University of Stavanger

Faculty of Science and Technology

MASTER'S THESIS

Study program/ Specialization: Konstruksjoner og materialer - Bygg	Spring semester, 2015 Open / Restricted access
Writer: Espen Framhus	…… (Writer's signature)
Faculty supervisor: Charlotte Obhrai	
Thesis title: Modeling of breaking wave loads on jacket structure in FEM software USFOS	
Credits (ECTS): 30	
Key words: USFOS Breaking of waves WaveSlam	Pages: 76 + enclosure: 23 Stavanger, 14.06.2015 Date/year

Front page for master thesis
Faculty of Science and Technology
Decision made by the Dean October 30th 2009

Preface

This thesis was done as to conclude my degree of Master of Science, at the University of Stavanger. The topic of the thesis, dynamic response of jackets due to breaking waves, was chosen out of interest for the offshore wind field.
In addition, this is a central theme in my line of study, and I felt that I had good academic foundation to work with it.
The project allowed me to further investigate the state of the industry and this thesis aims to present parts of the topics I have studied. The topics include hydrodynamics, breaking wave forces, signal analysis and structural dynamic response. In addition the thesis presented an opportunity to gain experience from learning both a finite element software such as USFOS and a powerful calculation tool like Matlab, and the experience gained is likely to prove useful.

I would like thank Professor Charlotte Obhrai for providing me with valuable study resources, aiding me during my work with the thesis and reading and correcting my thesis report.

Espen Framhus
Stavanger, June 2015

Summary

This thesis will in the first part present introduce and state the current development of offshore wind energy, and some of the motivations behind it. It will then present the current configurations and justify the need for better an understanding of the conditions, in designing and modeling the new foundations types like jackets are needed as the industry is expected to move into deeper waters. As a step in bettering the understanding of the conditions that are expected in deeper water, the WaveSlam project was lunched. This project had a goal to better understand the magnitude of the breaking wave forces one could expect to see on a jacket in deep water conditions.

The second part will go through some of the central used for theory for calculating breaking waves. With most of the theory being later applied directly in the report or indirectly through the use of the computer software tools.

In the third part the theory is applied to a model in USFOS in an effort to simulate the conditions expected to be observed. As the model is geometrically equal to that used in the WaveSlam, and the model was adjusted so its response in the simulation was comparable.

In the final parts of the report, the comparison of the experiment structure and the model allowed for an investigation into the problems that may arise from the use of an FEM software such as USFOS.
The central structural parts have to be fitted with the correct parameters individually, as the earlier adjustments was not sufficient for new load cases. Once responses of the model was in accord with the responses of the structure, it was possible to establish that there are inconsistencies that is introduced by USFOS wave generator. It caused the Eigen frequency of the model to shift to a lower value that it originally was fitted for. The cause of this Eigen frequency shift, and to how large an extent it effects the results was not established.
However the thesis was able to compare the model best fitted response to that of the experiment. The results from then introducing a load to the model based on a load case from the current monopile theories it is possible to see the extent of inaccuracy in the monopile theories when used on jackets. The thesis have not looked at accuracy of the load distributions on the jacket, and there might be some effects that are caused by an error in it. Therefore there are still some problems that have to be addressed before a certain conclusion can be drawn.

Concluding remarks

- USFOS is a FEM tool that can recreate slam events the associated dynamic response, there is still some inaccuracy that has to be addressed when the modeling the waves used in combination with the slam impulse.
- Monopile theory offers little coherence between the load and response calculated, and the actual observed loads on a jacket. Further investigations should focus on finding a correct way to represent the load distribution and duration accurately.

Table of content

List of figures

List of tables:

1. Intro

1.1 Scope and goals

The offshore wind industry is currently moving into deeper waters, with harsher conditions.
In these new waters, a new set of considerations becomes relevant. One of the main concerns is that the estimation of impact loads from breaking waves, are too large and are causing over conservative designs. Another concern is that the duration of these loads are close too, or the same as some of the Eigen frequencies of the structure and may cause resonance.

A breaking wave load and duration are often closely linked with the design of the structure that is affected by it. Since size and shape are closely related the breaking wave load. A change in structural shape, say from a single pile, to a jacket structure would therefore also cause a large change in breaking wave load.
To be able to make an accurate estimation of the loads and dynamic response is important, as this allows for better optimization of the design. High utilization and optimization are important for wind turbine projects. A small economic gain per turbine can give great savings for projects with numerous foundations.

The breaking wave load has been studied to some extent in previous experiments for single piles. However up until just recently there have been no such study of the same slam forces on a jacket structure.
An experiment called "WaveSlam" is the first to make such an efforts establish parameters such as, forces of a breaking waves on a jacket foundation of wind turbine. This has been done in through a large scale test during the summer of 2013. [1]

To get parameters regarding duration, magnitude and the distribution of the slam load, several tests was run. The data collected could then be numerically treated to find results that would be comparable with the previous studies and formulas that had been developed.

Using the data collected from the wave slam experiment, it is possible to model a jacket and try to recreate a slam event as observed in "WaveSlam". Data from the experiment can be used to ensure coherency between input into the finite element simulation, and the actual events, as there are many factors of the simulations that has to be assumed.
The output data from the model simulation can then be used in to verify that the model behaves the same as the jacket structure.

The main goal for this thesis is to investigate if the USFOS finite element software can be used to accurately model the dynamic response of a jacket structure subjected to a wave slam event. Using some of the data the WaveSlam-project has collected, this thesis aims to:

- Compare the calculated results from the model simulation with measured results from a scale model tests in the WaveSlam experiment, which will be used as reference for modeling and calculations.

- The finite element software USFOS can be used in combination with the current slamming theories to find a slamming factor that match the response observed in the experiment. If there are discrepancies between the simulated and the measured adjustments to the model maybe necessary to give a result similar to those observed in the experiment.

1.2 Background

Wind energy have been harvested for millennia. Primarily being used for simple mechanical labor, however by the time of the industrial revolution the first electrical production wind-mills (or turbines) where being built.
In 1888 electricity was first generated on a large scale (12kW) by a windmill, this was a windmill constructed by Charles F. Brush in Cleveland. After some initial improvements was made in the performance, using the aerodynamic principles developed in the aviation industry. Despite these improvements the industry was not able to compete with its non-renewable alternatives in the market, so there was little development in the area for a long time.

However the oil crisis of 1973 showed how important a reliable energy source is, and the vulnerability of any economy that does not have access to such resources. This forced industrial nations to consider renewable alternatives, like wind energy.
The crisis of 1973 gave the development of wind energy renaissance, and now wind energy is considered a viable alternative to non-renewable energy production. [2]

1.2.1 Development

Wind turbines are currently being developed as a part of a 2020 goal the EU has set for itself in terms of renewable energy production. In December 2008 the EU agreed to a target of 20% renewable energy by 2020. [3]
To be able to reach the 2020 goal, a large portion of the development has to happen offshore.
As of the beginning of 2012 the total installed capacity was about 3800 MW, with an ever greater number conceded and under construction, such that it is expected to increase to a total of 27 GW once they are completed. [4]

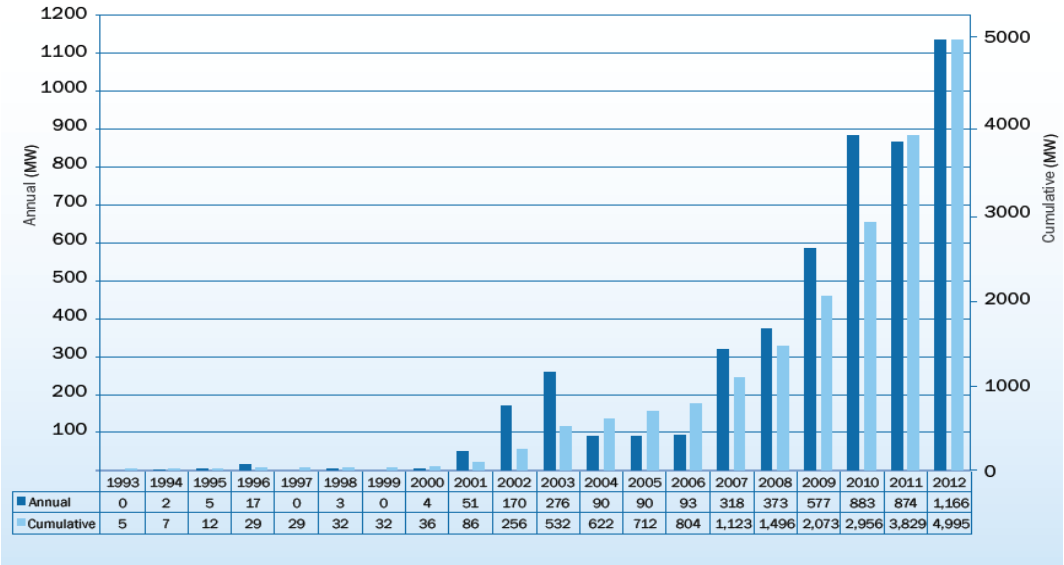

	1993	1994	1995	1996	1997	1998	1999	2000	2001	2002	2003	2004	2005	2006	2007	2008	2009	2010	2011	2012
Annual	0	2	5	17	0	3	0	4	51	170	276	90	90	93	318	373	577	883	874	1,166
Cumulative	5	7	12	29	29	32	32	36	86	256	532	622	712	804	1,123	1,496	2,073	2,956	3,829	4,995

Figure (1.1) Statistic of offshore development [5]

The goal is that by 2020 140 TWh of energy will be generated by offshore wind.
This number could be increased to 818 TWh by 2050 in some scenarios. [6]

1.2.2 Offshore Wind

The reasoning behind offshore winds likely importance in the future, stems from the site conditions offshore. They often have more stable wind conditions then their inland counterparts. Combining this condition with the higher average wind speeds, gives a (much) higher energy potential when compared with sites onshore. [4]
There are also relaxed restriction on both visual and noise impacts. It can therefore be easier to get concessions, and build larger turbines than what would be allowed on land. [4]
As for transport, it is generally thought to be simpler to organize and transport parts of such a massive scale by water, than by roads. [2]

1.2.3 Optimization and Standardization

A drawback for offshore wind compared with onshore, are costs. They tend to be much higher and grow with depth and distance to shore.
The increased costs are generally related to foundation and grid connections, both of these tend to grow with increasing depth and distance to shore. Optimization and standardization will help in this regard as both of these can be improved with research and increasing experience. [7]

Since foundations for offshore wind turbines often are produced in serial productions, and they make up a large portion of the investment[8], a small optimization of the design might give a great benefit economically.
For better optimizations, new standards have to be developed, as many of the currently used are blends between fixed bottom and oil and gas standards, which generally result an over-conservative design. Therefore correctly modeling deep offshore designs remain one of the key challenges in the deep water development.
One of the steps being made towards better optimization is to better understand the forces involved in waves breaking on the structure. Research into this field has so far been limited, and as there are different dynamic considerations when it comes to a wind turbine compared with oil and gas platforms. Research done in these fields are of limited use.

This is because a wind turbine is long and slender with the majority of its structural mass at its top, and it has therefore few dynamic similarities to an oil and gas platform. [9] The differences may make it more susceptible to breaking wave loads than those of oil and gas truss structures of similar configurations and size. A general rule has been to be very conservative when estimating the forces and through this ensure sufficient safety. [9]

Efforts have been made to improve methods of prediction breaking wave loads, several experiments have been conducted with focus on wave slam, but these have primarily been interested in forces on monopiles.

1.2.3.1 WaveSlam

WaveSlam was the first project that aimed to give a better understanding of these forces on jackets. During June of 2013 a jacket structure was build in the large wave fume GWK in Hannover, Germany. Fitted with sensors and gauges the structure, a large scale (1:8) model of a jacket foundation, was subjected to numerous breaking waves.

The experiments were designed to measure the breaking wave forces a jacket wind turbine foundation. As jackets foundations are expected to become more relevant as a substructure solution. [1]

The data used in this thesis originates form this experiment.

1.2.4 Foundation trends

The current construction of offshore wind power has primary been focused around shallow water. In shallow waters, it has been common to use single piles (called monopiles) or large concrete sections (referred to as gravity based structure or GBS) as they are considered the most cost efficient foundations. Per 2011, the monopoles consisted of over 70 % of the total foundation market share, while GBS made up around 21%. [4] The remaining 9 % being made up of less developed alternative foundation such as jackets and floaters.

Future foundation designs that are expected to change from those that are currently being employed. This is mainly because a large portion of the projects being proposed by developers are in waters that have greater depths then have been before. Giving new requirements to the design foundation. [7]
Foundations like jackets are therefore expected to become more in use in the coming years as it is thought to meet these requirements efficiently. [10]

As seen from the figure below the intermediate water depth (30-60m) contains a large portion of the consented projects.

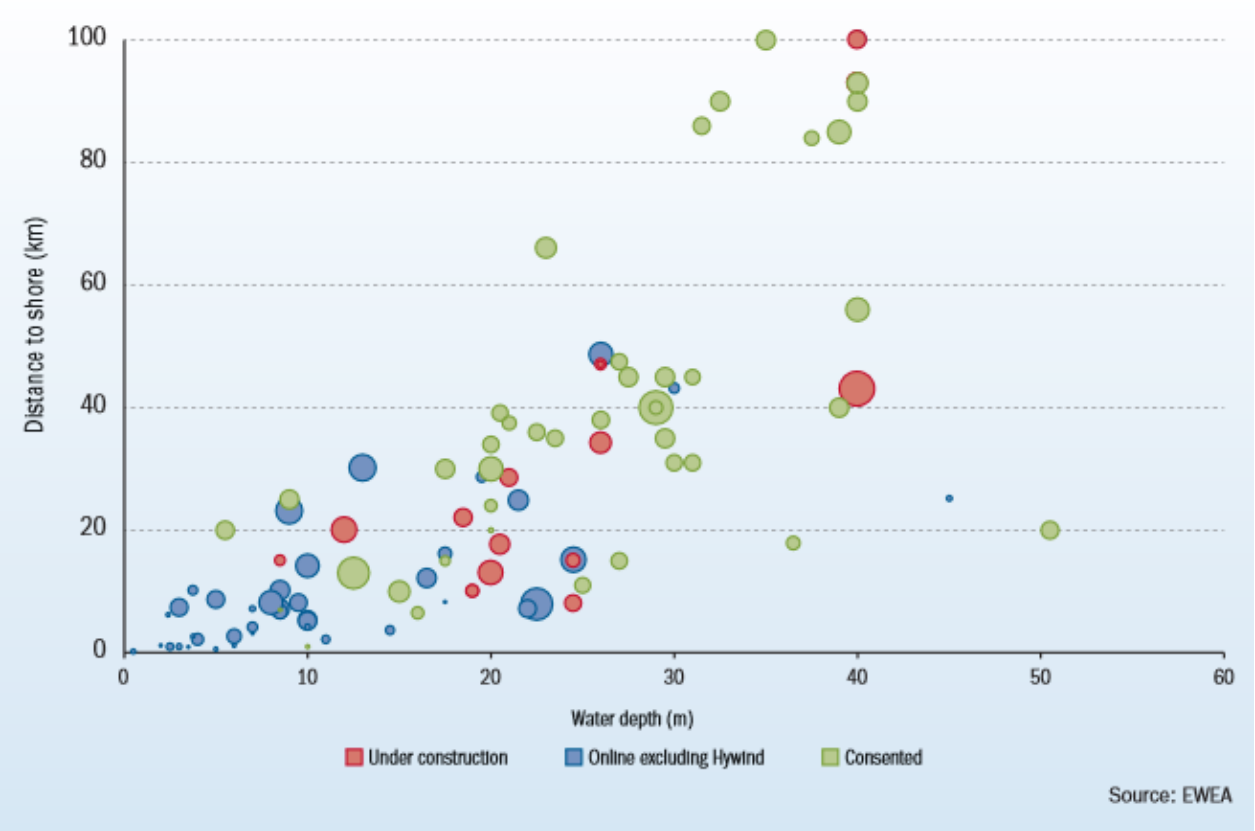

Figure (1.2) Chart of constructed, planned and consented of offshore turbines in European waters [11]

Reason behind the change in design is that in these areas, monopile and GBS types of structures are expected to be less cost effective and impractical compared to other alternatives.
Water depth are a major factors that have a large impact on cost and loads of the foundation, for monopile around 30 meter of water depths the required pile diameter and thickness becomes of such a size that installation is an issue.[12]
Jacket structures might require more work in fabrication and in installation, but in return exploit the material more efficiently, requiring less material, and therefore weighing less that a

monopole or GBS equivalent. Jacket structures are therefore likely to be more and more relevant for offshore wind farms in the near future. [13]

Floating structures have been suggested as viable in waters depths below the 50 meter [12], while floating structures are being developed, and certain floating wind turbines are in test stages, bottom-fixed structures are currently viewed the only commercialized design alternative in use for offshore wind energy. [10]

1.3 Bottom fixed support structures

1.3.1 Monopiles

The simple pile construction has a great advantage when it comes to pricing, as it is relatively simple to install and remove. The development of increasing and increasing diameter sizes have Allowed for deeper and deeper usage of monopoles.[10]

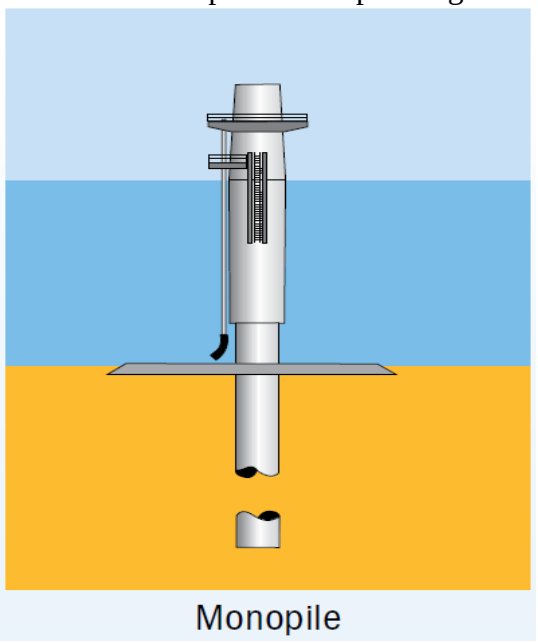

Figure (1.3) Illustration of typical monopile [7]

It is however not without problems. Due to its configuration, as a slender pole, the diameter has to be increased very rapidly as the depth increases to counter the increase in turnover-moment form current and wave loads.

This is big problem for monopole structure, as they become very heavy very fast when the depth is increased. This may make it unable to compete with different configuration such as a truss at depths greater than 20~25 m. Piles at larger depths can weigh as much as 800 tons or more, and only a few years back this would make it impossible to install them, as vessels found it difficult to install piles weighing greater than 500 tones. [10]

It is the most common support structure in use today, as most wind parks offshore have been placed in depths that are within optimal depths for use.

A major factor playing in favor of monopiles compared to more experimental solutions is that it has proven track record, thus giving ease of mind to financers whom are concerned with risk and risk management. [7]

The most common configuration of anchorage for monopiles is piling it into the seabed. [14] This makes it less attractive to use in some sea bed conditions. However since it is a single connection to the seabed, it is susceptible to scour [15]

1.3.2 Gravity based structures

The foundation concept where the idea is to utilize a massive dead load, and by doing this avoid any lifting force between the seabed and the structure. This dead load is preferably so large so that stability is ensured no matter what the surrounding conditions are. [16]

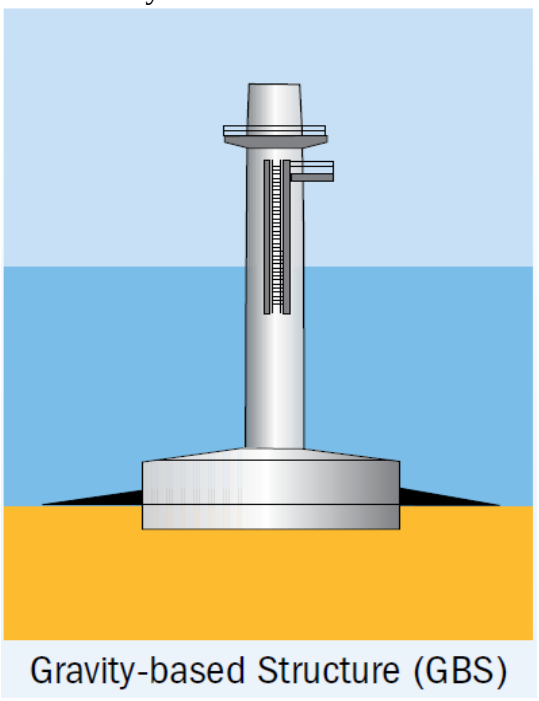

Figure(1.4) Illustration of typical gravity baseds structure [7]

Gravity based foundations are considered competitive in areas with modest environmental loads and water depths less than 30 meters. [11]
The nature of the configuration makes it well protected against ice and other impact loads. As it its massive weigh makes it less sensitive to impacts than its foundation alternatives.
Gravity based structures require large construction sites, like (ship) yard to be constructed. They mainly use concrete as building material, something that is relatively cheap compared to alternatives. The size and the dead load requirements are strongly dependent on the depth it is to operate. In small depths from 3 ~15 meters it is well suited as then these requirements are relatively small. Since these demands increase rapidly with depth it is not well suited for depths greater than 25 meters.
Transportation over large distances can be an issue as they are towed on barges. Preparations are required when installing the foundation. The installation process is comparably a bit costly from the placing of the ballast. [15]

1.3.2 Three/four legged jackets

Jackets are seen as the main alternative for monopiles when water depth or soil conditions are deemed to challenging/expensive for the monopole configuration. [10]
This makes them a likely go-to solution since for future development, as a major part of the consented turbines are in water depths over 30 meters. [5]
A welded triangular or four legged structure. It is often the preferred solution for medium depths. It takes less seafloor preparations than that of gravity bases structures. It is a well tried out way of designing supports for the oil and gas industry. [17]
Structures with this configuration may be unsuited to in icy waters since they generally have thinner tubular sections than those of monopiles. Therefore they are more sensitive to impact loads.

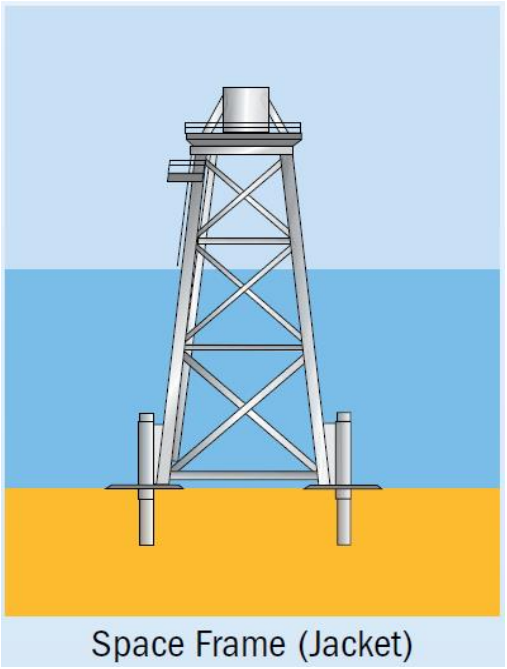

Figure(1.5) Illustration of typical jacket structure [7]

The legs of a jacket foundations have to be piled into the seabed to get anchorage and these types of configuration have been used previously in the oil and gas industry. Jacket foundations scales better to a much greater depth then both monopiles and gravity based foundations. They are also lighter compared to equivalent monopiles and gravity based structures, making them easier to transport to on site.
They requires deeper anchorage piles as they have smaller diameter. However small tubes are easier to handle when installing, compared with those used for the larger monopile. The hammer required for piling is also much smaller, reducing the equipment requirements. In rocky soils they may need to be drilled into the soil to get anchor footing.[15]
Even if there the jacket structure is well a researched foundation for oil and gas platforms, this research may not be as relevant for wind turbine construction.
The experience with jackets thus far have been good, with no structural failures to report. [10]

2. Theory

2.1 Wave Theory

A wave theory is needed to accurately describe the behavior of the water surface, as this very close linked to forces experienced by the truss there are many theories describing how waves behave. This paragraph will attempt to give some insight into those that are consider to be most relevant for this thesis and what assumptions and validity each holds given conditions of the experiment. [18]

2.1.1 Fluid dynamics of waves

Assume that there is that there exists a function, whose gradient represents the flow of a fluid through an arbitrary body[19]:

$$V = \nabla\phi \tag{2.1}$$

This function is called potential flow. Where V represent the total velocity of the flow.

Newton's 2nd law states that force is equal to the acceleration times the mass of the object affected, or

$$F = M * a \tag{2.2}$$

It can be applied to an arbitrary body of fluid giving[19]:

$$dF = dm * \frac{D\vec{V}}{DT} = dm * [u\frac{\delta\vec{V}}{\delta x} + v\frac{\delta\vec{V}}{\delta y} + w\frac{\delta\vec{V}}{\delta z} + \frac{\delta\vec{V}}{\delta t}] \tag{2.3}$$

The forces acting on a fluid body can be derived using a Taylor series expansion.
For any direction (here x-direction) a sum of the fluid body element forces can be written as[19]:

$$dF_{S_x} = \left(\frac{\delta\sigma_{xx}}{\delta x} + \frac{\delta\tau_{yx}}{\delta y} + \frac{\delta\tau_{zx}}{\delta z}\right) dxdydz \tag{2.4}$$

Accounting for gravity as well the equation can be written as:

$$dF_{S_x} = \left(\rho g_x + \frac{\delta\sigma_{xx}}{\delta x} + \frac{\delta\tau_{yx}}{\delta y} + \frac{\delta\tau_{zx}}{\delta z}\right) dxdydz \tag{2.5}$$

Newtons 2nd law can be substituted for the "dF" in the fluid body equation, this gives a set of equation of motion that will satisfies the continuum assumptions.[19]

$$\rho g_x + \frac{\delta \sigma_{xx}}{\delta x} + \frac{\delta \tau_{yx}}{\delta y} + \frac{\delta \tau_{zx}}{\delta z} = \rho(u\frac{\delta u}{\delta x} + v\frac{\delta u}{\delta y} + w\frac{\delta u}{\delta z} + \frac{\delta u}{\delta t})$$

$$\rho g_y + \frac{\delta \tau_{xy}}{\delta x} + \frac{\delta \sigma_{yy}}{\delta y} + \frac{\delta \tau_{zy}}{\delta z} = \rho(u\frac{\delta v}{\delta x} + v\frac{\delta v}{\delta y} + w\frac{\delta v}{\delta z} + \frac{\delta v}{\delta t}) \qquad 2.6$$

$$\rho g_z + \frac{\delta \tau_{xz}}{\delta x} + \frac{\delta \tau_{yz}}{\delta y} + \frac{\delta \sigma_{zz}}{\delta z} = \rho(u\frac{\delta z}{\delta x} + v\frac{\delta z}{\delta y} + w\frac{\delta z}{\delta z} + \frac{\delta z}{\delta t})$$

Water can be assumed to be an incompressible Newtonian fluid, meaning that the shear stress is directly proportional to its deformation. [19]
Incompressibility keeps the density constant over the whole fluid body.
This assumption with respect to the fluids properties, is not exactly correct but the error is small compared to the gravitational effects, so small that they may be neglected.

They greatly simplifies the equation of motion, which then can be rewritten as a form of the Navier-stokes equations [19]:

$$\rho\left(u\frac{\delta u}{\delta x} + v\frac{\delta u}{\delta y} + w\frac{\delta u}{\delta z} + \frac{\delta u}{\delta t}\right) = \rho g_y - \frac{\delta \rho}{\delta x} + \mu(\frac{\delta^2 u}{\delta x^2} + v\frac{\delta^2 u}{\delta y^2} + w\frac{\delta^2 u}{\delta z^2})$$

$$\rho\left(u\frac{\delta v}{\delta x} + v\frac{\delta v}{\delta y} + w\frac{\delta v}{\delta z} + \frac{\delta v}{\delta t}\right) = \rho g_y - \frac{\delta \rho}{\delta y} + \mu(\frac{\delta^2 v}{\delta x^2} + v\frac{\delta^2 v}{\delta y^2} + w\frac{\delta^2 v}{\delta z^2}) \qquad 2.7$$

$$\rho\left(u\frac{\delta w}{\delta x} + v\frac{\delta w}{\delta y} + w\frac{\delta w}{\delta z} + \frac{\delta w}{\delta t}\right) = \rho g_z - \frac{\delta \rho}{\delta z} + \mu(\frac{\delta^2 w}{\delta x^2} + v\frac{\delta^2 w}{\delta y^2} + w\frac{\delta^2 w}{\delta z^2})$$

By assuming the motion to be frictionless ($\mu = 0$) the Navier-Stokes equations reduces to the Euler's equation:

$$\rho\left(u\frac{\delta u}{\delta x} + v\frac{\delta u}{\delta y} + w\frac{\delta u}{\delta z} + \frac{\delta u}{\delta t}\right) = \rho g_y - \frac{\delta \rho}{\delta x}$$

$$\rho\left(u\frac{\delta v}{\delta x} + v\frac{\delta v}{\delta y} + w\frac{\delta v}{\delta z} + \frac{\delta v}{\delta t}\right) = \rho g_y - \frac{\delta \rho}{\delta y} \qquad 2.8$$

$$\rho\left(u\frac{\delta w}{\delta x} + v\frac{\delta w}{\delta y} + w\frac{\delta w}{\delta z} + \frac{\delta w}{\delta t}\right) = \rho g_z - \frac{\delta \rho}{\delta z}$$

These assumptions and equations of motion form the general basis for wave theories. Often the equations are written as derivative of a function potential that represents flow, often referred to as potential flow, as it is presented in formula 2.1.

2.1.2 Airy theory / Stretched Airy theory

Linear wave theory (LWT) also known as Airy wave theory, was developed by Airy (1845), it is based on the assumption that the amplitude is relatively small compared to the $\frac{H}{2\lambda} \ll 1$.

For small amplitudes compared with water depth, it is possible to neglect nonlinear terms in the Bernoulli equation, this process called as linearizing. This can be done for small amplitudes because then the non-linear terms effects on the solutions are small.
Airy theory have proven to give good estimates within its realm of validity,
Outside its domain it gets large errors, especially close to the surface boundary. [20]

Integrating the Navier-Stokes equations using the assumptions stated produces the Bernoulli equation. [21]

$$\frac{p-p_0}{p} = -\phi_t - \frac{1}{2}(\nabla\phi)^2 - gy \qquad 2.9$$

Where ϕ represents the potential flow equation

Then the equation can be rewritten as the Bernoulli equation is given as:

$$p + \rho g\xi + \rho\frac{\delta\phi}{\delta t} + \frac{1}{2}\rho V * V = C \qquad 2.10$$

From the kinematic boundary condition we have that a fluid cannot pass through solid boundaries such as walls or bottoms, this can be expressed as:

$$V * n \equiv \frac{\delta\phi}{\delta n} = U * n \qquad 2.11$$

We use the kinematic condition combined with a dynamic condition saying that the pressure at the free surface must match prescribed reference pressure.
We assume that the free surface given as:

$$\zeta = f(\xi, \eta, t) \qquad 2.12$$

Where:
ζ: 0 at surface
ζ: -h at depth h

Implementing the kinematic boundary condition on the free surface formulation gives the following derivative.

$$\frac{\delta f}{\delta t} + \frac{\delta\phi}{\delta\xi}\frac{\delta f}{\delta\xi} + \frac{\delta\phi}{\delta\eta}\frac{\delta f}{\delta\eta} - \frac{\delta\phi}{\delta\zeta} = 0 \quad on\ \zeta = f \qquad 2.13$$

Now implementing the dynamic boundary condition, results in an equation that looks like this:

$$gf + \frac{\delta\phi}{\delta\xi} + \frac{1}{2}V * V = 0 \qquad on\ \zeta = f \qquad 2.14$$

The surface have an unknown location, and the boundary condition of the free surface is dependent on the derivatives on of

$$\phi \wedge f \qquad 2.15$$

The derivatives of the functions $\phi \wedge f$ can be expressed using a Taylor series expansion. The expansion can be simplified greatly by assuming linear conditions, thus setting all except the first derivative to zero. [20]
Combining the boundary conditions into one equation.

$$\frac{\delta f}{\delta t} - \frac{\delta \phi}{\delta \zeta} = 0 \; on \; \zeta = 0 \qquad 2.16$$

$$gf - \frac{\delta \phi}{\delta t} = 0 \; on \; \zeta = 0 \qquad 2.17$$

$$\frac{\delta^2 \phi}{\delta^2 t} - g\frac{\delta \phi}{\delta \zeta} = 0 \; on \; \zeta = 0 \qquad 2.18$$

Solving the Laplace equation gives a potential solution [21] :

$$k\xi cos(x) + k\eta sin(x) - \omega t \qquad 2.19$$

$$\phi = \frac{gA}{\omega}\frac{cosh\, k(h+\zeta)}{coshkh} sin(x) - \omega t \qquad 2.20$$

From this potential function, velocity and acceleration fields can be found.
If stretching of the equation is done, the equation will still have to satisfy boundary conditions
The boundary conditions are modified to give :
Dynamic:

$$\frac{1}{2g}(u^2 + v^2) + z - \frac{1}{g}\frac{\delta \phi}{\delta t} = c(t), z = \eta \qquad 2.21$$

Kinematic:

$$\frac{\delta \eta}{\delta t} + u\frac{\delta \eta}{\delta x} = v, z = \eta \qquad 2.22$$

The new potential is then given as [22]:

$$\phi = \frac{g*H}{\omega*2}\frac{cosh\, k(h+\zeta)}{coshk(h+\eta)} \sin(kx - \omega t) \qquad 2.23$$

Where $\frac{cosh\, k(h+\zeta)}{coshkh}$ is changed to $\frac{cosh\, k(h+\zeta)}{coshk(h+\eta)}$ in order to represent the factor of stretching [23]

Note: *while it satisfies the boundary conditions, it does not satisfy the Laplace equation.*

Using this formulation of the Airy theory, a set of equations to calculate the wave properties can be evaluated.

From this potential function a set of parameters can be found [24]:

Wave length: $$\lambda = \frac{gT^2}{2\pi} \quad (2.24)$$

Wave number: $$K = \frac{2\pi}{\lambda} \quad (2.25)$$

Celerity: $$C = \sqrt{\frac{g}{K}\tanh(kd)} \quad (2.26)$$

Surface elevation: $$\eta = \frac{H}{2}\cos\theta \quad (2.27)$$

Extracted from [24]

2.1.3 Stokes theory

Stokes (1847) was able to find a solution for waves that where outside the Airy wave theories steepness and relative height limitations. His trigonometric expansion of the Airy wave have been used with good results for waves that are in too shallow waters, or are too steep to be covered by Airy theory. [25]
His reasoning can be simplified to be, as a number of sine wave potentials will always satisfy the continuity and bottom boundary conditions the same as a single potential. The problem is then that there are several free surface boundaries. The sum of waves are added as a potential with half the period and half the length of the previous order. The next issue is to satisfy two surface boundary conditions. [22]
High order Stoke approximations are unsuited to describe waves of small magnitude compared to the depth, as stokes expansions under these conditions were diverging. [25]
The stream theory incorporates the same reasoning as the Stokes theory, but instead of finding the analytical solution it solves the problem numerically. [26]

A general expression for stokes/stream theory is given as:
[27]

$$\psi(x,z) = cz + \sum_n^N X(n)sinh(nk)(z+d)cos(nkx) \quad (2.28)$$

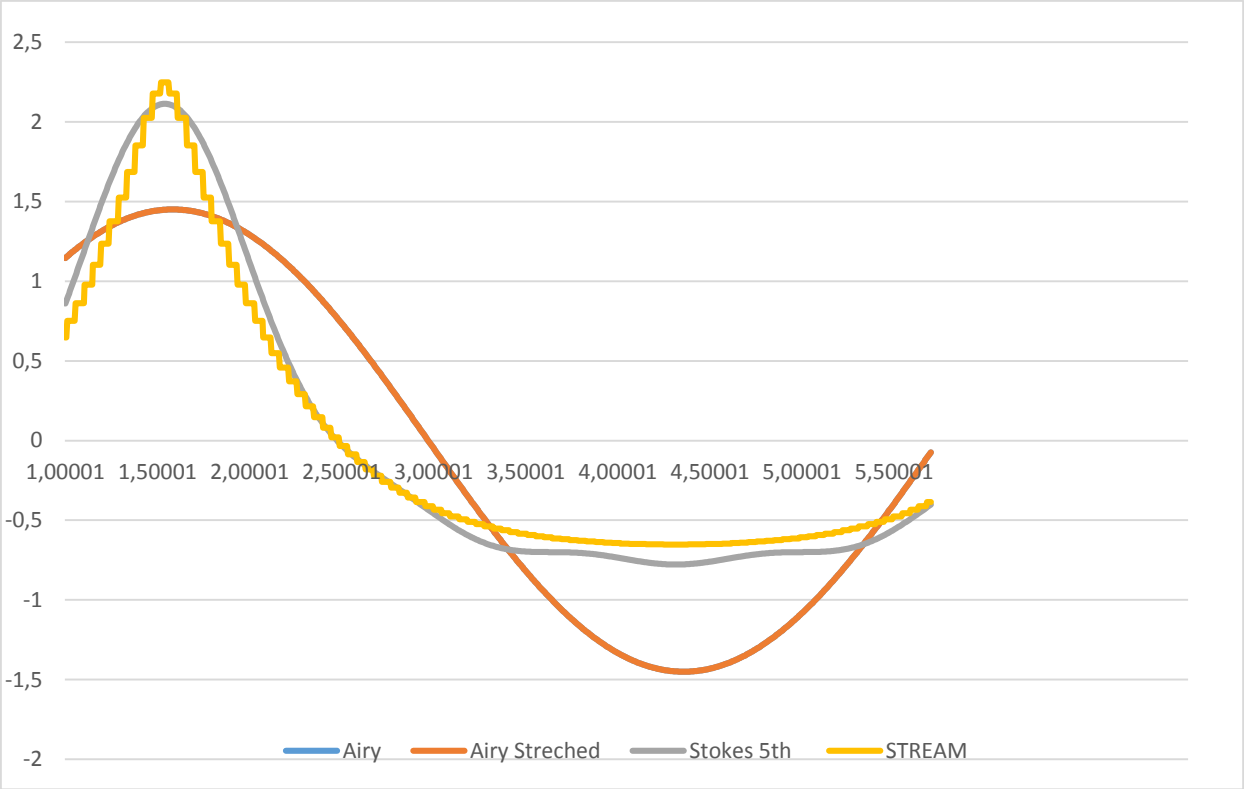

Figure (2.1) – Plot of Surface elevation of different theories in USFOS.
(Wave height = 2.9 m, Depth = 4.3, Period 5.5 seconds.)

To give an approximation of the breaking waves Stokes or Stream theory will be applied in USFOS. Alternative theories such as Higher order Cnoidal theory is unsuited for describing waves close to breaking because it has inhomogeneous convergence issues, similar to those the stokes theory experience in small amplitudes.[25]

2.2. Applicability of Wave theories

The wave theories are often limited by a combination of wave depth and height. A good way to illustrate the validity of a theory is through the use of logarithmic plots of wave height and depth. [28]

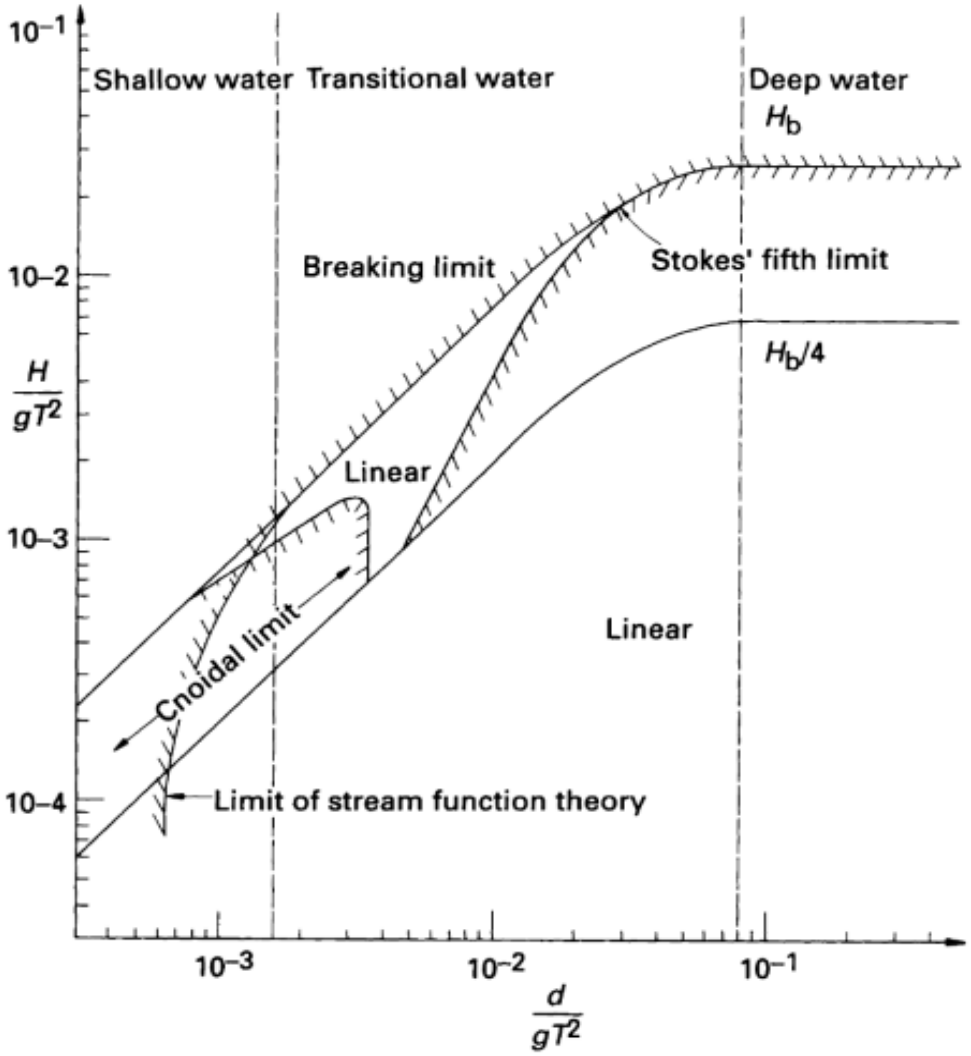

Figure (2.2) Chart of the applicability of wave theories from [28]

This figure offers a good illustration of the validity of the wave theory employed based on wave steepness $\left(\frac{H}{gT^2}\right)$ and depth limitation$\left(\frac{d}{gT^2}\right)$. If a wave reaches the breaking limit it breaks. This event can take several forms, spilling, plunging, collapsing and surging. What type of wave break occurs is dependent on the circumstances.

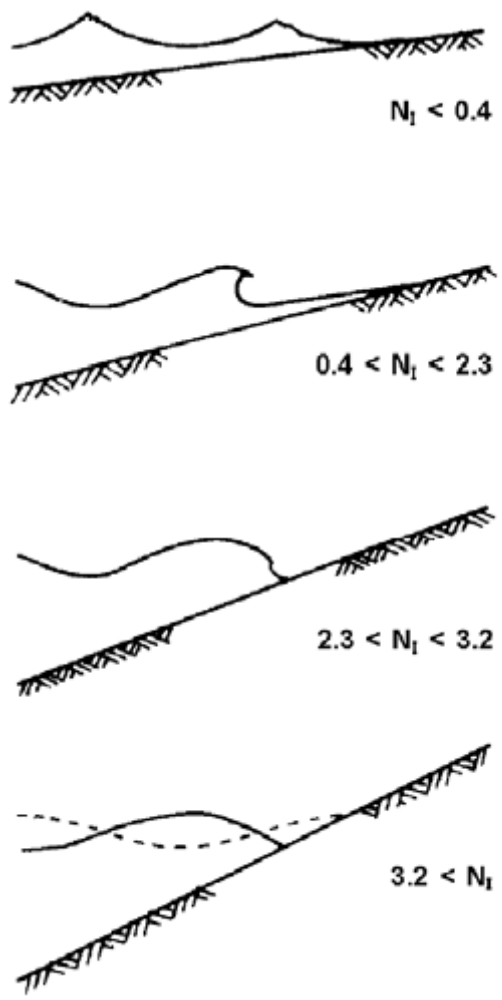

Figure (2.3) Types of breaking waves[29]

What type of breaking event occurs is described by the Iribarren number [30]:

$$N_I = \frac{tan\beta}{\sqrt{H/L_0}} \qquad 2.29$$

$$L_0 = gT^2/2\pi \qquad 2.30$$

$\beta - Wave\ steepness$

Spilling	$N_I < 0.5$
Plunging	$0.5N_I < 3.3$
Collapsing or Surging	$N_I > 3.3$

Most relevant for this thesis are the spilling and plunging. This is because these can cause high pressures and impulse loads structures. The loads expected are over a small area and over a short amount of time.

2.2.1 Breaking criteria

In an effort to predict when waves become unstable and break, criteria for breaking have been developed. To account for both deep water and shallow water breaking:

Breaker height to depth ratio [30]:

$$\gamma_b = \frac{H_b}{d_b} \tag{2.31}$$

γ_b the ratio can vary between 0.7 and 1.2

Miche (1944) found general limiting steepness of waves to be

$$\left(\frac{H}{L}\right)_b = 0.14 tanh\left(2\pi \frac{d_b}{L_b}\right) \tag{2.32}$$

As depth increases to deep water this limit goes towards: 0.14 (1/7)
Waves with greater steepness becomes unstable and break.
This formulation only holds under the assumption that the seabed is a flat surface. For sloped seabed and shoaling, some modifications are needed to the criteria [25]

$$\frac{H_B}{H_0} = 0.14 tanh\left((0.8 + 5S)2\pi \frac{d_b}{L_b}\right) s < 0.1 \tag{2.33}$$

$$\frac{H_B}{H_0} = 0.14 tanh\left((0.13)2\pi \frac{d_b}{L_b}\right) s > 0.1 \tag{2.34}$$

In shallow waters, the Cnoidal theory offers the best results on wave height, but over estimates the wave length and wave celerity. The Stokes and stream theory will therefore be the ones applied in this thesis, as the celerity is important for the breaking wave load (see section 2.3.2)
For deep waters, the limit can be assumed to be around [25]:

$$\frac{H}{L} = \frac{1}{7} \tag{2.35}$$

2.3 Wave forces

2.3.1 Morrison's Equation

The Morrison Equation is a way of estimating the load due to non-breaking waves on slender piles. It uses the wave particle potential derivatives combined with empirical factors to get a resulting force from the passing waves. Since both acceleration and velocity will cause resulting forces on the pile, the equation is separated into two terms. Each of these accounts for a part of the force that is exerted on the cylinder.
The inertia term in the equation records force due to the water particle acceleration, while the drag term accounts for water particle velocity. This method has been used to estimate forces that are in good agreement the actual measured loads. [31]

The drag coefficient is determined as a dimensionless function of viscosity and Reynolds number.[32]

$$R_e = \frac{u_0 D}{\upsilon} \qquad 2.36$$

Relation between Reynolds number and drag coefficient:

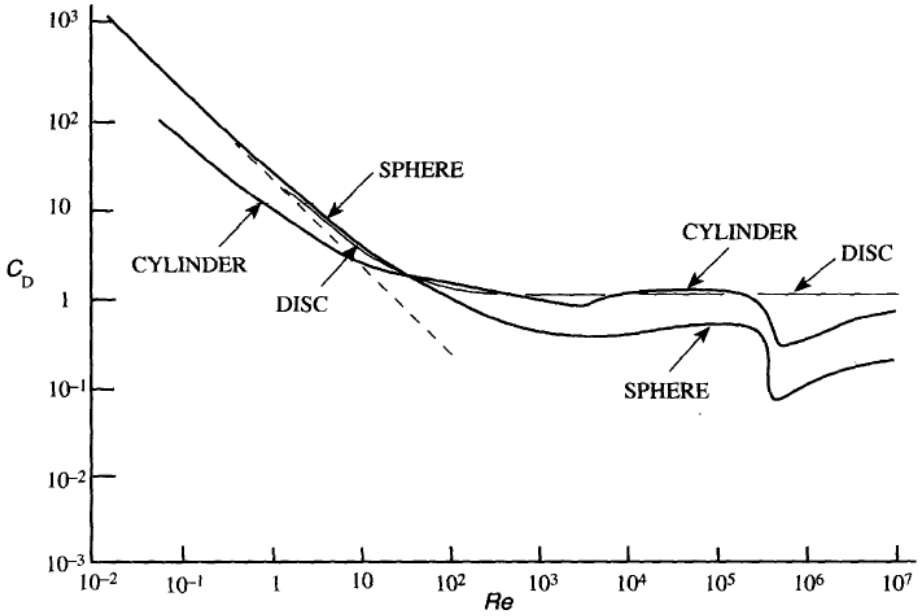

Figure (2.4) Reynolds number and related drag coefficient [32]

The inertia coefficient is estimated as the force produced by the Froude Krylov force whereas the acceleration of current would cause an increase in pressure on the surface of the cylinder. When cylinders are small comparatively to the wave length, this acceleration is assumed to be constant.

The fluid around small cylinders will be dragged along as the fluid passes the cylinder. This additional mass acceleration results in an increase in the force on the cylinder.

The ratio of additional mass with respect to the actual mass of water affected is used to produce the mass coefficient $C_M = \left(1 + \frac{M_{added}}{M}\right)$ that is used to scale the inertia term of the Morrison equation.

The Morrison equation is given as follows [31]:

$$F_{total} = F_D + F_I \qquad 2.37$$

$$F_D = \int_{-d}^{\eta} \frac{1}{2} \rho C_d D u(z,\theta) \vee u(z,\theta) \vee dz \qquad 2.38$$

$$F_I = \int_{-d}^{\eta} \rho C_m \pi D^2 \acute{u}(z,\theta) dz \qquad 2.39$$

These equations can be used to represent the quasi static response and are indirectly applied, as these calculations are done by using the wave generator in USFOS.

2.3.2 Wave slamming force

When a wave phase passes a structure while breaking or just prior to breaking, the wave can have a form that is near vertical, causing a rapid change in pressure as it passes.
The short duration and large magnitude of this force makes it unpractical to adjust and implement it into one of the existing terms and therefore it is added in as a separate term of the total force equation. The term is usually referred to as "Wave slamming force".

$$F_{total} = F_D + F_I + F_s \qquad 2.40$$

For cylindrical sections it is assumed that the water acts like a flat surface hitting a flat plate. The resulting pressure calculated using Bernoulli equation and considering the potential flow. This was the assumptions made by Von Karman as basis for his consideration of a wave slam event.
Von Karmans formulation [31]:

$$F_S = \rho_w R C^2 C_s \text{ , } C_s = \pi\left(1 - \frac{C}{R}t\right), \text{ at t= 0 => } C_s = \pi \qquad 2.41$$

$$F_S = \rho_w R C^2 \pi \qquad 2.42$$

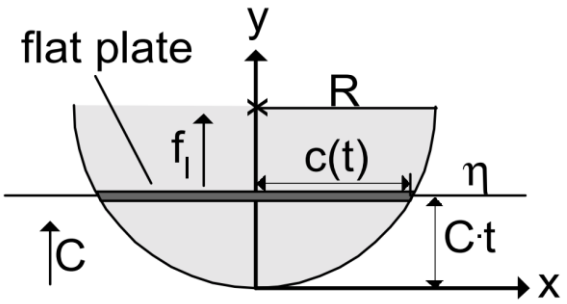

Figure (2.5) Illustration of Von Karman's formulation[31]

$\rho_w = waterdensity\ C = wavephasespeed\ R = cylinderradius$

When a wave moves past a cylindrical cross section, the free water surface will deform. This is effect is not accounted for in Von karman's formulation of a slamming event. This effect described as pile-up effect, will cause the actual slamming event occurs a bit ahead of the wave phase. Wagner's formulation modifies the formulation proposed by Von Karman to account for this effect.
Wagners Formulation [31]:

$$F_S = \rho_w R C^2 C_s, \text{ at t= 0 => } C_s = 2\pi \qquad 2.43$$

$$F_S = 2\rho_w R C^2 \pi \qquad 2.44$$

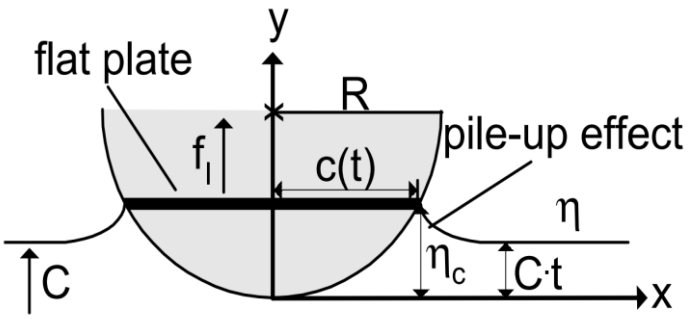

Figure (2.6) Illustration Wagner's formulation

The pile up effect increases the line force estimated because it decreases the impulse duration. Wagner's model estimates the line force to be twice that of Von Karman.
The general equation for slamming is then formulated with a slamming factor, which is dependent of which interpretation is preferred.
The general wave slam equation is as follows [31]:

$$F_S = \rho_w R C^2 C_s \qquad 2.45$$

For the dynamic analysis the impacts duration is a major factor. Impact duration is dependent on the diameter of pile, breaking wave celerity, inclination, rise time, and wave particle velocity. It is also dependent upon the amount of air entrainment. Air may cause a cushioning effect, increasing the impact duration and reducing the impact force on the cross section.
For monopiles the duration of a plunging breaker wave is estimated as[24]:

$$Tdruation_{Standards} = \frac{13D}{64c} \qquad 2.46$$

2.3.2.1 Curl

The Von Karman/Wagner formulation only account for a unit length of the cylinder, so to find the total load, a relation to the size/length of the impact area is needed.

Goda(1966) uses a curling factor to account for the "impact" length, the curling factor is a percentage of the surface elevation at the highest point of the crest compared to Stillwater level. The inclination of the water surface also plays a role in the duration and severity of the impact. Goda states that a vertical wall of water the inclination and rise time is assumed to zero.
An inclination further from vertical and an increase in rise time of the max impact force tends to reduce the slamming force. The rise time is also vital since it greatly affects the dynamic response of the structure. [33]

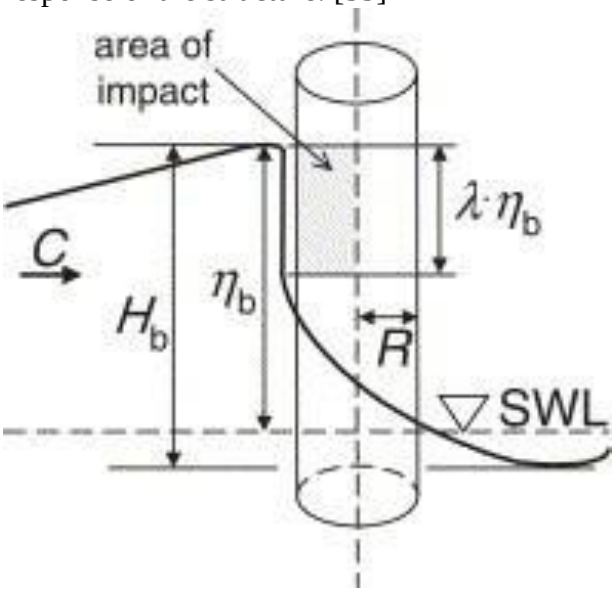

Figure (2.7) Illustration of curl effect

The total force of slamming on a cylinder is then:

Modified equation [31]:

$$F_S = \lambda \eta_b \rho_w R C^2 C_s \qquad 2.47$$

Using the theory proposed by Wagner, it has investigated different inclinations of a cylinder to find an appropriate curling factor for each inclination. For zero inclination (pile is vertical) was a curling factor equal to 0.46. [31]

2.3.2.2 Slamming factor

The pressures on increasing angles of the wave direction on the impacted cylinder. They proposed a Cs factor that varies with time history based with starting point at Wagner peak pressure. [31]

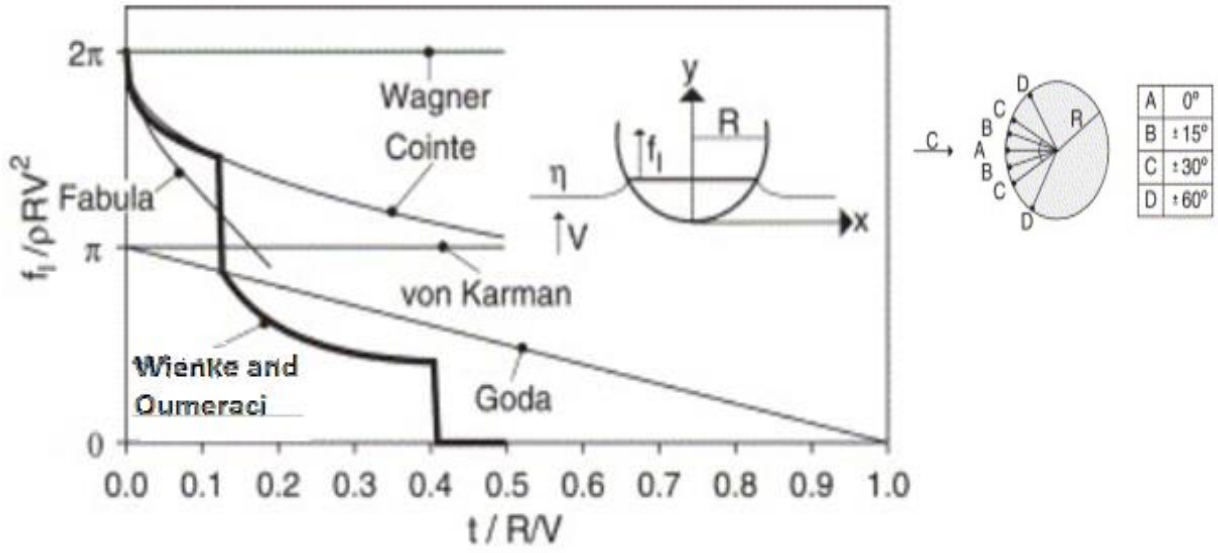

Figure (2.8) – Slamming coefficients of different theories [31]

Some of the Slam coefficients at time = 0

Name	**T = 0**	**Cs**
Wienke & Oumeraci	0	2π
Wagner	0	2π
Von Karmans	0	π

2.4 Structural analysis

Offshore wind turbines are subjected to numerous loads, some cyclic, some self-imposed, and some impulse based. The total load picture and load history affects how these loads translate into a structural response.

A wind turbine is a multi-degree dynamic system that have many Eigen-frequencies that may produce dynamic effects from periodic loading. Vibration control is important regulate as to avoid resonance at these frequencies. This is why complex dynamic analysis are needed.

Computer software is a very helpful tool in this, as it allows for quickly calculation of numerous Eigen frequencies based on the model and data inputted. From such an analysis, it is possible to compare the loads that might affect the structure and the resonating frequencies. If there is likely to be a resonating load, it is often best to avoid it. This can be achieved by either by changing design or modifying properties of the structure in some way. Computer tools like USFOS are therefore helpful very helpful in design as they usually allows for quick modifications to their models as well.

2.4.1 Loads in USFOS

USFOS uses two node Beam elements. These beams has 6 degrees of freedom and can be used as columns as well as beams. As a results, it is effective at modelling requiring few elements even for large structures. It represents loads and stresses on the element with local coordinates.

The beam can be represented by a 4th degree differential equation, which can be solved resulting in a trigonometric and exponential shape function.

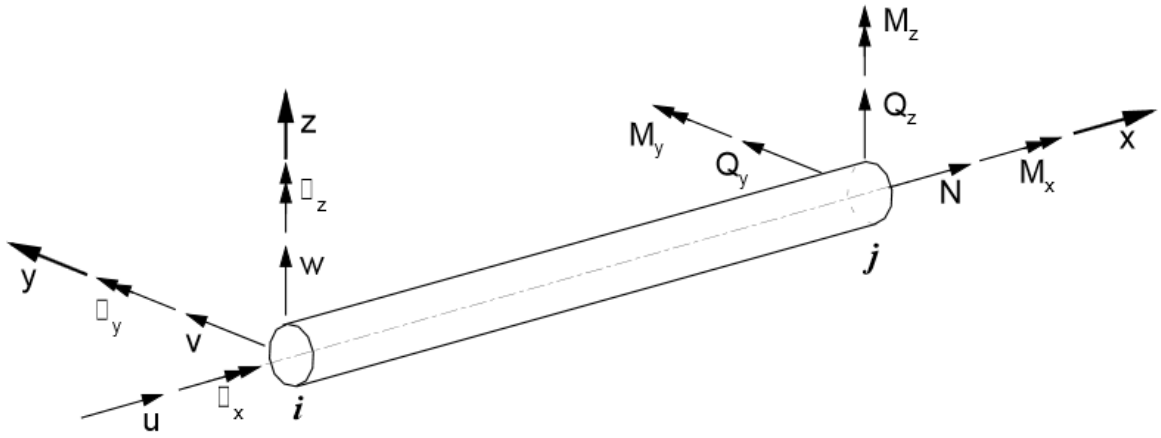

Figure (2.9) Load decomposition in USFOS [27]

For the software to be useful it needs also to be able to replicate the loads in a way that is similar to that seen in the reference structure.

Loads can be represented as both point loads and distributed loads over the element. Distributed loads are allowed to vary linearly over the elements length.

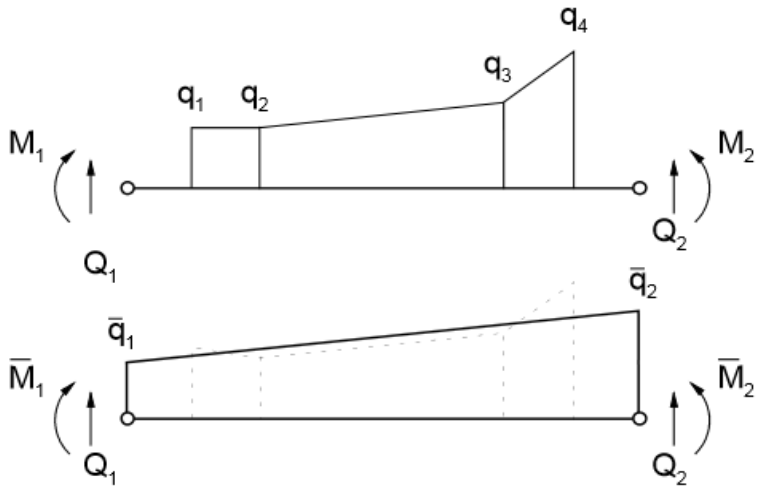

Figure (2.10) Load distribution over the elements in USFOS [27]

For jackets, joint-connections are of special interest, as these get large stress concentrations from the surrounding elements. Structures with joints that have eccentricity have to be taken into consideration when modelling in order to account properly for their geometric configuration. This properties are often of interess if the modeling is done for example to find values for fatigue assessments, but it is not a property that is used in this thesis.

2.4.2 Dynamics in USFOS

USFOS can perform dynamic analysis using the predefined load histories. It dose this analysis numerically based on mass matrix that can be set to either Consistent or Lumped mass matrix. The dynamic response is highly dependent upon the duration and intensity of the load applied. Both of these parameters can be regulated with the "timehistroy" command(see figure 2.11)

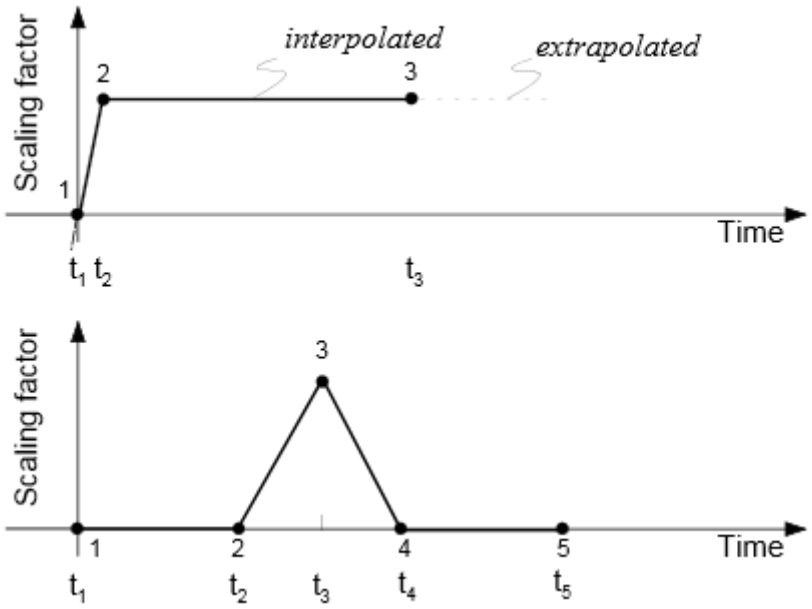

Figure (2.11) graphical representation of defined load histories [27]

The response is calculated using the dampening model that is a form of Rayleigh dampening. Two constants representing dampening, one for high order vibration, and one for low order vibration. The numerical method involved in calculating the response is a modified Newmark method called HHT-α [27]. This method is in essence similar to Newmark method, with the exception of "α".
A factor that is set to produce an artificial dampening effect for high order vibration. This is done to increase the accuracy of the numerical solution.
The integration can be set to either solve as a direct integration, solving the equation set for each time set. Alternatively as predictor –corrector approach, where the acceleration is assumed to be zero and then the dynamic equilibrium is solved through iteration, resulting in a new acceleration value. From this both the next time step of velocity and displacement can be found and updated accordingly.
It is suggested that the predictor- corrector approach might produce the best results when comparing accuracy and economy of CPU consumption. [27] As the thesis would make use of high resolution calculation to find the response, large amounts of resources where required.

2.4.3 Eigen frequencies of model

One of the main concerns with wave slamming is that the loads impact duration is close to the Eigen frequency of the main structure. When the natural frequency of vibration is close to the duration of external loads a phenomena occurs know as resonance. There have been many examples of systems that have broken down due to this phenomena.[34] In addition to extreme cases that causes total failure.

An impulses response can be translated into a general spectrum response based on the shape and length of the impulse. Using this shape, combined with a known response, gives an idea

about the Eigen frequency relative to the length of the impulse. [35]

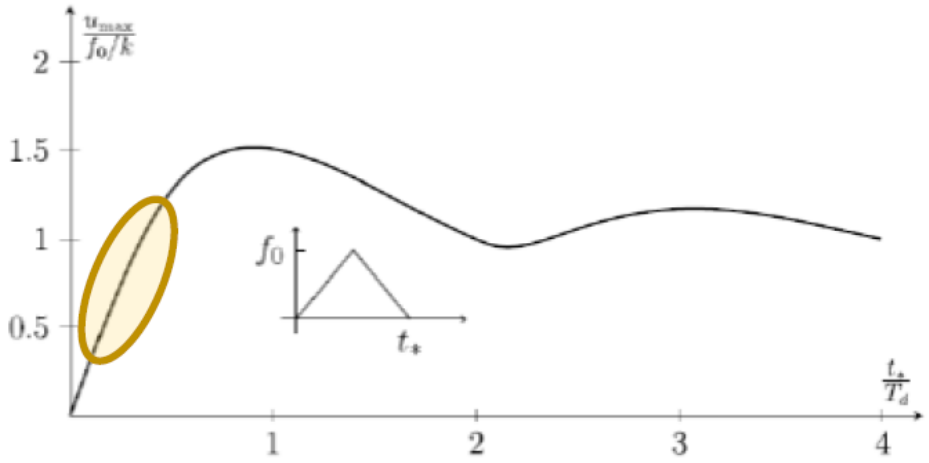

Figure (2.12) Illustration of an example response spectrum for triangular load [35]

Response spectrum are predefined spectrums of expected response based on the shape of impulse introduces, often developed for single degree of freedom systems. Commonly used in simplified earthquake engineering to find loads of small structures.[34]

A response spectrum could be helpful when applied to the model structure as it could give a general idea about the response based on of the Eigen frequency exited compared with the duration of load applied. However since the jacket is a multiple-degree of freedom system it should be considered an inaccurate assumption. Therefore it should not be used as a tool for establishing parameters and/or to form the basis for calculations.

2.4.4 Fourier transform

In signal analysis a time response will in most cases not give much information that is useful. A frequency response spectrum is in many cases better suited as it shows around what frequency the energy in located. USFOS produces a signal in the time domain for each simulation that is run. To better visualize the data from this signal, it has to be transformed.
A transform function moves a function from one domain to another. In this case the transform moves a signal in the time domain, to the frequency domain.
The corresponding frequencies can in some cases be easier to analyze, than the original signal.
The Fourier transform can be described by the formula:

$$F(\omega) = F[f(t)] = \int_{-\infty}^{\infty} f(t)e^{-i\omega t}dt \qquad 2.47$$

The distribution of a response signal, when plotted with respect to frequency will for instance reveal the associated Eigen frequencies. In this new domain it is possible to preform mathematical operations on the response that normally would be unavailable in the time domain.

3. Model

3.1 Modelling in USFOS

Jacket model in USFOS is based on the model used in GWK wave slam experiments. [36] Through papers and reports form the experiment, most of the parameters and properties could be determined, those that were not, had to be assumed.

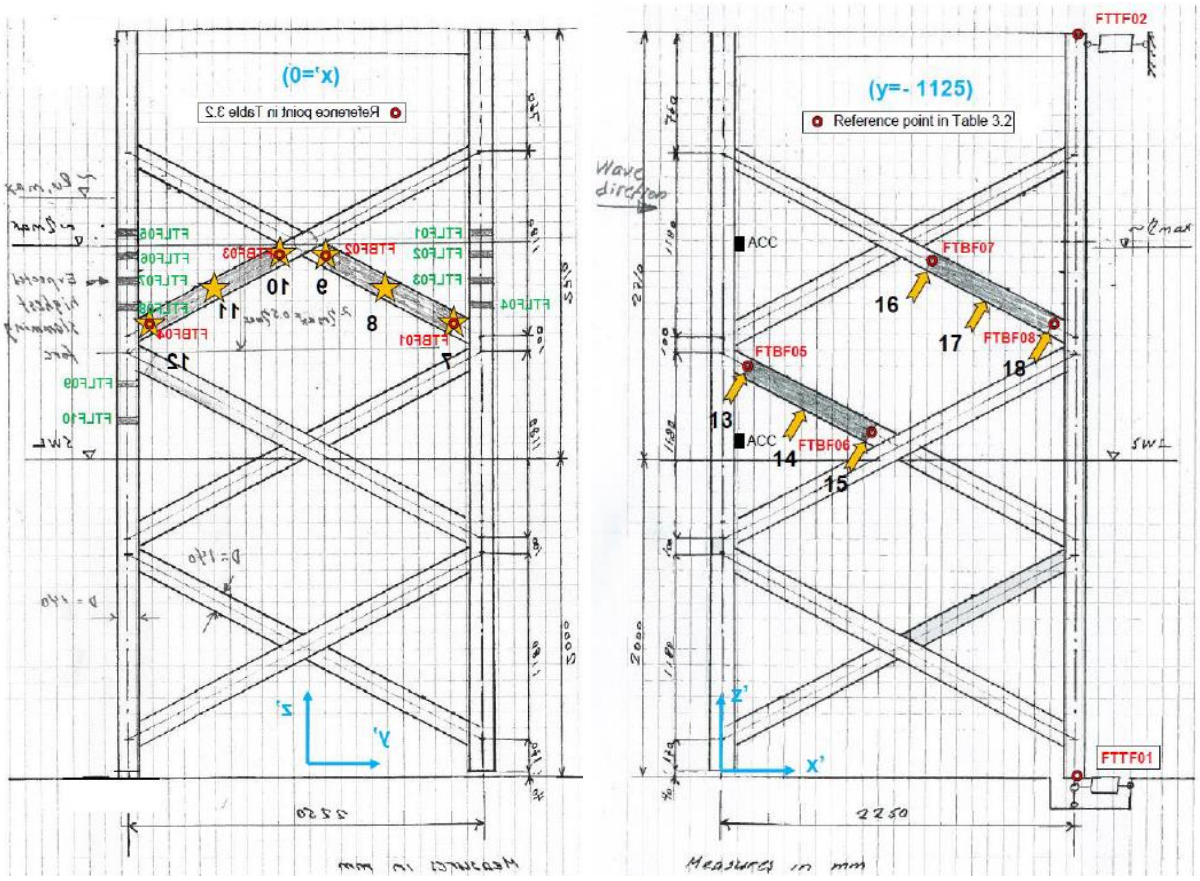

Figure (3.1) front(left) and side(right) sketch of the model, used as a basis for USFOS model[36]

3.1.1 USFOS model file

USFOS uses a simple node-beam system, where coordinates for nodes are given relative to a global origin, and beams are defined as lines between the nodes with both a material and a geometry property that are also defined in the model file numerically. This offers for an easy and flexible system that can be modified quickly to fit the needs of the user.

As USFOS reads the model files line by line, nodes have to be defined before the beams. The correct coordinates where worked out by hand, based on the sketches provided (see Figure 3.1 above), and the structure itself was assumed to be rigid. This rigid property could be set in the boundary code, as a 6 digit code placed at the end of each Node line. *(Sketch is available in full in the attachments)*

Reaction-nodes get their support property from this code as it restricts movement and/or rotation at each node, given that it is activated.

The boundary code represented the number of degrees of freedom available to at the node. In the model Y and Z directions where assumed as directly fastened in the boundary code, while

in the X direction, there where force transduces that also had to be accounted for.

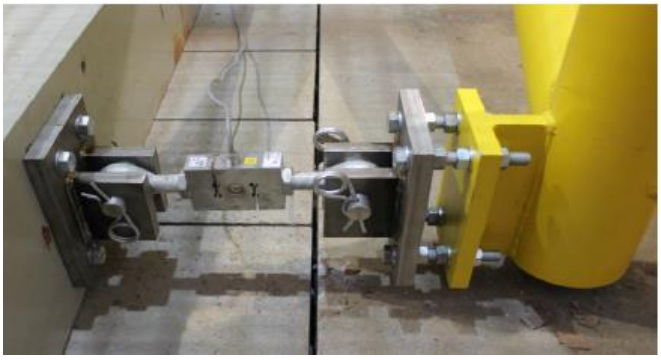

Figure (3.2) "Force Transducer FTTF03" [35]

Force transducers connected between the reaction point and the structure itself are assumed to have a stiffness property and were much lower than that of the structure itself, and therefore expected to play a major role in adjusting the models response to that measured in the experiment.

	A	B	C	D	E	F	G	H
1	'	NODES axis A						
2				'x= 0				
3			'id	x	y	z	Boundary code	
4		NODE	1	0	0	-1.96	0 0 0 1 1 1	
5		NODE	2	0	2.25	-1.96	0 0 0 1 1 1	
6		NODE	3	0	0	-1.79	0 0 0 1 1 1	
7		NODE	4	0	2.25	-1.79	0 0 0 1 1 1	
8		NODE	5	0	1.125	-1.2	0 0 0 1 1 1	
9		NODE	6	0	0	-0.61	0 0 0 1 1 1	
10		NODE	7	0	2.25	-0.61	0 0 0 1 1 1	
11		NODE	8	0	0	-0.51	0 0 0 1 1 1	
12		NODE	801	0	0	-0.06	0 0 0 1 1 1	
13		NODE	9	0	2.25	-0.51	0 0 0 1 1 1	
14		NODE	10	0	1.125	0.08	0 0 0 1 1 1	
15		NODE	11	0	0	0.67	0 0 0 1 1 1	
16		NODE	111	0	0	0.53	0 0 0 1 1 1	
17		NODE	1111	0.344	0	0.489	0 0 0 1 1 1	
18		NODE	112	0	0	0.53	0 0 0 1 1 1	
19		NODE	12	0	2.25	0.67	0 0 0 1 1 1	
20		NODE	13	0	0	0.77	0 0 0 1 1 1	
21		NODE	132	0	0	0.91	0 0 0 1 1 1	
22		NODE	14	0	2.25	0.77	0 0 0 1 1 1	
23		NODE	143	0.344	2.25	0.95	0 0 0 1 1 1	
24		NODE	142	0	2.25	0.91	0 0 0 1 1 1	
25		NODE	15	0	1.125	1.36	0 0 0 1 1 1	

Figure (3.3) Illustration of the coordinates from USFOS in excel

Most of the element geometry used in the model are tubular cross-sections, USOFS uses a command called "pipe" to define this type of section.

The cross-sections had in general diameters of 140 millimeters and pipe wall thickness at 5 millimeters whereas the center pipe has a different dimensions. The top square consists of I-beam profiles with a height of 140 millimeters and flange width of 140 millimeters.

	A	B	C	D	E	F	G	H	I
1	'	BEAMS in ax	'id	N1	N2	Materialgeometry			
2									
3		BEAM			1	1	3	1	1
4		BEAM			2	2	4	1	1
5		BEAM			3	3	5	1	1
6		BEAM			4	4	5	1	1
7		BEAM			5	5	6	1	1
8		BEAM			6	5	7	1	1
9		BEAM			7	3	6	1	1
10		BEAM			8	4	7	1	1
11		BEAM			9	6	8	1	1
12		BEAM			10	7	9	1	1
13		BEAM			11	8	10	1	1
14		BEAM			12	9	10	1	1
15		BEAM			13	10	11	1	1
16		BEAM			14	10	12	1	1

Figure (3.4) Illustration of the Beam element from USFOS in excel

The geometries and material properties are determined by lines of code called material models, each model is given a unique numerical value that is then related to the elements that should have this property (See Table (3.2) at the end of section 3.1.2).

The resulting Finite element model:

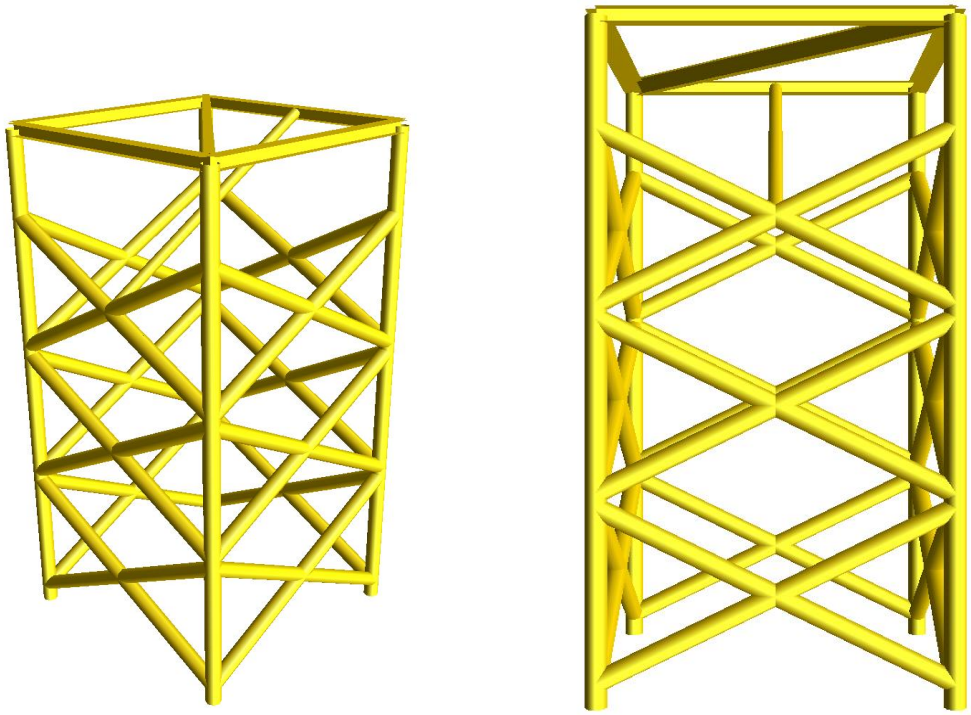

Figure (3.5) A side view of the jacekt model from USFOS

To remove any buoyancy effects the model is filled with water up to the still water level. Using an USFOS command called INTFLUID will assume the pile elements to be filled with fluid based on a predefined time history. The fluid has to be given a correct density to represent water.

3.1.1.1 Instrumentation

Certain parts of the model were of different materials and cross-sections since some parts of the structural sections where replaced by instruments. These have to be accounted for in order for the model to have the correct response in simulation and be a computational representation of the actual structure. Apart from instruments there were also cables attracted to the model, and these are assumed to be averagely distributed along the top beams and down towards the instrumentation parts. To account for the cables, the density of the material that where relevant

got their density increased by:

$$Densicy_{Cable} = 500 \frac{N}{m^3} \quad 3.1$$

As the geometry of the tubular sections is predefined the resulting load per meter can be calculated as

$$A_{pipe} * Densicy_{Cable} = 0.00431m^2 * 500 \frac{N}{m^3} = 2.15875 \frac{N}{m} \quad 3.2$$

This number is relative to the average distributed mass of the model quite small (see Figure 3.6)

An assumptions is made about the connection between the structural parts as well, the connections are assumed to be rigid, and the nodes are therefore non-rotational. This causes the model to be calculated much stiffer than what is actually the case. This is unlikely to be the case in the actual structure. As a result the Young's modulus of some of the materials may have to be reduced to provide a realistic representation of the model in the experiments. (See section 3.2.2)

The initial simulation material parameters are chosen from the parameters stated in [35].

The Model file is available in full in the attachments

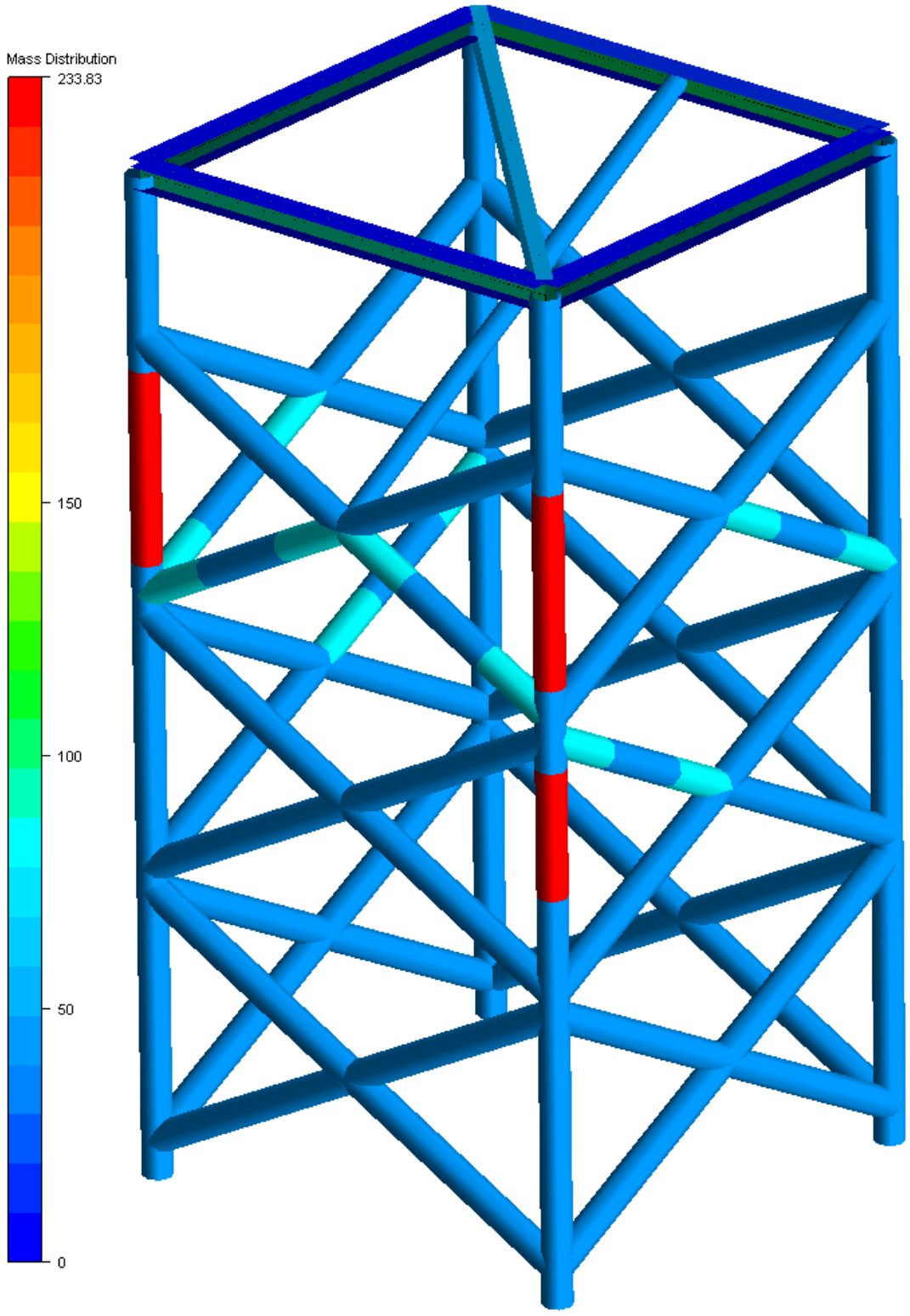

Figure (3.6) Illustration of the mass distribution of the model

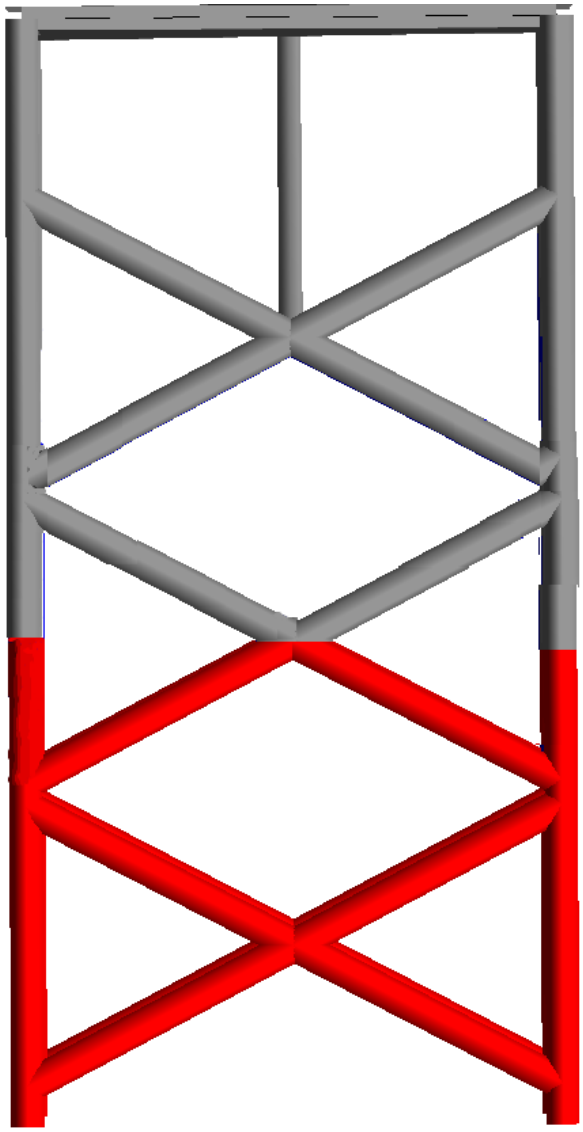

Figure (3.7) Illustration of the internal fluid distirbution in the model

3.1.2 Control file

To successfully run an analysis in USFOS two files are required, a model file as discussed above, and a control file. The control file regulates the type of analysis, its properties, resolution and conditions applied during the analysis. In this file it is possible to regulate many parameters, such as wave height, wave period, surface elevation, dampening and hydrodynamic coefficients among other things.

Many of these parameters, like gravity are kept unchanged during the analysis, some values had to be changed to different values depending on the simulation run. In this thesis these values have been named “Simulation parameters” and will be presented as a table (Figure (3.7)).

Wave height, depth and wave period could be regulated using the same command in the control file called “Wavedata”, while duration of slam was regulated using a “timehistory” command. (See figure 2.11) This command is also used when describing the impulse shape of the slam loads.

As a way to provide overview of what parameters currently are being used, they will be: Presented in a table as show in Figure (3.7)

SIMULATION PARAMETERS		
H- wave height	**1.9**	**m**
d- water depth	**2.275**	**m**
P- wave period	**5**	**s**
Slam duration	**0.075**	**s**

Table (3.1) Illustrative table of the Simulation parameters

The file provides the user good overview over the analysis settings and allows for change and adaptation if needed. *The Control file is available in full in the attachments*

TABLE MATERIAL MODEL:

Material models		
ST-37		
-Density	Kg/m^3	7850
-Young's	N/m	2.10E+11
Aluminum		
-Density	Kg/m^3	3380
-Young's	N/m	7.00E+10
Instruments		
-Density	Kg/m^3	12700
-Young's	N/m	2.10E+11
ST-37 (with cable)		
-Density	Kg/m^3	8350
-Young's	N/m	2.10E+11
Internal fluid		
-Density	Kg/m^3	1025
-Young's		N/A
Force transducers(1&3)		
-density	Kg/m^3	N/A
- Young's	N/m	1.00E+07
Force transducers(2&4)		
-density	Kg/m^3	N/A
- Young's	N/m	1.25E+07

Table (3.2) Illustrative table of the material parameters

3.1.3 Filter

The generated response data is expected to need filtering the program Matlab has functions that quickly can generate a filter based on the user specifications, the specification requirements can vary based on what filter function is used but the one used.
In this analysis a cut-off frequency, order of magnitude of the filter and filter direction (low-pass/high-pass) was required.
A low pass filter would suppress/reduce the amplitude of signals that had a frequency above the cut-off frequency, while a high-pass does the exactly opposite.

Illustrative examples of filters used:

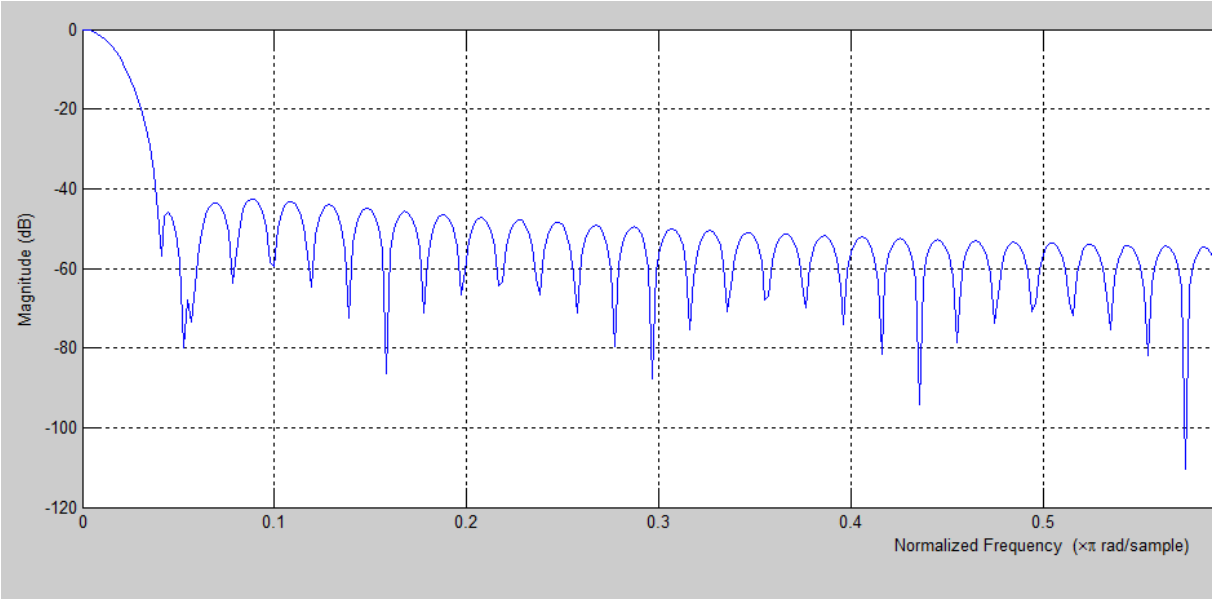

Figure (3.8) Illustrative plot of low pass filter

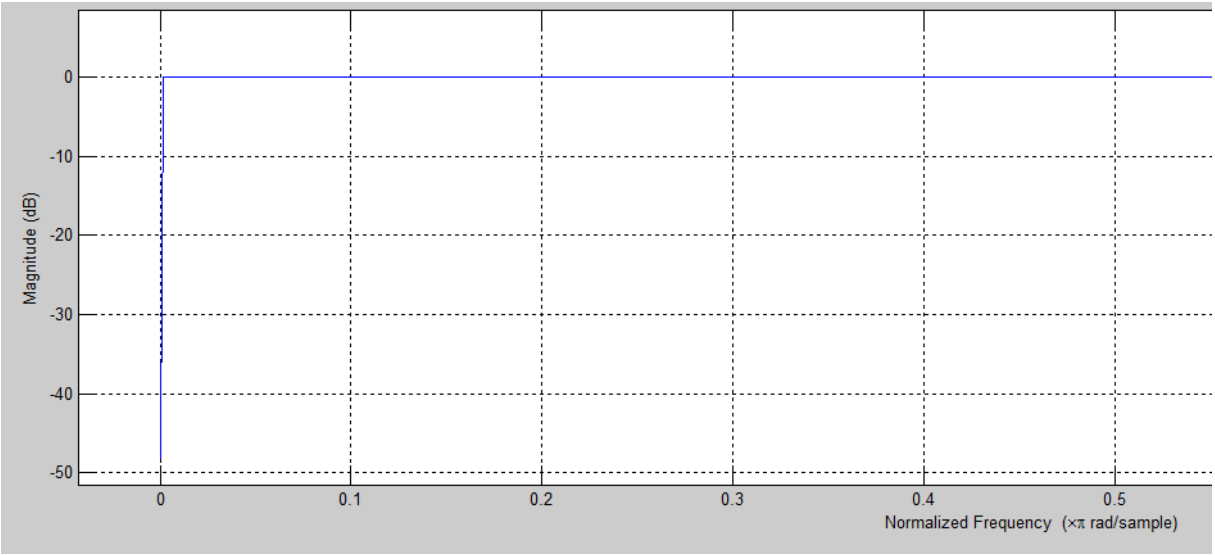

Figure (3.9) Illustrative plot of high pass filter

3.2 Verification of Structure in USFOS

To be able to use USFOS strengths, as a finite element modeling tool it is first needed to verify it the USFOS model using measured data from the large wave fume.
There are several aspects that require verification. A simple way of verifying is by submitting the model to known conditions and see what USFOS calculates the results to be, and then compare these results to those measured in under the same conditions.

Calibration hammer tests were performed during the experiments in Germany, the structure where subjected to a known impulse load introduced by a special hammer with force gauges. By comparing both the impulse force of the hammer and the response measured in the reaction points gives a lot of information about the properties of the structure. It is also very useful for calibration of the computer modeling. In USFOS such data can be used to find and compare the similarities in Eigen period and dampening between the experimental structure and the USFOS model.

It was also preformed several breaking wave measurements. Some of this data, if filtered correctly can be used to find the quasi-static response.
The comparison of quasi-static load of the model and that measured in the experiment can reveal the load ramp up, that would indirectly indicate the passing wave-steepness. The duration of the load would give a good clue about the passing wave period.
It is important to determine what and how large effects the water level has on the dynamic output, as it may be a source of inaccuracy when comparing to the experimental data.

3.2.1 Data from hammer experiment

The data collected from the hammer tests are used to calibrate the model so it behaves in a way close too or the same as the structure in the experiment. To be able to do a simulation with comparable values, the data used first needs to be reviewed.

3.2.1.1 Hammer impulse

The hammer signal was recorded using a special hammer that had force measurement sensors placed into it. The signal was collected at a rate of 10 000 Hz. The point where the impact was introduced was at what is equal to the location of Node 501(see Figure (3.12)).

The impulse force signal could be plotted as a function over time:

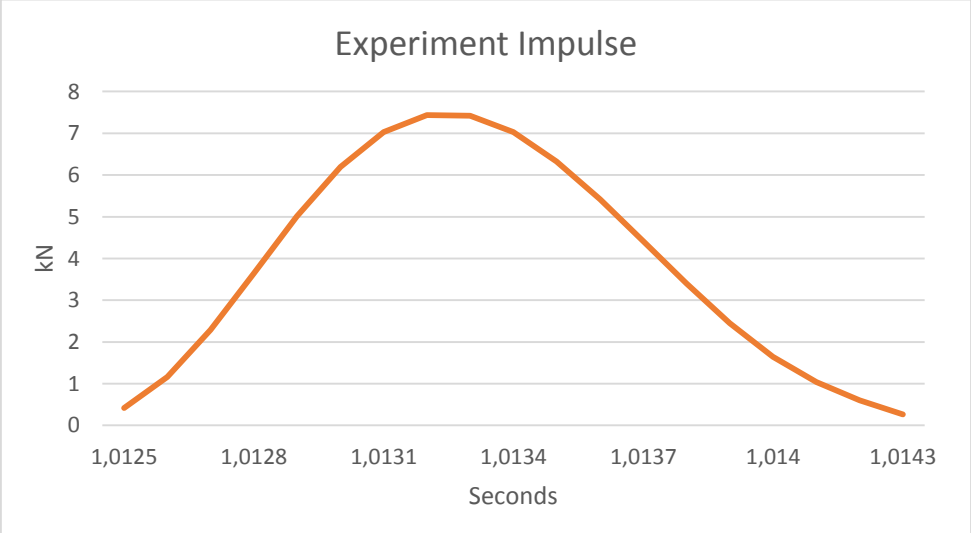

Figure (3.10) plot of recorded impulse

The maximum impulse can be established from the plot as 7.4 kN.
It can also be observed that the impulse is distributed in a shape close to a triangular shape.
The duration of the impulse is around 2 milliseconds. This impulse forms the basis for the load impulse used in USFOS.

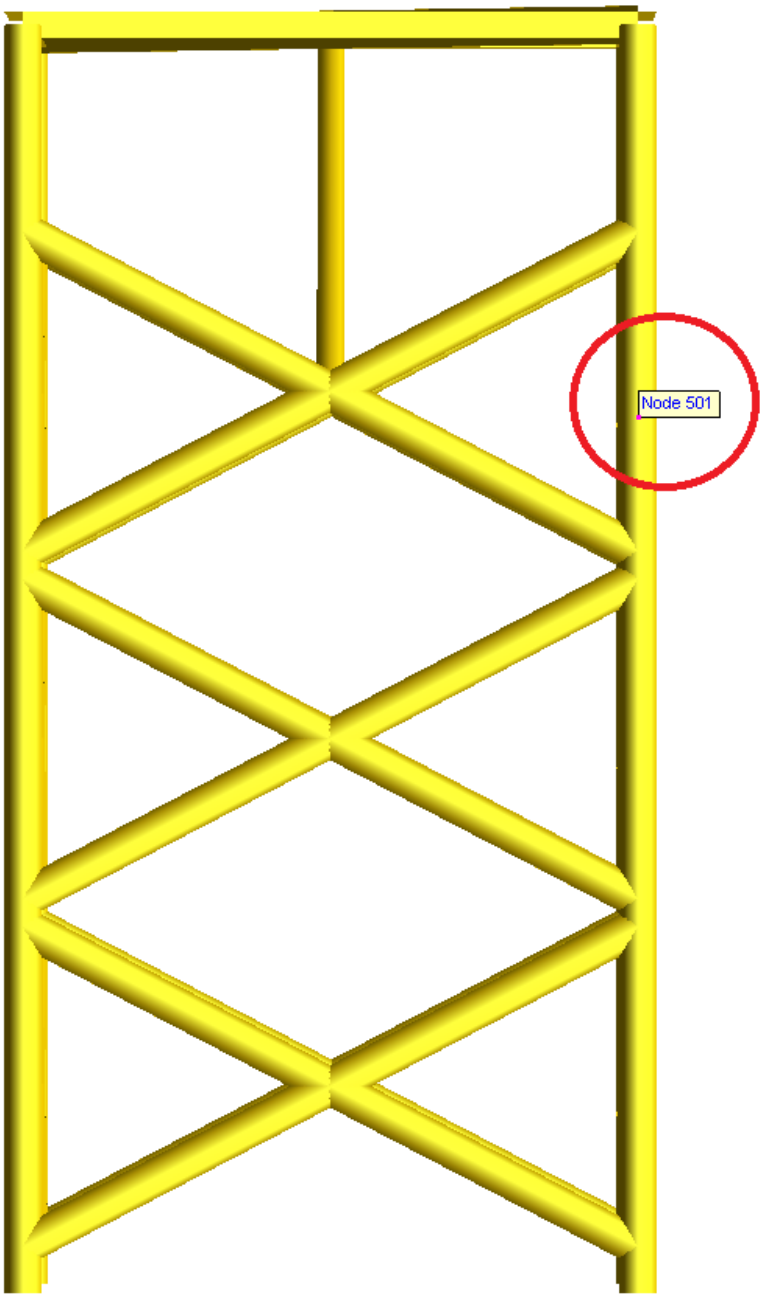

Figure (3.11) location of hammer impact point

3.2.1.2 Reactions

Reactions was recorded with the same frequency as the impulse at 10 000 Hz. The reaction forces was recorded at four force transducers.
The sum of these represents the total x-directional response of the experimental structure.
A problem with the loads was pointed out in [36]; the excitations of the top transducers are smaller than that of the bottom ones. This is problematic as FTTF02 and FTTF04 are placed closer to the impulse location, and therefore would be expected to have larger excitation than that of FTTF01 and FTTF03. (See Figure 3.12)
This problem should be kept in mind as it will cause the response in section 3.222to be a bit off.

All the data collected in the hammer test was collected while there was water in the wave fume, the water depth was 2 meter.

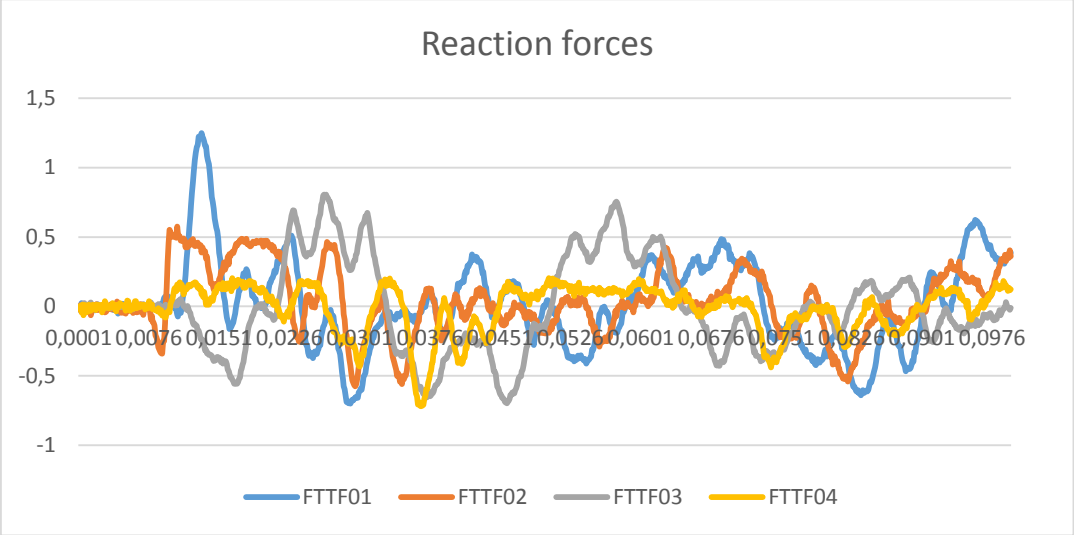

Figure (3.12) Reaction forces from the recorded hammer impulse

3.2.2 Hammer response comparison

USFOS is capable of simulating loads as impulses based using the "time history" command (see Figure (2.11)), and the impulses can be induced by both as beam loads (N/m) and node loads (N).
Using the "node load" option and imposing a load with same intensity and duration as a measured with a hammer, the reaction forces of the model can be compared with those measured on the jacket-structure. The load should be imposed at the exact same location in the geometry of the model as the structure, to avoid discrepancies.

In USFOS the Node 501 is defined with coordinates at the location as the hammer load was delivered to the experiment structure.
On this node the load impulse is introduced, and its location is marked in Figure (3.12) (previous page)

From the review of the hammer data (section 3.2.1), the measured the imposed load is 7.4 kN, and can be assumed to have a close to triangular load distribution. The duration is set based on experiment data to be 2 milliseconds (or 0.002 seconds). (See Figure (3.16))

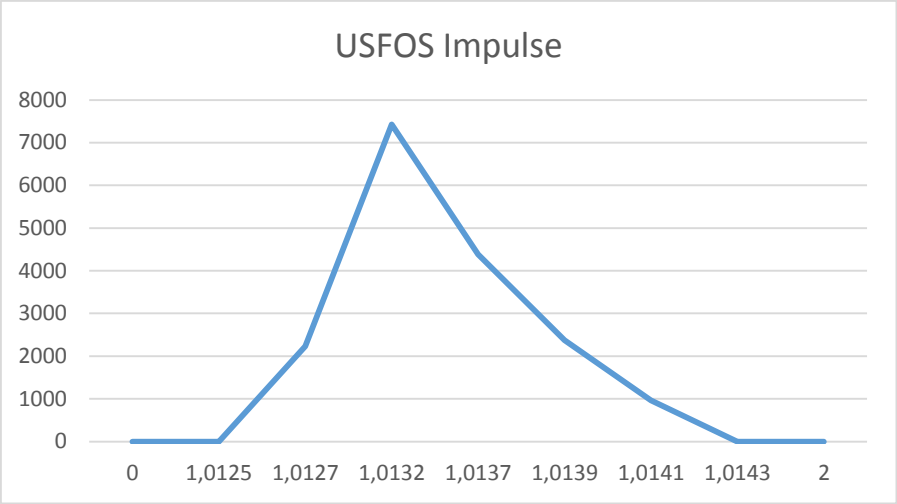

Figure (3.13) Impulse load assumed in USFOS

Using the information provided, an impulse that can be used in USFOS has been constructed. This impulse has about the same values can be the one observed in the experiment, and can be imported into USFOS as a "timehistory".

Since the data in section 3.2.1 was recorded while there was water in the tank, this option was also implemented in USFOS using the "wavedata" command, where the wave height was set to zero, to avoid and quasi-static effects from the waves.

The impulse was then introduced to the model using the properties that was has been provided. The structural data used in the initial simulation based on material properties from [35]

CONTROL FILE	**Comment:**	**Value:**
-Calculation resolution		0.0001
Simulation duration		
-Static	end time	1
-Dynamic	end time	2.238
Hydro dynamics		
-Water	depth :	2
-Wave		0
Imposed loads		
-Impulse	Node 501	7430
Dampening		
-25Hz	%	0.015
-125Hz	%	0.015
Structural data		
Geometry models		**unchanged**
Material models		
ST-37		
-Density	Kg/m^3	7850
-Young's	N/m	2.10E+11
Aluminum		

-Density	Kg/m^3	3380
-Young's	N/m	3.00E+10
Instruments		
-Density	Kg/m^3	12700
-Young's	N/m	2.10E+11
ST-37 (with cable)		
-Density	Kg/m^3	8350
-Young's	N/m	2.10E+11
Internal fluid		
-Density	Kg/m^3	1025
-Young's		N/A
Force transducers(1&3)		
-density	Kg/m^3	N/A
- Young's	N/m	1.00E+07
Force transducers(2&4)		
-density	Kg/m^3	N/A
- Young's	N/m	1.25E+07

Table (3.3) Material properties used in simulation

The calculation resolution is set to be high, by defining the simulation increment to be small. Size of the increment makes each load set the same length as the samples of the experiment data. To have the same experiment data sample length and the load step length simplifies some aspects of the comparison, in addition a resolution needs to be able to give a detailed plot of the data.
Using values prescribed in the table above, the resulting model simulation can be is presented in two graphs, one describing the models and structure vibrations in time domain, the other showing the frequency response spectrum of each of the signals.

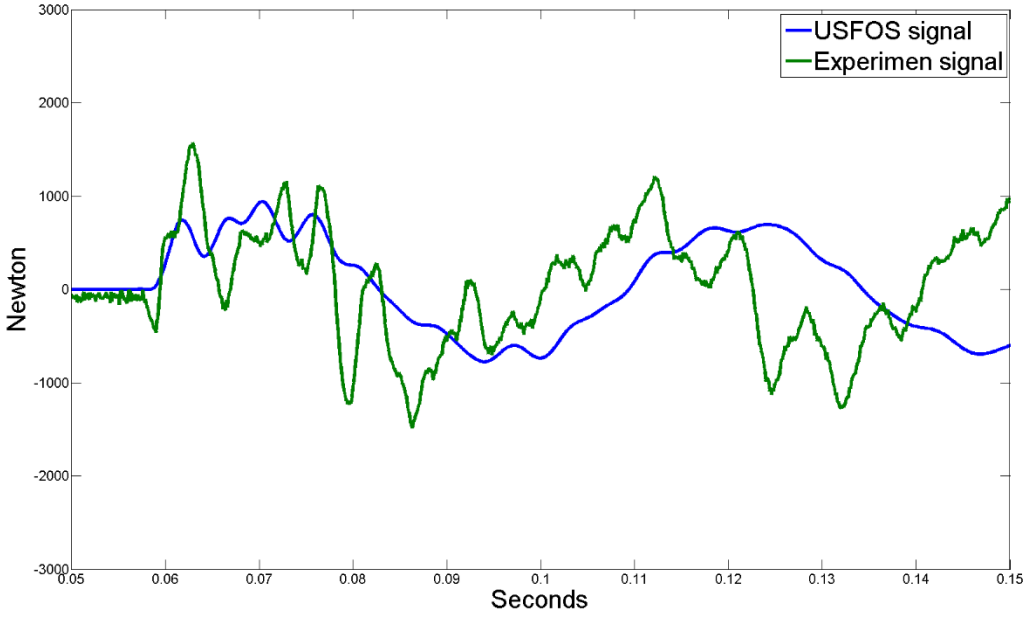

Figure (3.14) comparison of experiment and USFOS signals using properties in Table (3.3)

The graph shows reaction forces load extracted from USFOS and the structure response based on the sum of all forces in from the Figure (3.15). Both signals are have much smaller amplitudes than the impulse load they have been subjected too. When the data extracted from USFOS is plotted together with the experiment data, it is clear to see that the model is inaccurate. Both the data from the experiment and the simulated data can be further analyzed by transforming them to frequency spectrums. The transformation is done using Matlab's Fast Fourier transform function.

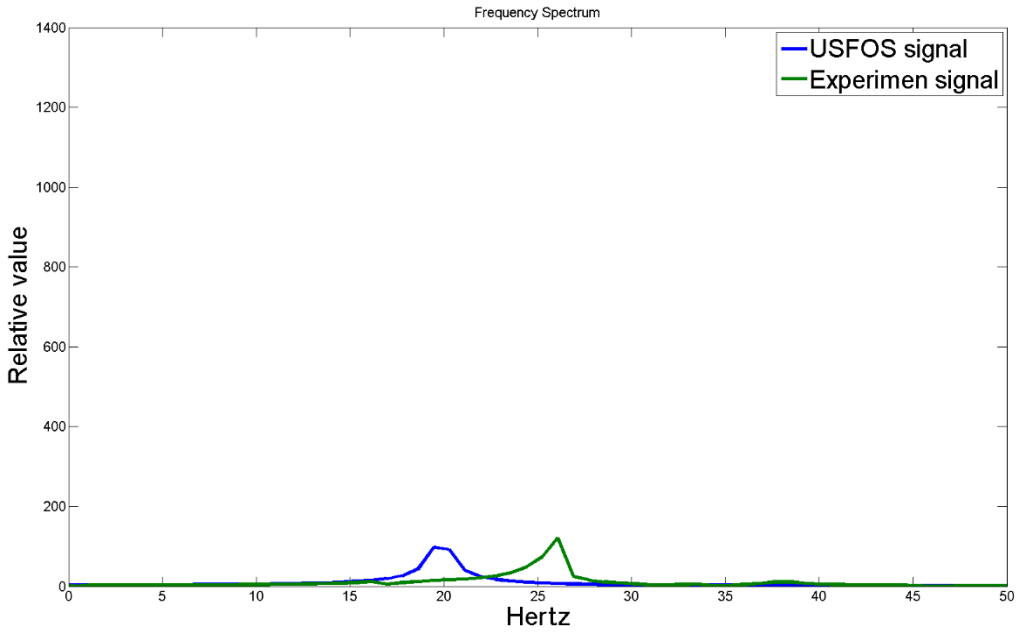

Figure (3.15) Frequency spectrum of signal Figure 3.14

The frequency transform reveals that the USFOS model is too soft to be an accurate representation of the structure used in the experiment. As the component with the greatest impact on the frequency spectrum, the force transduces are likely to have been modelled to soft. A closer inspection of the Figure (3.15) it is possible to see that the rest of the USFOS spectrum lacks the small irregularities observed in the experiment structure's spectrum.
The model signal lacks these small peaks, could be an indication of the model having to high a stiffness when disregarding the main vibration frequency.

This might be due to the nature of the USFOS as a modelling software, since nodes have been modeled as fastened they may also be unable to rotate.

Regardless of the cause, these inaccuracies have to be addressed in order to get results that are usable for comparison later. A way to negate the problem could be by reducing the general stiffness of all materials used while tuning the stiffness for the transducers slightly up.
New material values are therefore chosen based on this assumption.
The several simulation is done with values taking into account frequency spectra distribution. When attempting to match the models with the structures.

After several iterations with different parameters, a strong improvement in the accuracy is seen by using the material parameters as follows:

CONTROL FILE	**CHANGE**	**Comment:**	**Value:**
-Calculation resolution	**No**		0.0001
Simulation duration	**No**		
-Static		end time	1
-Dynamic		end time	2.238
Hydro dynamics	**No**		
-Water		depth :	2
-Wave			0
Imposed loads	**No**		
-Impulse		Node 501	7430
Dampening	**YES**		
-25Hz		%	0.0175
-125Hz		%	0.0175
Structural data	**No**		
Geometry models			**unchanged**
Material models	**YES**		
ST-37			
-Density		Kg/m^3	7850
-Young's		N/m	5.15E+10
Aluminum			
-Density		Kg/m^3	3380
-Young's		N/m	3.50E+10
Instruments			
-Density		Kg/m^3	12700
-Young's		N/m	5.15E+10
ST-37 (with cable)			
-Density		Kg/m^3	8350
-Young's		N/m	5.15E+10
Internal fluid			
-Density		Kg/m^3	1025
-Young's			N/A
Force transducers(1&3)			
-density		Kg/m^3	N/A
- Young's		N/m	1.4575E+09
Force transducers(2&4)			
-density		Kg/m^3	N/A
- Young's		N/m	1.4600E+09

Table (3.4) Adjusted material properties

The signal that is extracted form USFOS using these parameters have a shape and form very close to that of the experiment signal. This is also reflected in the frequency response spectrums.

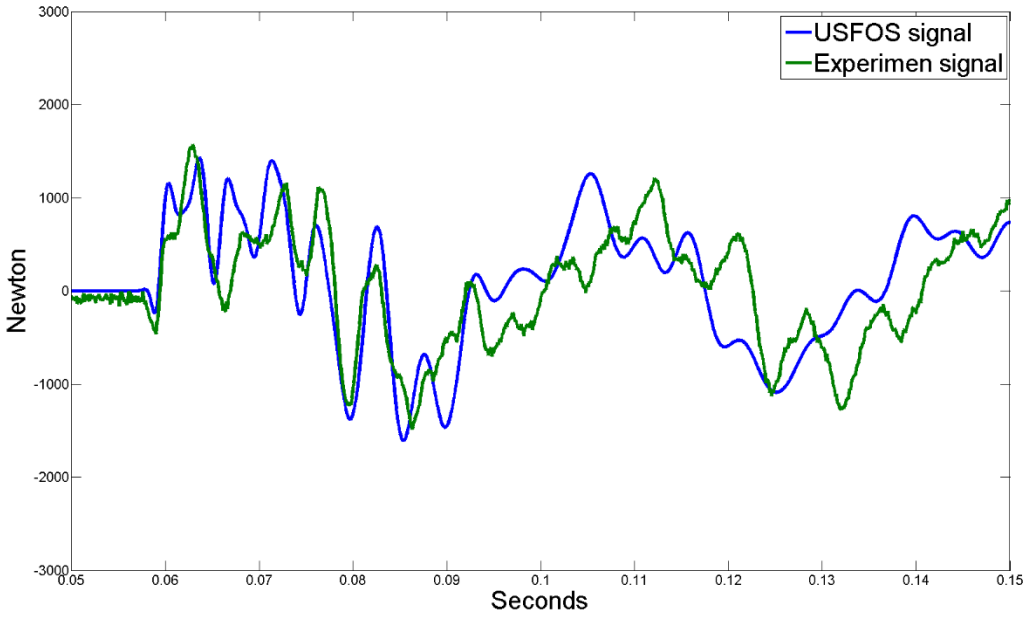

Figure (3.16) Comparison of experiment and USFOS response

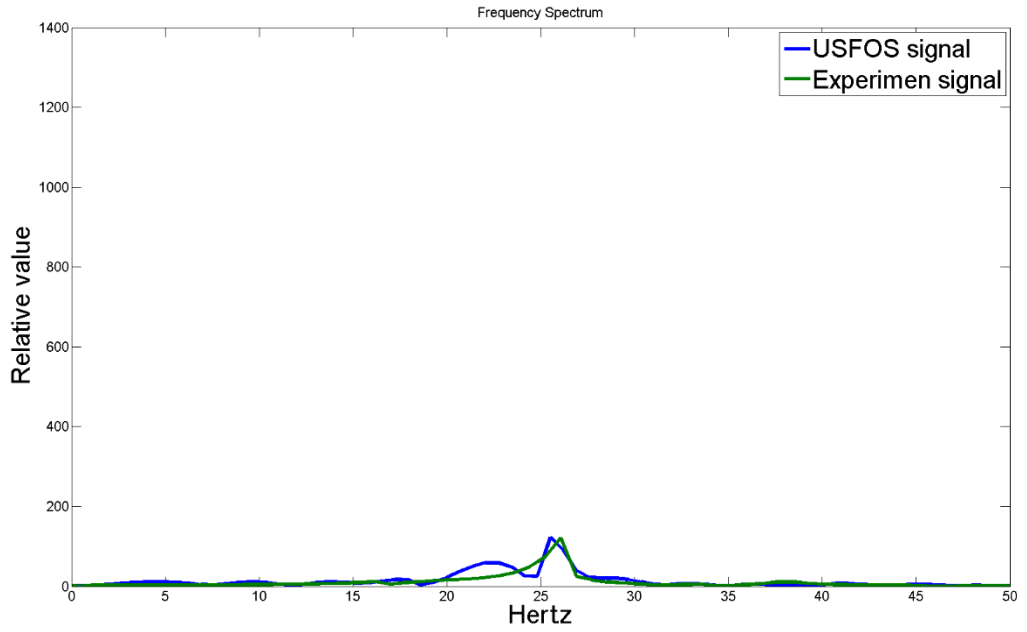

Figure (3.17) Frequency spectrum of signals in Figure (3.16)

As is seen from Figure 3.17, the models response is similar to that measured in the experiment data. In the frequency distribution there is both a strong degree of accuracy in the largest peaks of the spectrum, and a similar shape in the irregularities. Ideally these minor peaks should also be similar, however to fit them proved difficult, and therefore have not been further pursued.

Based on the visual observation of the response signal it is can be assumed that the model and the structure now behaves in a similar manner. The adjustments done are assumed to be sufficiently correcting for any misrepresentations of properties in the model.

3.2.3 Wave comparison

To correctly estimate the dynamic response, a wave has to be established that is the best possible fit to the wave observed wave. The observed wave can be established through visual inspection.

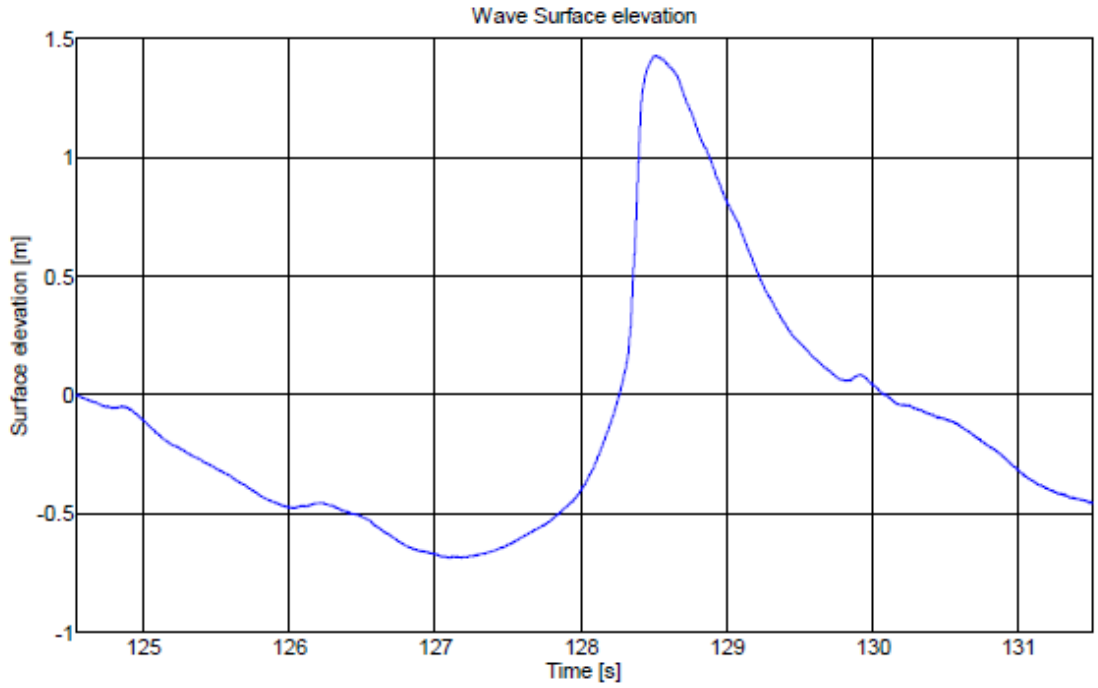

Figure (3.18) Surface elevation of breaking wave [36]
Based on a visual inspection:

$$H = 1.9\ m \tag{3.1}$$

$$Period = 5.0\ s \tag{3.2}$$

In the of the experiment the total response force was measured to be as shown in Figure 3.25 The total response force can be separated thought correct filtering into two signals, one representing the quasi-static load, and one representing the slam load.

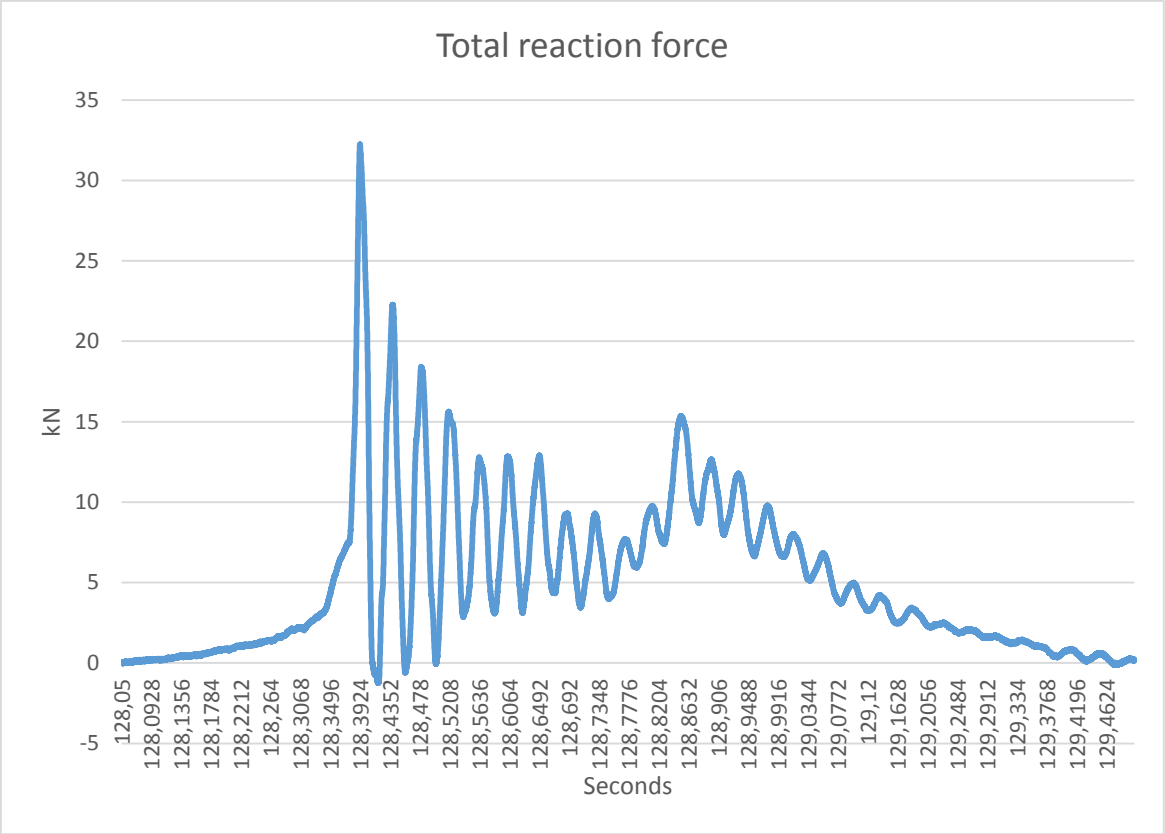

Figure (3.19) Total response force for a breaking wave

Separating the forces using filtering of the response signal, the quasi-static was established to be:

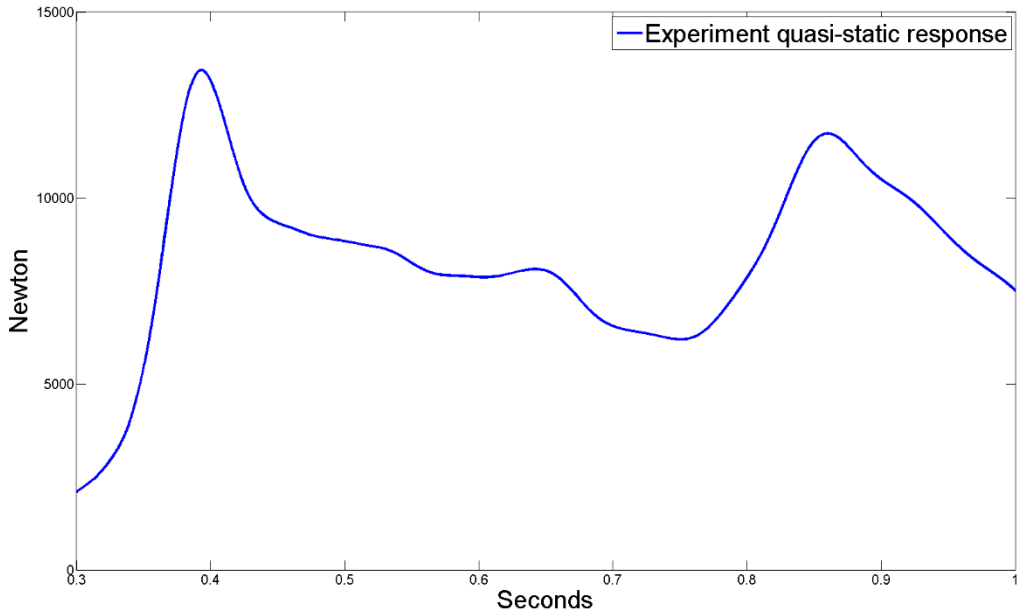

Figure (3.20) quasi-static from the total response (see Figure 3.19)

The wave described in the experiments data have a very steep shape (Figure 3.24), as USFOS has don't allow for simulation of waves that are outside the applicability chart(Figure 2.2) such as those that are in the breaking wave region are, this may be problematic.

There may also be problems from inaccurate representation of the passing wave. If the wave is too long compared to what is done in the experiment, the quasi static load will be overestimated, and the amount of the structure that is submerged will be too large, and that can affect the dynamic response. Another point is that a shallow water wave is steeper than that of a deep water, the slamming load can be applied much closer to the maximum quasi-static response giving a higher total max load. To observe the extent of the effects mentioned above, waves of different wave heights has to be simulated.

While USFOS calculates ideal conditions with an ideal wave shape. In reality most waves will differ from this ideal shape. In addition since USFOS does not allow for close to/ breaking waves in their simulation, an alternative method is required.

The first attempt at generating similar quasi-static loads used Stokes theory, USFOS was not able to perform the based on the current parameters. This was because the water depth relative to the period placed the wave in shallow water region. (See Figure 2.2) The theory applied was changed to Stream. The stream theory was not able to run a simulation at the estimated height of H= 1.9m.

It could however preform the simulation at H = 1.7m:

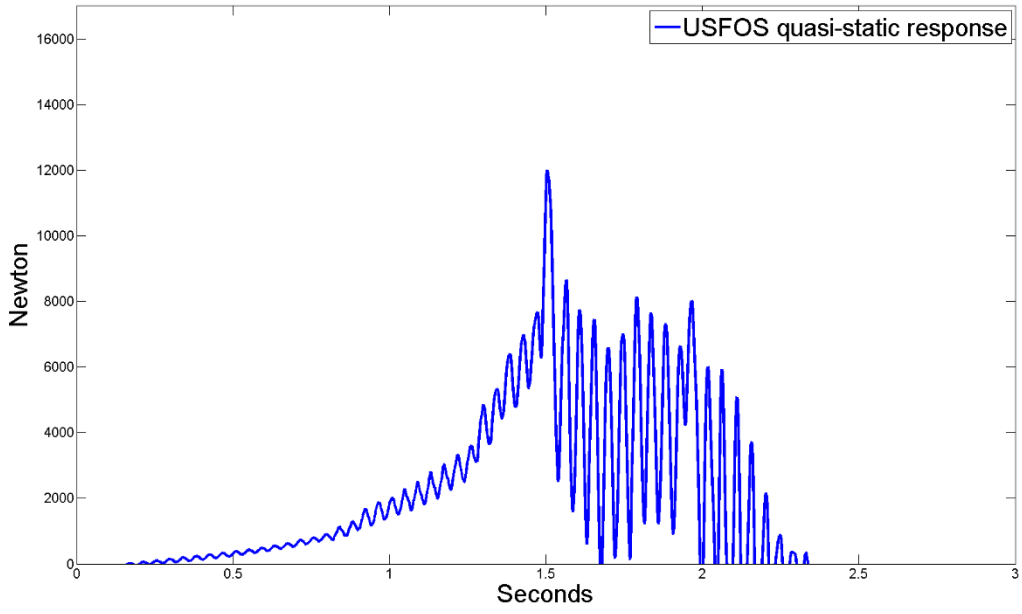

Figure (3.21) Stream function 1.7 Meters at 2 meter depth

As can be observed from Figure (3.21) the simulation shows a large degree of variation of the load intensity, so much that it should not be used. If a load of this shape was used in conjunction with a slam impulse, it would be difficult to separate the response produced from the impulse to that of the quasi-static load.

The wave is still in the breaking area of Figure (2.2), by reducing the wave height the wave can be moved into the region of non-breaking waves.

By reducing the wave height from 1.7 which is outside the breaking criteria down to 1.5 it could be that this variation is reduced or removed. Using Figure 2.2 in combination with the calculated values for different values of depth, a new values is found as:

$$Depth\ 1.7m: \quad \frac{H}{gT^2} = \frac{1.7}{9.81*5^2} = 8.15 * 10^{-3} \qquad 3.3$$

$$Depth\ 1.5m: \quad \frac{H}{gT^2} = \frac{1.5}{9.81*5^2} = 6.11 * 10^{-3} \qquad 3.4$$

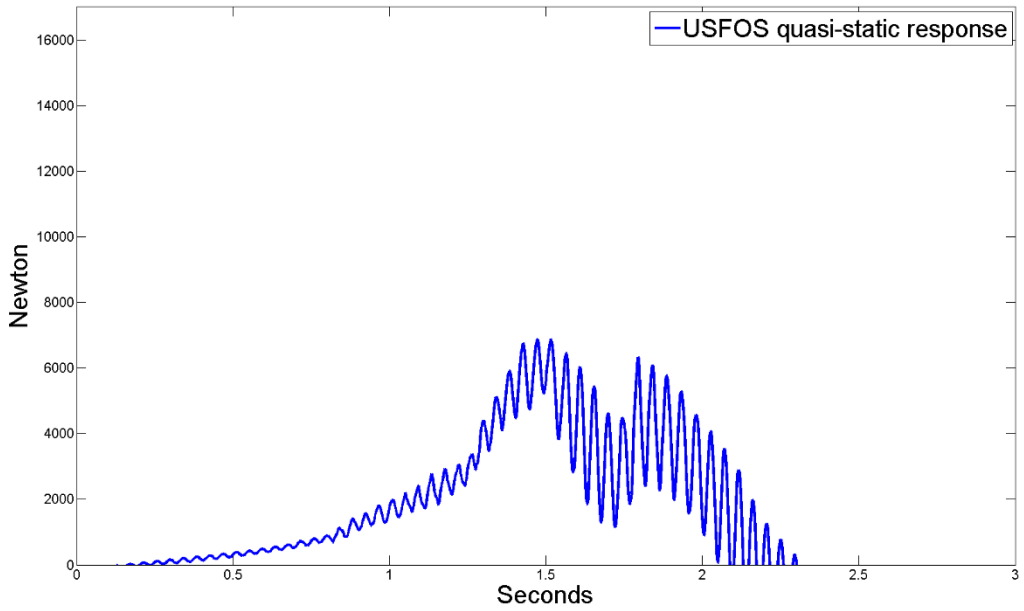

Figure (3.22) Stream function 1.5 meter at 2 meter depth

The wave of 1.5 meters provides too little quasi-static load to applicable, and the tendency of variating load is still present.
The Stokes theory is thought to provide a much smoother load distribution (see Figure 2.1), the Stream theory will therefore no longer be pursued.

According to Figure 2.2, the depth has to be increased be able to match the wave height and given period for stokes theory.
In the first simulation the depth was set at the same value as in the original experiment at:

$$Depth = 2.00\ m \qquad 3.5$$

USFOS was unable to generate the wave at depths as low as this for Stokes theory. Through trial and error the new value is set at:

$$Depth = 2.75\ m \qquad 3.6$$

Running a simulation gave the response signal:

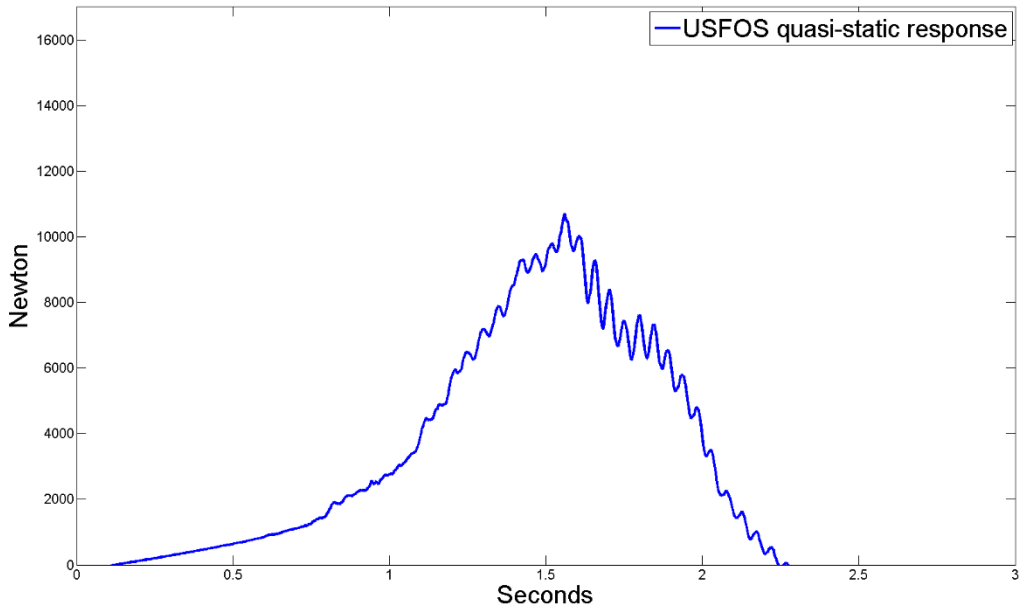

Figure (3.23) Stokes theory wave 1.9 meters at depth 2.75 meters

And plotted with the meassured experiment values:

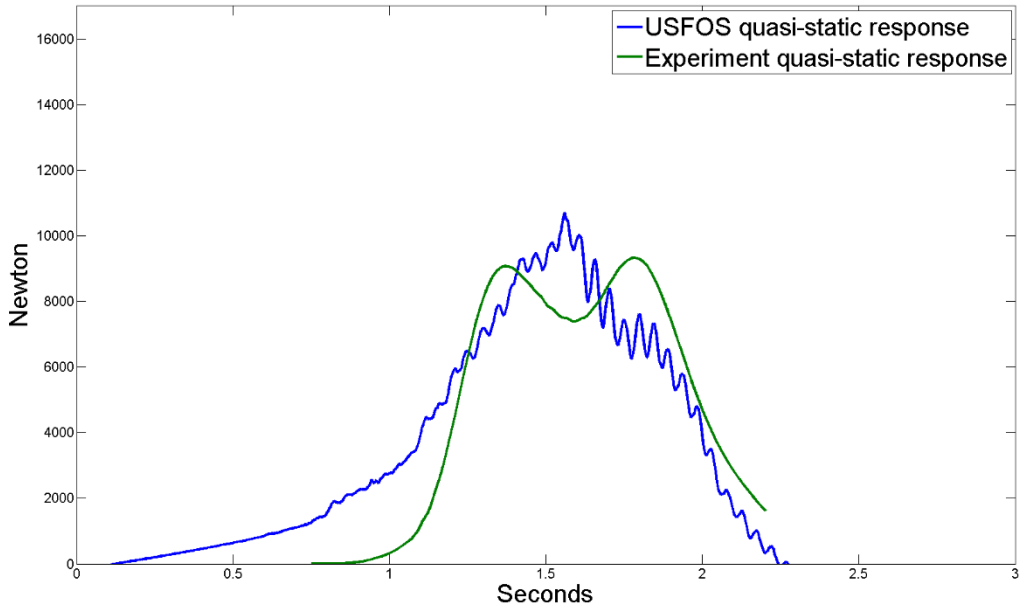

Figure (3.24) Best fitted load signal in USFOS (see Figure 3.23) and experiment load.

The behavior that diverges from that observed in the experiment are unfavorable.
However from around the first peak of the experiment signal it is seen that they have around the same duration and nearly the same value. Since it is at this from this point the slamming load will be have effects, the error prior to this isn't necessarily that important. In addition a lot of the quasi static effects are filtered out it, so it may be possible to use this a wave as a quasi-static component in a wave slam simulation without too creating a large error.
The Figure 3.29 also gives an indication of the magnitude of accuracy lost due to the quasi-static wave load.
One inaccuracy that can be observed is the fluctuation in load intensity. The Stokes wave shows, as the Stream theory waves that was first applied (See Figure 3.21, Figure 3.22), variation in the load applied to the structure. Although the fluctuation is less intense and it is uncertain to what degree this inaccuracy will cause.
The wave used in Figure 3.24 is assumed to be the best fit and will be applied throughout the rest of the simulations where wave loads are to be applied.

4. Responses due to slam loads

As it is assumed that the model now behaves in a similar manner as the structure, it should provide a similar result under similar conditions. A wave has been developed in section 3.2.3 that gives loads close to those observed in the experiment. Data from a slamming event provided from [36] is available.
Imposed on the structure, the response can be reviewed ad should be similar to the response seen by the experiment structure. If a large degree of discrepancy is observed, some additional tuning of the structure may be required.

4.1 Slam load from experiment

The data provided from the experiment of a slamming event consisted of two data sets, a reaction data set, containing all the reaction forces for the provided slam load unfiltered. Also a data set of containing the sum of forces measured in-front of the structure.

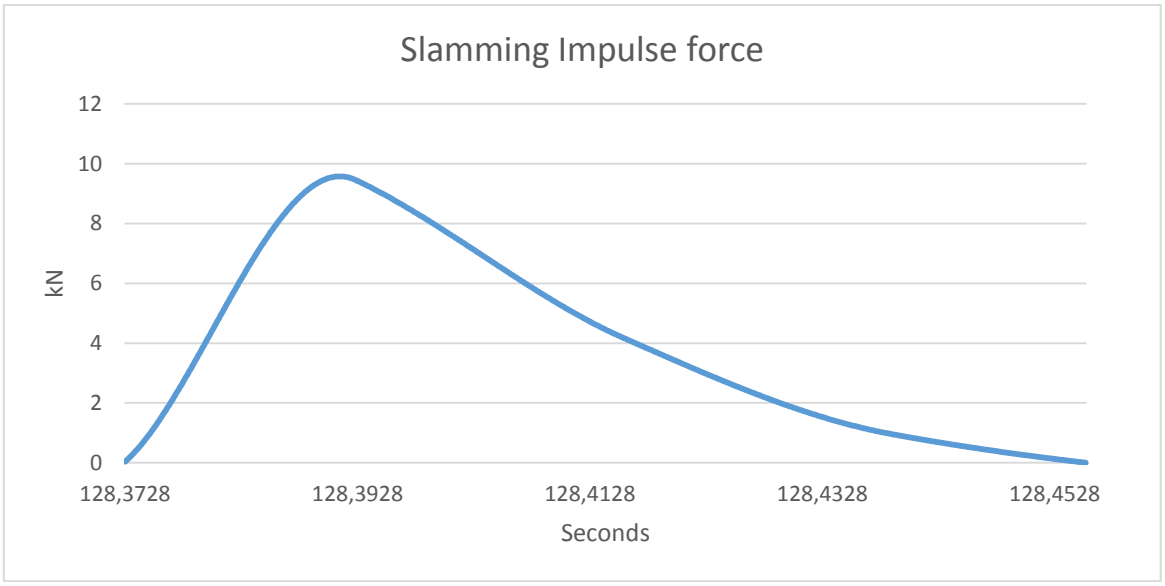

Figure (4.1) Calculated slamming force front brace[36]

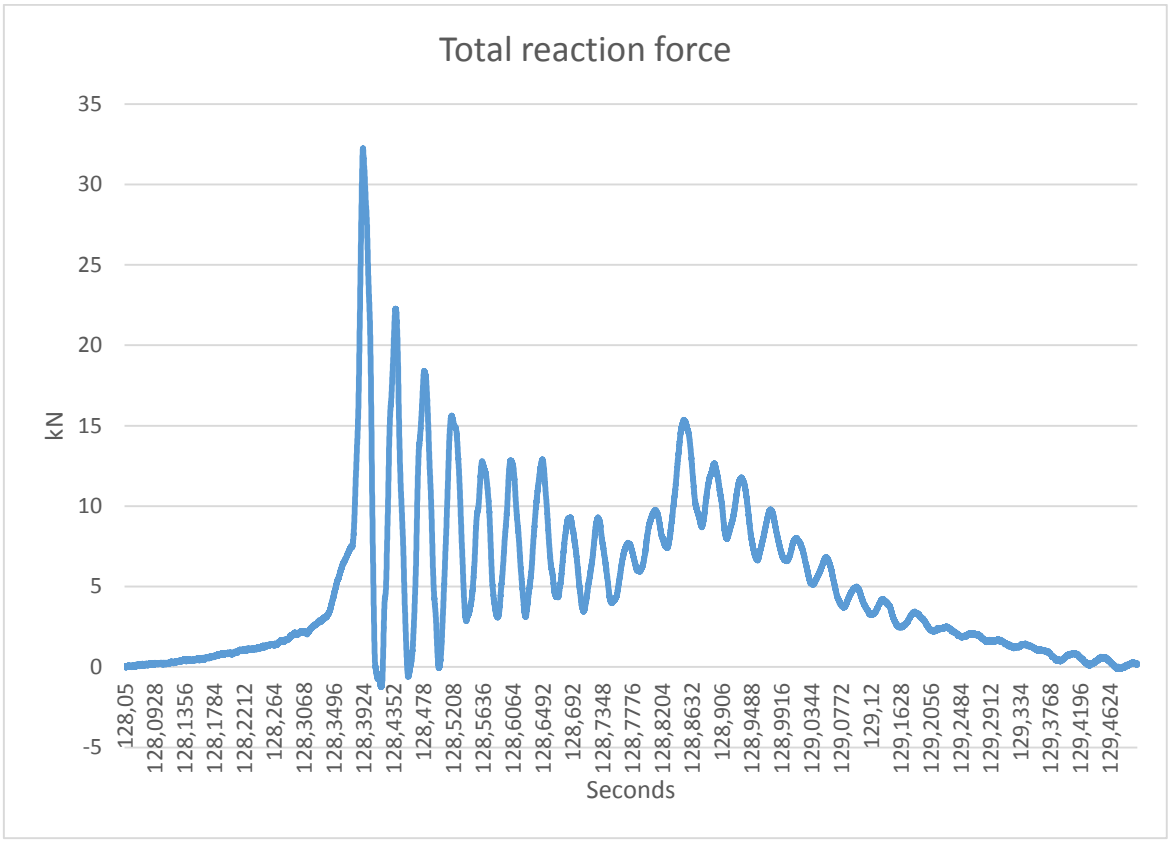

Figure (4.2) Related total response from slamming force(see Figure 4.1) [36]

Based on the hammer response comparison, the model should now response in a similar manner to that of the structure given that the same impulse is employed.
To check this assumption, the model can be now be submitted to a load impulse constructed to have the same magnitude and duration as that of Figure (4.1).

To fit the impulse to the correct duration, the "timehistory" command was used in a similar manner as was done in section 3.2.2.
Since the slam impact is distributed over a larger area of the structure than in section 3.2.2, a new distribution of the load is needed. To get an accurate representation of the load distribution, the impulse was distributed into four point loads placed on the front brace of the model as seen in Figure (4.5).

Each individual node will have a max impulse can be estimated form the impulse plot in Figure 4.1 to be:

$$Node\ Load_{Max} = \frac{9500}{4} = 2375\ N \qquad 4.1$$

The duration of the impulse can be estimated from Figure 4.1 it is visually estimated as:

$$T_{Experiment} = 128.4478 - 128.3728 = 0.075\ s \qquad 4.2$$

The constructed impulse can be illustrated as:

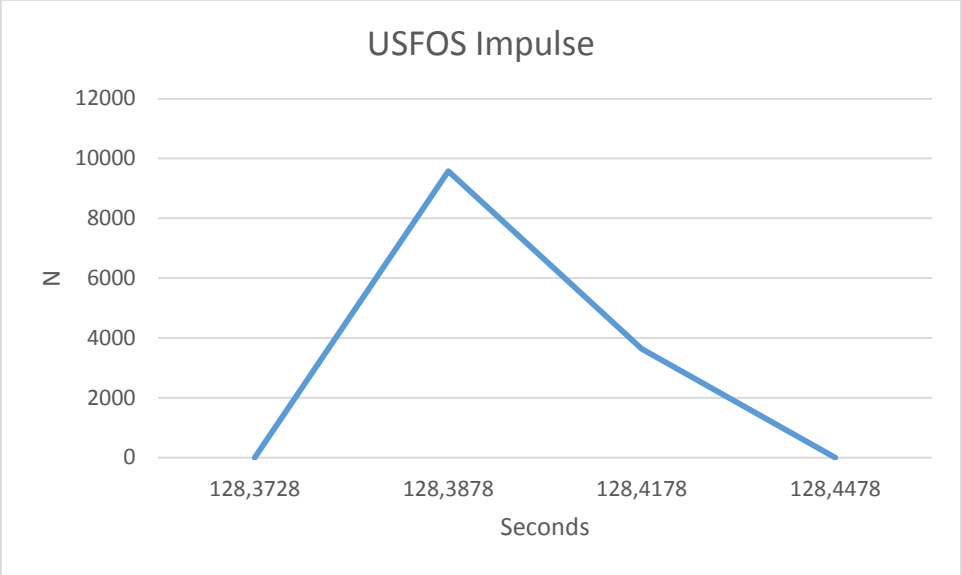

Figure (4.3) Slamming impulse assumed in USFOS

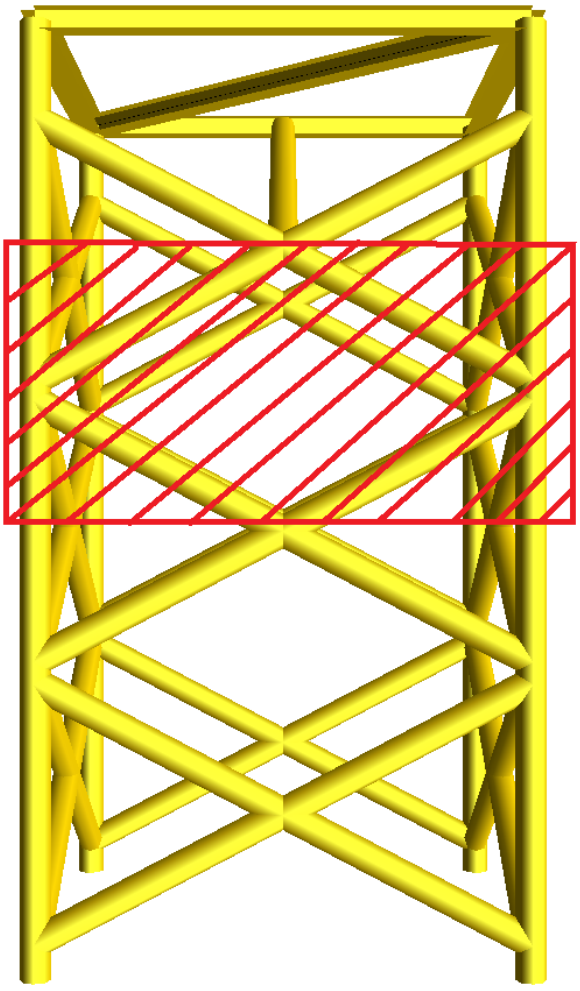

Figure (4.4) Slam affected zone

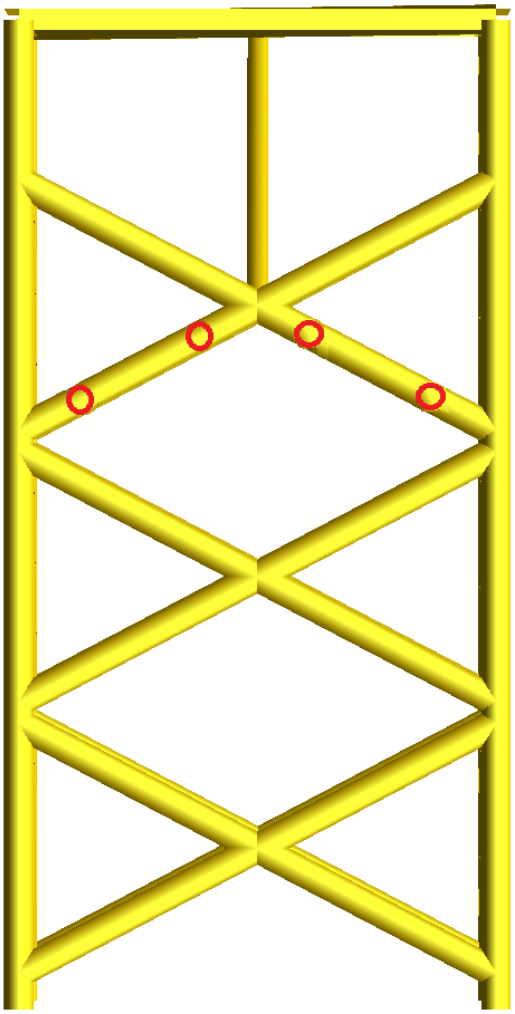

Figure (4.5) location of impulse loads

For the simulation to have equal conditions of the structure, it has to be loaded with a quasi-

static response as well. The wave observed in the experiment for this load case is the same that was used in the section 3.2.2. The values for period, depth and wave height are imported:

$$H = 1.9\ m \tag{4.3}$$

$$Period = 5.0\ s \tag{4.4}$$

$$Depth = 2.75\ m \tag{4.5}$$

This gives the control file parameters as follows:

SIMULATION PARAMETERS		
H- wave height	1.9	m
d- water depth	2.275	m
P- wave period	5	s
Slam duration	0.075	s

Table(4.1)

The simulation is run using these data, the response is extracted. The signal is plotted in graph together with the experiment response.
As can be observed by Figure (4.8) bellow, the response has a much smaller maximum peak compared with the observed response from the experiment.

$$ForcemaxPeak_{Experiment} = 25\ kN \tag{4.6}$$

$$ForcemaxPeak_{USFOS} = 15\ kN \tag{4.7}$$

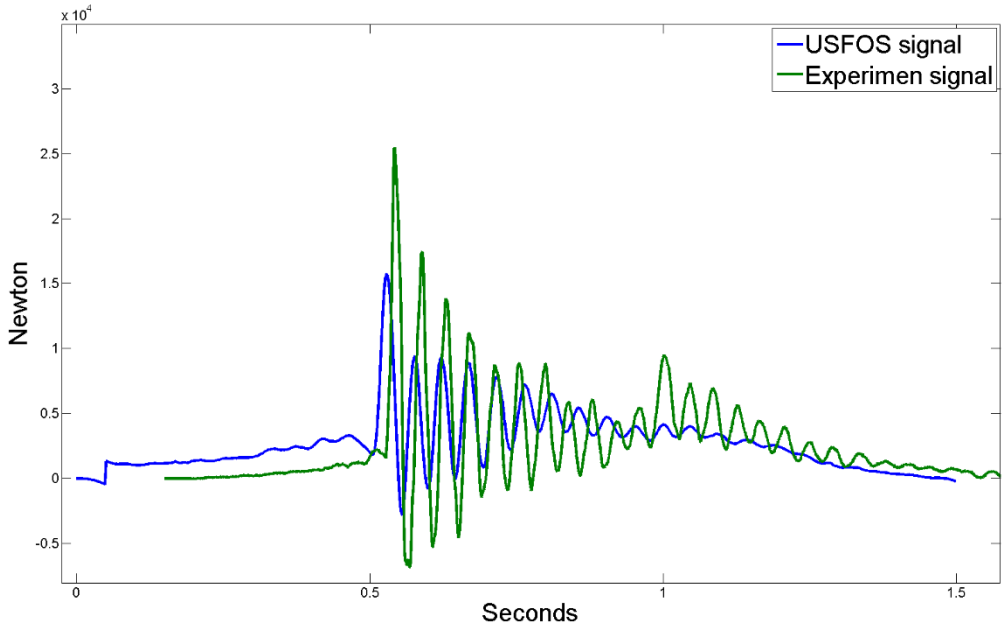

Figure (4.6) Signal response of USFOS simulation compared with experiment

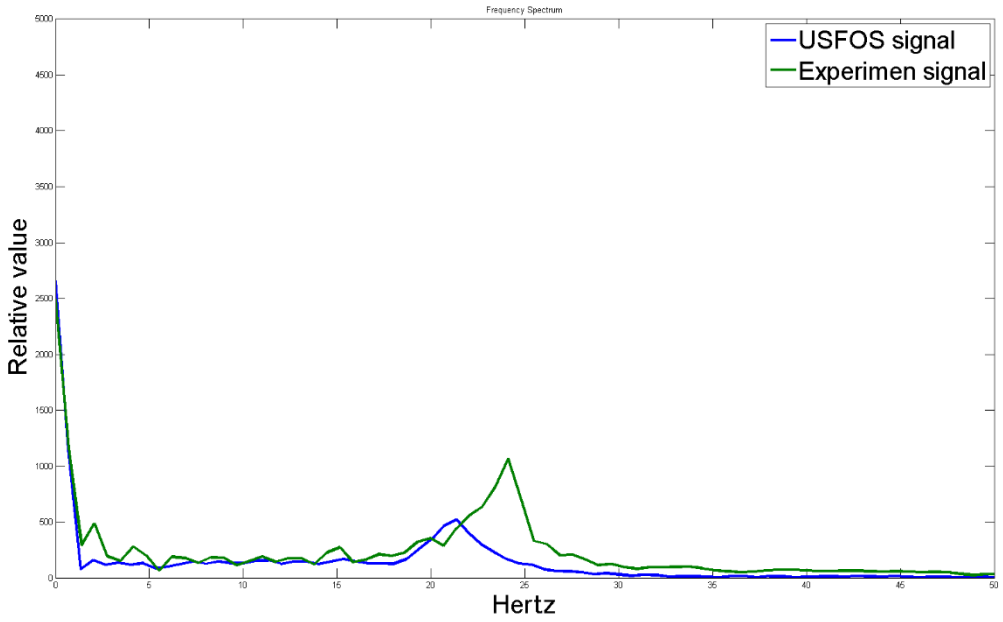

Figure (4.7) Frequency spectrum of Signal (see Figure 4.6)
The frequency spectrum illustrates the difference as well, it appears that the new location of loads have been unfavorable when it comes to the accuracy. Since that the model now vibrates at a lower frequency that what would be expected if it had behaved as the experiment structure.

There are numerous possibilities to why the vibration shifts towards a lower frequency as seen in Figure 4.7. It can also be seen that the models ability to respond is much lower than the experiment signal.

One possibility is that there are hydro dynamic effects of the passing wave that causes the shift. In an attempt to address this issue the wave height have been reduced to an artificially low level compared with the experiment height. This is done because it was observed that a lower wave height could produce a response that vibrated around a higher frequency. That in-turn suggested that the water surface height will affect the response in USFOS.

An issue with this approach is that, the wave used, as in the previous Section 3.2.3 was shown to produce loads that are in good agreement what has been observed. (See Figure 3.24)
Also the reduced wave height do not sufficiently explain why signal response of the model as illustrated in Figure (4.6) is a lot smaller than that of the structure, which might instead be attributed to different Eigen frequencies of the loaded parts. This discrepancy could instead suggest that there have to be done adjustments to the model to get a matching signal

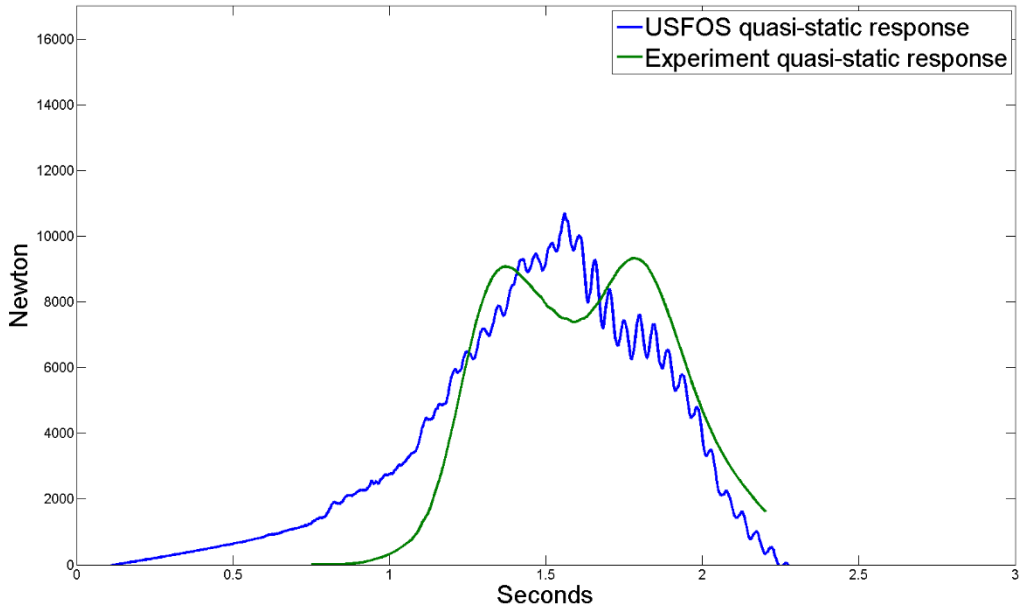

Figure (3.24)

To check if the assumption that it is the wave that is causing the reduced response vibration, a suited value should exist between the current wave height of 1.9 meters and no wave, that produces the a similar frequency response as the seen in the experiment. Running an USFOS simulation, keeping the impulse at the same level and duration, while reducing the wave height for each iteration found that the best fitted wave height as 0.9 meters.

The best fitted result is found through trial and error at:

SIMULATION PARAMETERS		
H- wave height	0.9	M
d- water depth	2.275	M
P- wave period	5	S
Slam duration	0.075	s

Table (4.2) Simulation parameters for reduced wave height

The reduced wave height provided a response frequency much closer to that observed in the experiment load case.

The peak maximum response force will however not be changed much by a change in the passing wave height. As can be seen by Figure (4.12) below.

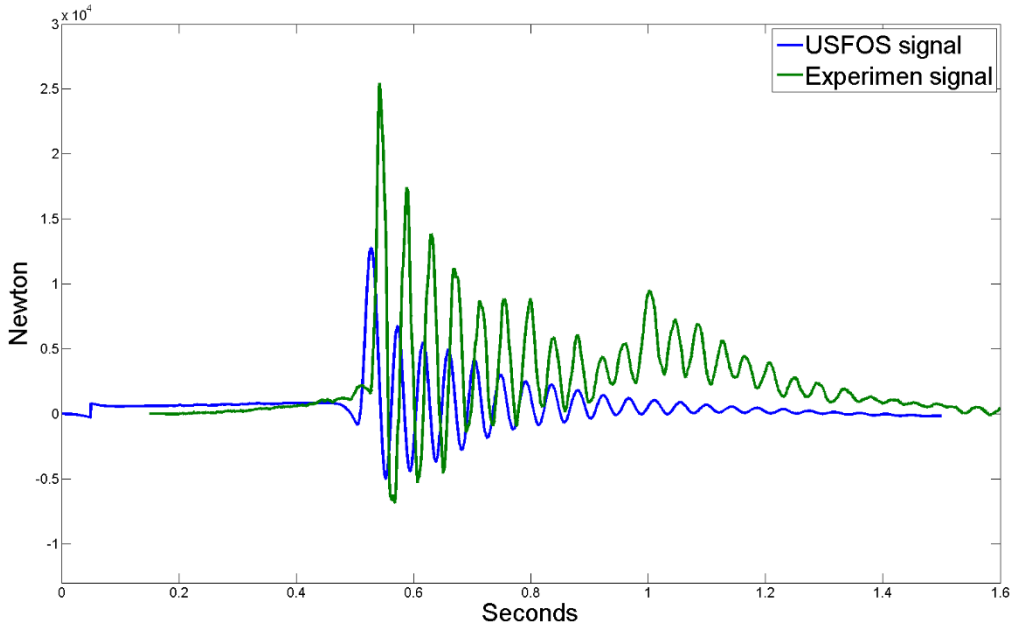

Figure (4.8) Signal response of USFOS simulation with reduced wave height

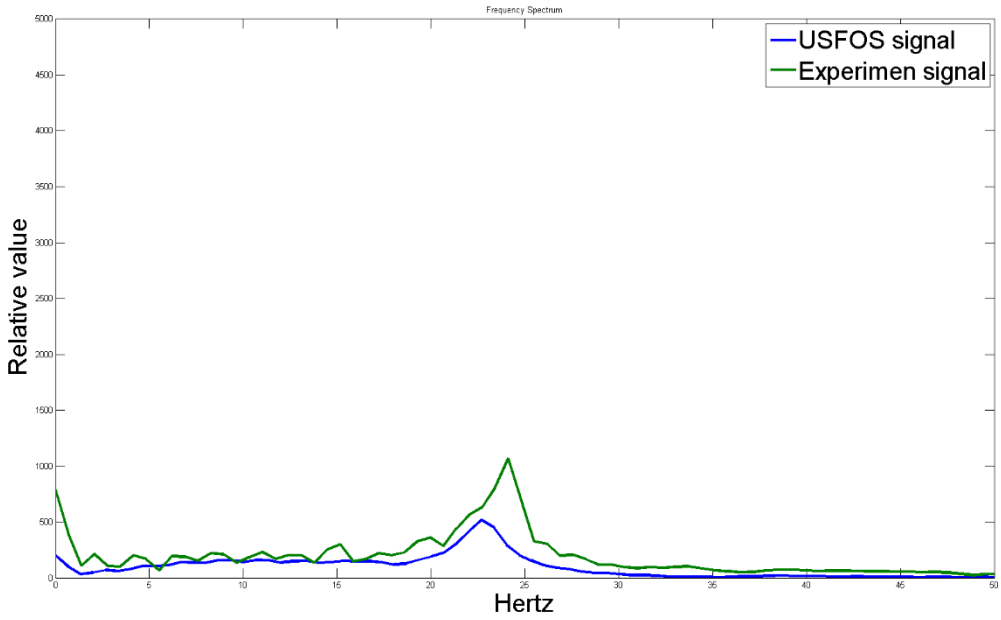

Figure (4.9) Frequency spectra of signal (see Figure 4.8)

The change in wave height did not improve with the max response, however the frequency matches better. This suggests that the problem of max response lies in the model, since the loads are distributed on the front brace, a component of the structure that has only has been indirectly tuned in the section 3.2.2.

The changing wave heights effect on the Eigen frequency could be related to either hydrodynamic effects, or calculation of the quasi static forces, or both, as there can be made arguments for both.

A hydrodynamic effect that could affect the Eigen period, could be related to the mass of the surrounding water, which also would be expected increase for larger wave heights. Such an effect of increased mass would cause the models Eigen period to shift towards a lower frequency.

An effect on the frequency distribution by the quasi-static load, could be caused by the variation in the intensity of the quasi-static loads, as can be seen in Figure 3.24. The variation of intensity would cause vibration effects that could cause a shift in the frequency distribution and explain the change.

Regardless of the cause, the effect is observed to appear consistently and is assumed to be the cause of slight shift in frequency in the remaining simulations that is reviewed.

The difference in responses in Figure 4.7 could be caused by the braces' frequency being too different than that of the impulse duration. This suggests that new values of stiffens of structural parts related to the brace has to be found.

Running several simulations with different material properties, a good agreement was found using the values as described in Table 4.3.

After multiple trail and errors a better fit is found given the values:

CONTROL FILE	**CHANGE**	**Comment:**	**Value:**
-Calculation resolution	**No**		0.0001
Simulation duration	**No**		
-Static		end time	1
-Dynamic		end time	2.238
Hydro dynamics	**No**		
-Water		depth :	2
-Wave			0
Imposed loads	**No**		
-Impulse		Node 501	7430
Dampening	**YES**		
-25Hz		%	0.0175
-125Hz		%	0.0175
Structural data	**No**		
Geometry models			**unchanged**
Material models	**YES**		
ST-37			
-Density		Kg/m^3	7850
-Young's		N/m	5.05E+10
Aluminum			
-Density		Kg/m^3	3380
-Young's		N/m	3.50E+10
Instruments			
-Density		Kg/m^3	16000
-Young's		N/m	**7.05E+09**
ST-37 (with cable)			
-Density		Kg/m^3	8350
-Young's		N/m	**7.05E+09**
Internal fluid			
-Density		Kg/m^3	1025
-Young's			N/A
Force transducers(1&3)			
-density		Kg/m^3	N/A
- Young's		N/m	1.4575E+09

Table (4.3) Material parameters for the adjusted brace

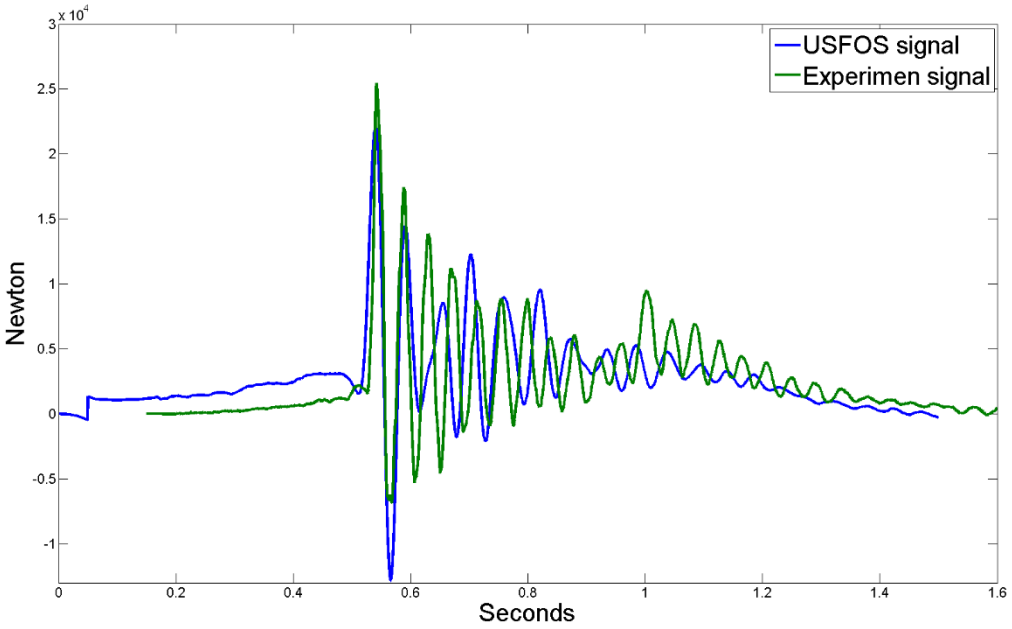

Figure (4.10) Signal response of USFSOS simulation compared with experiment, adjusted brace stiffness.

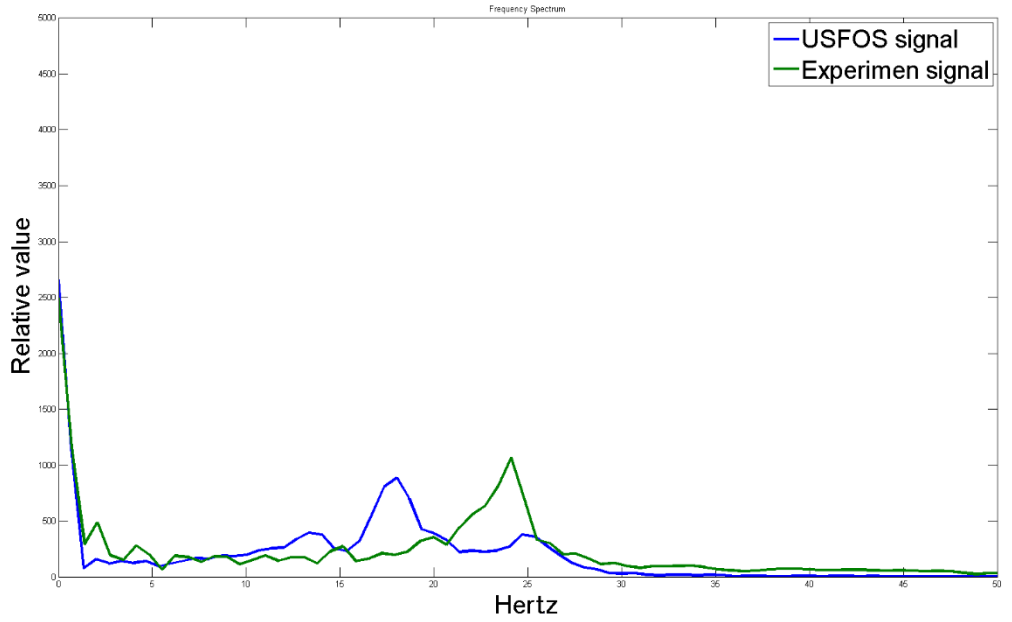

Figure (4.11) Frequency spectra of signal (see Figure 4.10)

As can be seen from figure (4.11), the response of the model with the retuned material stiffness provides a much better representation of the structural behavior. The error in the frequency spectrum is assumed to be caused primarily by the wave effect. (See previous simulation and Figure 4.9)

4.2 Slam based on monopile theory

When the model behaves correctly compared with the slam from the experiment, would be to of interess to see the effects and response of a breaking wave according to the current breaking wave theory when is applied to the model.
As there are little documentation about the braking waves on jacket, the monopile formulation is used. The model is subjected to a slamming event in accordance with a current recommended practice to observe to what extent it over estimates the forces the truss structure will be subjected to. The formulation of the slam force therefore based on the findings in [31]

For the models response from simulation to be comparable to the experiment response, the models material properties are kept the same as those found in Section 4.1.
These values are preferred over those found section 3.2.2, as the load that will be in use here have more similarities with the load found in "Slam load from experiment". The simulation should then provide results that can give a good idea about magnitude of a dimensioning slam response would produce, and this can be compared with that found in the experiment.

CONTROL FILE	**Comment:**	**Value:**
-Calculation resolution		0.0001
Simulation duration		
-Static	end time	1
-Dynamic	end time	2.238
Hydro dynamics		
-Water	depth :	2
-Wave		0
Imposed loads		
-Impulse	Node 501	7430
Dampening		
-25Hz	%	0.0175
-125Hz	%	0.0175
Structural data		
Geometry models		**unchanged**
Material models		
ST-37		
-Density	Kg/m^3	7850
-Young's	N/m	7.00E+10
Aluminum		
-Density	Kg/m^3	3380
-Young's	N/m	3.50E+10
Instruments		
-Density	Kg/m^3	16000
-Young's	N/m	7.00E+08
ST-37 (with cable)		
-Density	Kg/m^3	8350
-Young's	N/m	7.00E+08
Internal fluid		
-Density	Kg/m^3	1025

-Young's		N/A
Force transducers(1&3)		
-density	Kg/m^3	N/A
- Young's	N/m	1.4575E+09
Force transducers(2&4)		
-density	Kg/m^3	N/A
- Young's	N/m	1.4600E+09

Table 4.4 Material parameters with tuned brace

4.2.1 Slam force

To be able to replicate a slam as it would be according to the standards. Some parameters dependent on the wave that is assumed first needs to be established.
For simplicity we assume that the Airy theory is valid in order to establish the wave period and the wave celerity. The wave assumed is based on the earlier section 3.2.3. Where the wave period was visually estimated from the graph bellow.

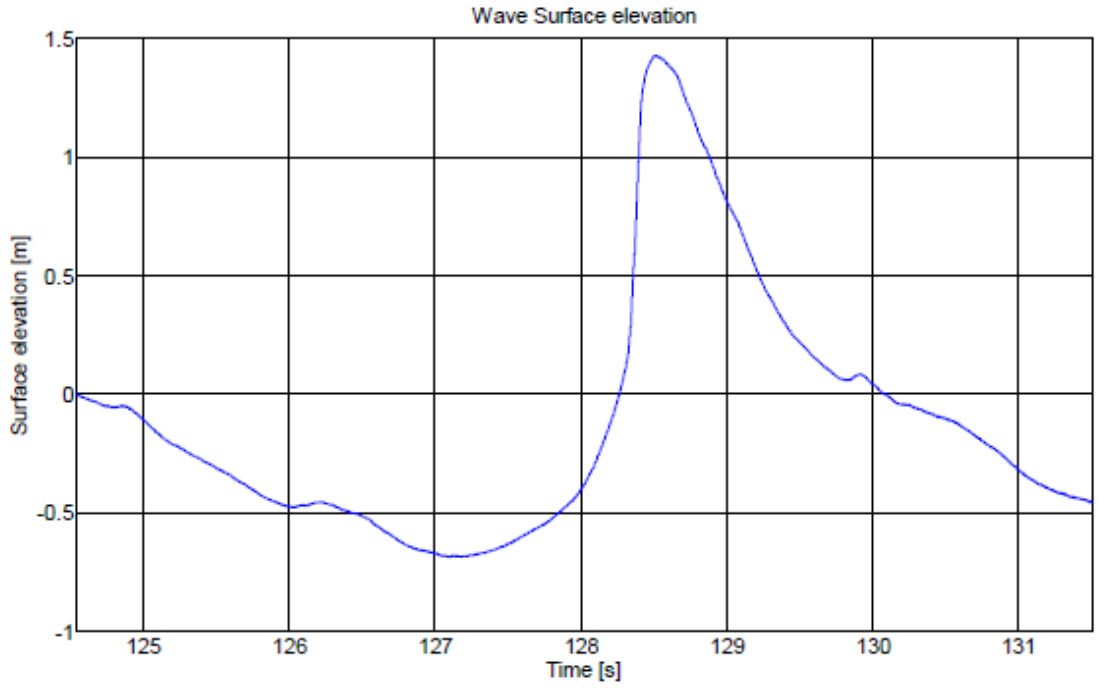

Figure (3.8) Surface elevation a wave from the experiment

Wave period is visually estimated to be 5 seconds
Under the assuming that Airy theory is valid, the wave number K can be calculated from the formulas from table in Airy theory:

Wavelength:

$$\lambda = \frac{gT^2}{2\pi} = 39\ m \qquad 4.8$$

Wave number:

$$K = \frac{2\pi}{\lambda} = 0.1611 \qquad 4.9$$

Wave celerity:

$$C = \sqrt{\frac{g}{K}\tanh(kd)} = 5.55 m/s \qquad 4.10$$

- *Where d - Depth is set as (2.00 m + 0.45 m)*

The parameters in needed to calculate the slam load of the wave have been estimated. A slamming coefficient is assumed based on the slam theory applied.
Using Wagner's formulation earlier described in the wave force paragraph:

$$F_S = \rho_w R C^2 C_s \qquad 4.11$$

Where Cs is assumed to be 2 Pi.

$$F_S = \rho_w R C^2 C_s = 1025 * 0.07 * 5.55^2 * 2\pi = 13886.33\ N/m \qquad 4.12$$

Duration is estimated by assuming plunging breaker and using the formulation given in [24]:

$$T_{Standards} = \frac{13D}{64c} = \frac{13*0.14}{64*5.55} = 0.0051\ s \qquad 4.13$$

This number clearly differs from that witch is observed in the experiment.

$$T_{Experiment} = 0.075\ s \qquad 4.14$$

All load parameters that are required to run a simulation in USFOS is now known, the slam load can be assumed as a line load along the elements from the sill water level and to the highest part of the structure that would be submerged in the wave passing wave.
Using this information, a line load impulse is created and loaded onto the model into USFOS. Running this simulation produces the following signal.

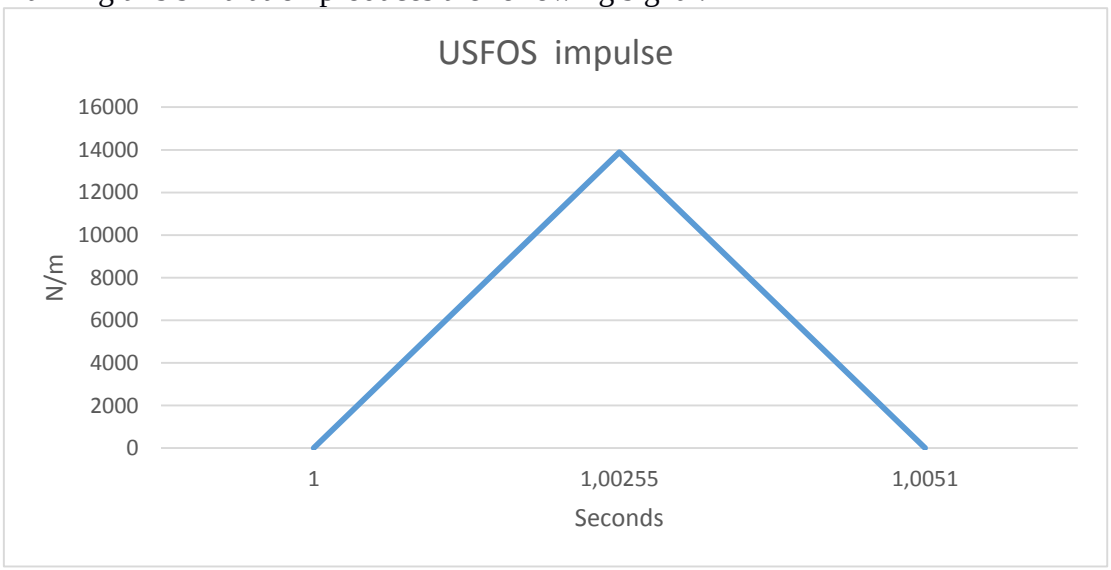

Figure (4.12) Line load impulse applied in USFOS

The assumption that the slam load is equal to an impulse loaded as a line load from the still-water level to the highest "wet" part of the structure could be translated as that entire wave hits the structure like a vertical wall of water. This is an unrealistic scenario, to give a more realistic representation of a slam event, a curl factor should also be accounted for.
A curl factor states how large a portion of the wave in the slam zone (hatched area Figure 4.13) have zero rise time and slam like behavior.
From the curl paragraph we have that the curl factor for zero inclination piles could be assumed as:

$$\lambda = 0.46 \qquad 4.15$$

To translate the curl factor into the computer model, the loads outside the assumed curl area (green hatch Figure 4.13) will not have impulse load from the slam applied to them.
This leaves only the elements that have been highlighted in green in Figure 4.13, these will have the slam impulse applied to them.

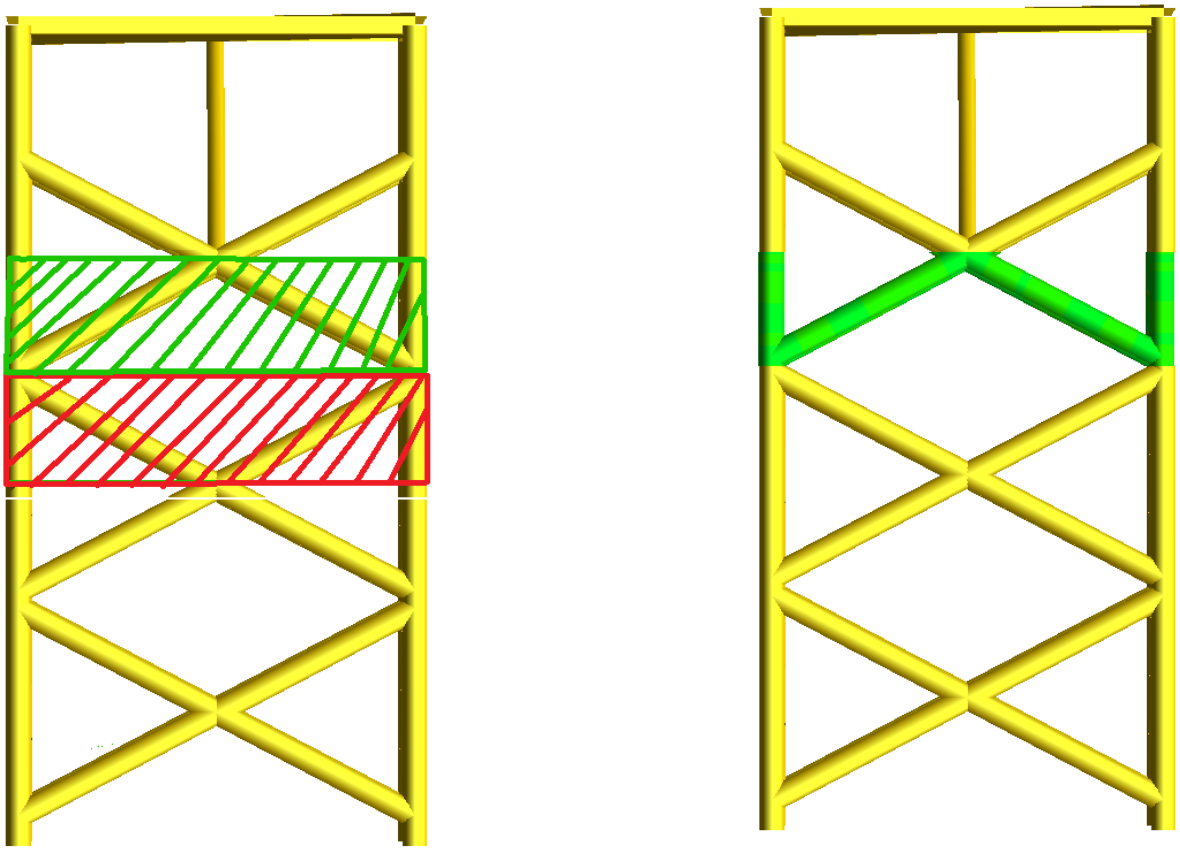

Figure (4.13) Illustration of the elements assumed to be loaded when curl is accounted for

4.2.2 Calculated response

Now that the slam loads magnitude, its duration and the elements that should be subjected to it is known, the USFOS simulation can be run.
The parameters defined in the control file are given as:

SIMULATION PARAMETERS		
H- wave height	**1.9**	**m**
d- water depth	**2.275**	**m**
P- wave period	**5**	**s**
Slam duration	**0.0051**	**s**

Table 4.5 Simulation parameters for monopile theory slam

The resulting total response from the impulse was filtered using a high-pass filter to remove the quasi-static effects.

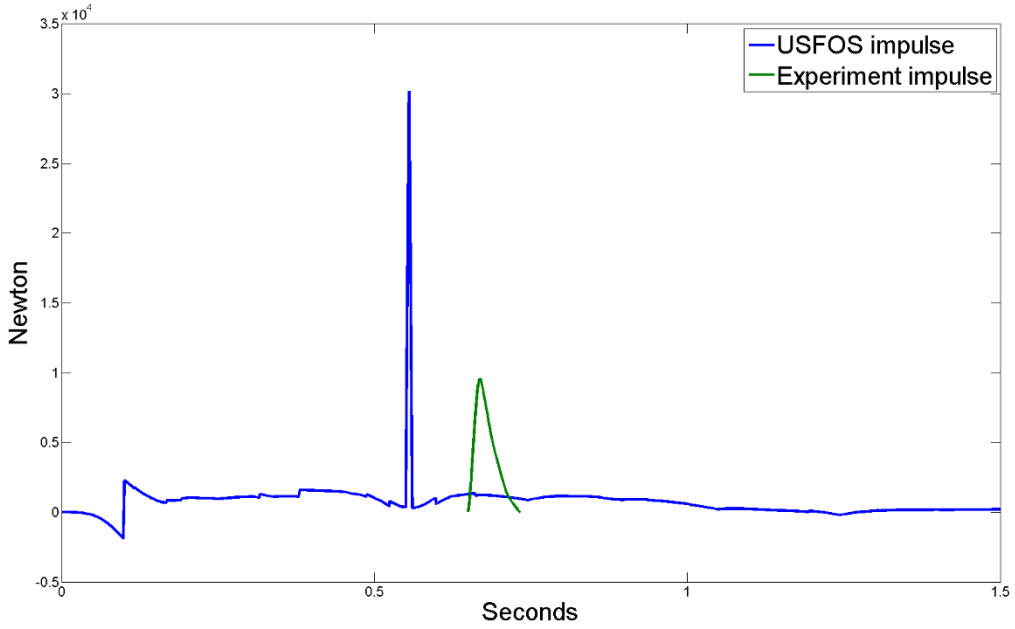

Figure (4.14) Comparison of total impulse force as calculated in USFOS based on monopile theory and experiment slam load.

The USFOS max impulses can be found as:

$$Fpeak_{USFOS} = 28000\ N \tag{4.16}$$

While the experiment peak by comparison is:

$$Fpeak_{Experiment} = 9543\ N \tag{4.17}$$

The response was also filtered to remove the quasi-static effects. Giving a resulting signal that could be compared to the experiment results:

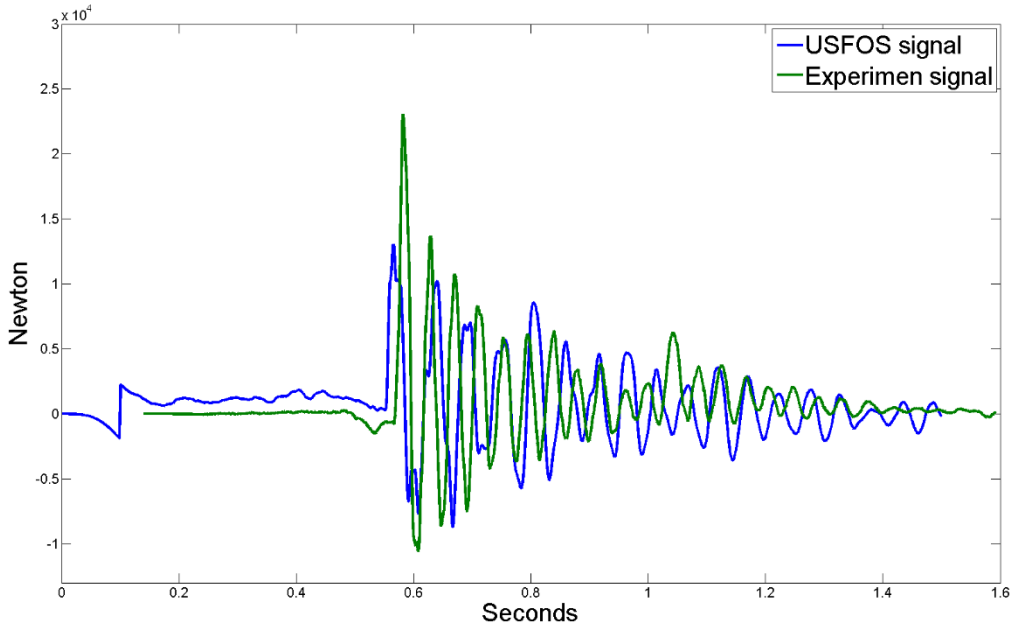

Figure (4.15) Signal response of USFOS simulation based on monopile theory slam load

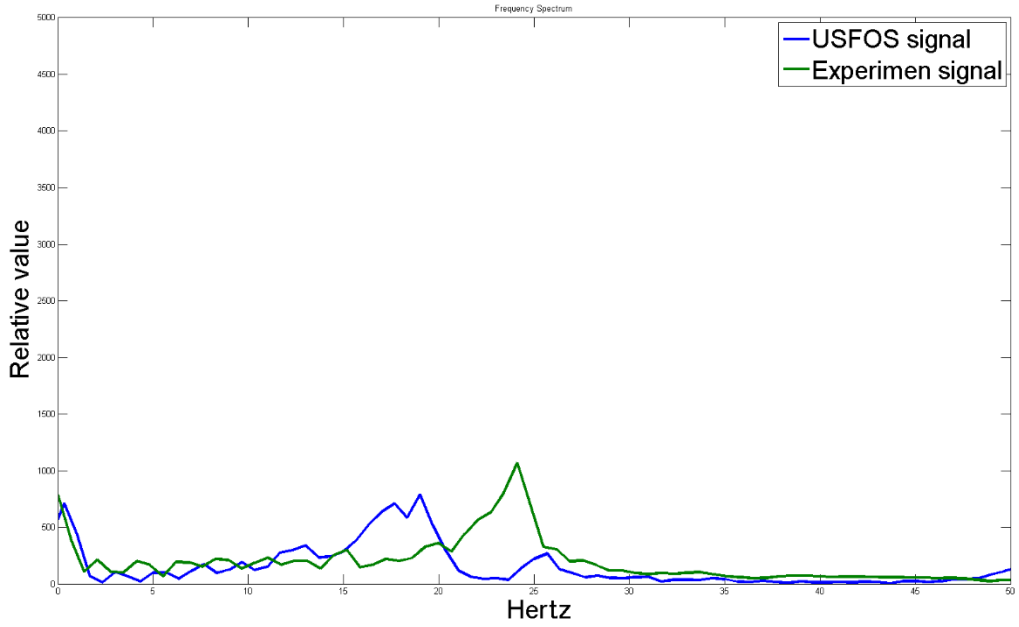

Figure (4.16) Frequency spectra of signal (see Figure 4.15)

The Eigen frequency still is shifted around a lower value than was observed in the experiment. As a simple verification to confirm that this effect still can be related to the error from the passing wave as discussed in section 4.1. The USFOS simulation is run again using the exact same parameters as used when calculating the result in Figure 4.15 and Figure 4.16, this time with the wave height set to zero.

The parameters defined in the control file are given as:

SIMULATION PARAMETERS		
H- wave height	**0.0**	**m**
d- water depth	**2.275**	**m**
P- wave period	**5**	**s**
Slam duration	**0.0051**	**s**

Table 4.6 Simulation parameters without wave interaction

The USFOS simulation gives the resulting signals:

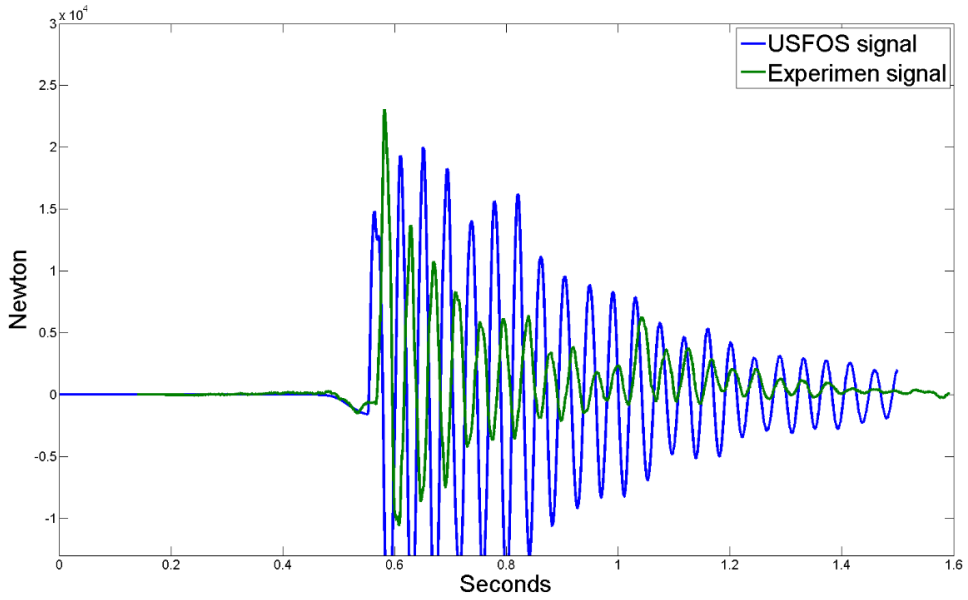

Figure (4.17) Signal response USFOS simulation no wave

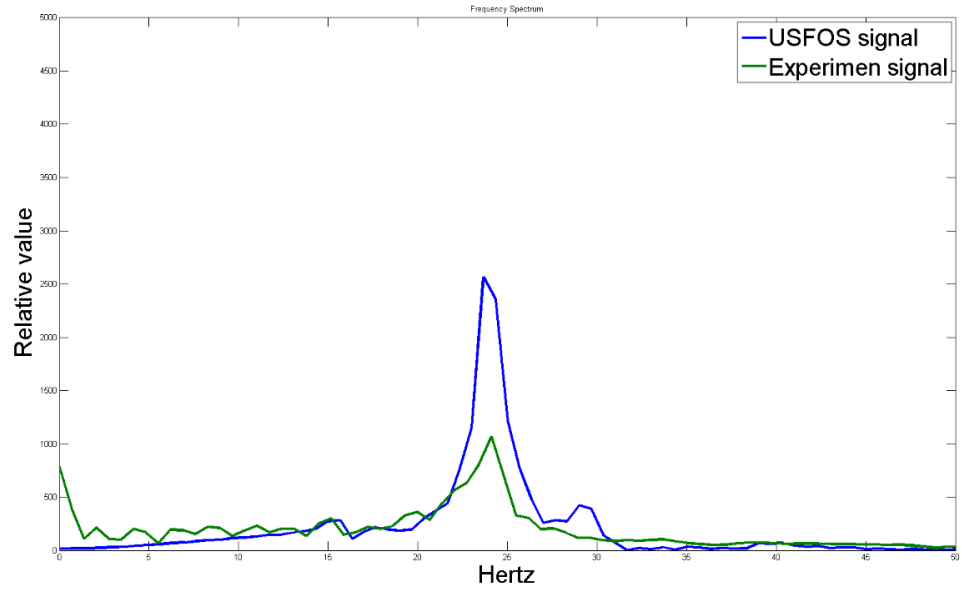

Figure (4.18) Frequency spectra signal (see Figure 4.17)

It can be observed form the frequency distribution in Figure 4.18, the response of the model vibrates around the same frequency as the structure under the condition that there is no wave load applied. Thus confirming that the error of the frequency distribution in Figure 4.16 is in some way related to the passing wave as discussed in section 4.1.

4.3 Result

The estimated response for each of the load case is presented here comparable with the experiment values.

Load case	Impulse (N)	Duration (Second)	Amplification factor	Max response (N)
Experiment	***9556***	***0.075***	***2.30***	***22000***
Simulations:				
Slam from experiment	*9556*	*0.075*	*1.56*	*15000*
Slam from experiment with tuned front-brace	9556	*0.075*	*2.09*	*20000*
Slam based on Monopile theory with tuned front-brace	28000	0.0051	0.42	12000

Table (4.7) Summary of impulse and response

The model with material parameters that have been established through comparing response of a hammer impact and an impulse node load as was shown in section 3.2.2. It can be observed from Figure (4.7) section 4.1, that the result indicates that the model has an Eigen frequency that is too far off from the duration of the slam when compared with the experiment. This causes less of an amplification effect in the resulting response, as can be illustrated by Figure 2.12.

The model using the material parameters that was chosen to match the slam event of the experiment, provides results that are much more "in tune" with the experiment response, as is seen in Figure (4.10). An issue with this solution is that the retuning of the model based on this experiment change the response compared with that which was observed in the section 3.2.2. The tuning also lowers the frequency response (Figure (4.11), showing that the Eigen frequency of the model is lower than that of the structure, given the same conditions.
This may be impart due to the wave effect.

Since the slam forces is distributed over the brace as a line load, the model configuration that have been tuned to match the response of the experiment slam was expected to be most correct representation of the actual structure in USFOS.
There is a large difference in the duration of a slam based on the recommended practice and the duration of the measured slam. This is shown most clearly in the effect it has on the response, even if the impulse used in section 4.2(Figure 4.14) is larger, the relative amplification of the resulting response is much smaller, as can be seen in table (4.7).

5. Discussion and conclusion

The finite element software USFOS is able to reproduce a slam event and simulate a dynamic response with a reasonable accuracy. There were however an uncertainty that was introduced when finding the parameters that can made the results form a simulation comparable to a reference structure.
The response of the model is strongly dependent upon material parameters and geometry parameters. As the geometry is predefined, the only parameters that are available for change are the material parameters. To make the model to behave like structure used in the experiment adjustment of the material parameters were required. As a model is an ideal representation of the actual geometry and materials, and the actual structure is likely different from the ideal the model is based on.
In addition it was could be assumed that USFOS over-estimates the structural stiffness about the joint and beam connections. As the model was modelled with rigid nodes (non-rotational) to mimic welded connection.

It was therefore not surprising that the model lacked the correct response when subjected to comparable load cases. The solution was to shuffle around the parameters for stiffness for the model, a finding a combination that gave results with similarities to that of the experiment signals. As it can be seen from the plots in section 3.2.2, the error in the frequency distribution was improved a lot from Figure (3.15) to Figure (3.17).

The solution strategy of trial and error, making educated guesses about the correct stiffness for a single material model based on the previous iteration of the simulation. In hindsight the model coding should have been in a way that better accommodated this type of solution strategy, for example in manner that would allow for adjustment of each of the central component individually. This would have allowed for better options when fitting of the models response.

After finding a fitting combination of parameters, the model was subjected to a load case that was assumed to be equal to a wave slam event observed in the experiment. The simulation revealed that the hammer response comparison was insufficient in correctly adjusting the models parameters. The response using the parameters form the hammer comparison produced a response that was inaccurate when compared to the experiment value.
The frequency of the response was also wrong compared to that observed in the experiment. While the error in response was negated by readjusting the parameters for the brace component that the slam was directed at. The error in frequency distribution had to be assumed to originate from the quasi static load and could not be removed without the compromising hydrodynamic effects that otherwise would be present.

As the change in frequency seamed to only be dependent on the wave. It appeared to be linked with the passing wave directly, as an increase in mass or indirectly, as an artifact inaccuracy in the modeling of quasi-static forces. A connection between wave height and a shift in the structures Eigen frequency was an observed.

The results in section 4.3 gave an indication of how the current theories for monopile differ from the forces observed on a jacket. When the slam based on monopile theory was applied, the impulse despite it having a much greater amplitude than previous load cases, failed to match them in response.
It is evident from this that the current monopile considerations are not directly transferable to the jacket for breaking waves based on the modeling done in finite element software.

5.1 Recommendation for future work

Some of the future work could include a more specific investigation of the load distribution on the jacket and find if it can be justified to increase the duration for jackets, by loading each element with an impulse with the duration as assumed in section 4.2, at different time steps.
There is also a consideration to why USFOS waves shifts the Eigen frequency of the structure as a wave passes, to apply wave forces in a manner than that better matches the measured load as seen in section 3.2.3, and finding a way that would allow for applying stable quasi-static loads at the correct magnitude would eliminate some of the uncertainty introduced by the wave generation when using USFOS for breaking wave of simulations.

References

1. Navaratnam, C.U., *Preliminary Analysis of Wave Slamming Force Response Data From Tests on a Truss Structure in Large Wave Flume, Hannover, Germany*. 2013. p. 63.
2. Busby, R.L., *Wind power : the industry grows up*. 2012, PennWell Corporation: Tulsa, Okla.
3. Fouquet, D., *Policy instruments for renewable energy - From a European perspective.* Renew. Energy, 2013. **49**: p. 15-18.
4. Kaldellis, J. and M. Kapsali, *Shifting towards offshore wind energy-Recent activity and future development.* Energy Policy, 2013. **53**: p. 136-148.
5. EWEA, *The European offshore wind industry key trends and statisitcs 2012.* 2013.
6. Jacobsson, S. and K. Karltorp, *Mechanisms blocking the dynamics of the European offshore wind energy innovation system - Challenges for policy intervention.* Energy Policy, 2013. **63**: p. 1182-1195.
7. EWEA, *EWEA 2013 Deep water*. 2013.
8. Green, R. and N. Vasilakos, *The economics of offshore wind.* Energy Policy, 2010. **39**(2): p. 496-502.
9. Mayilvahanan Alagan Chellaa, A.T.a.D.M., *An Overview of Wave Impact Forces on Offshore Wind Turbine Substructures.* Energy Procedia 2012. **20** (Technoport RERC Research 2012): p. 217 – 226.
10. Seidel, D.-I.M., *Substructures for offshore wind turbines, Current trends and developments.* Festschrift Peter Schaumann, 2014.
11. EWEA, *Wind in our sails*. 2011.
12. Myhr, A., et al., *Levelised cost of energy for offshore floating wind turbines in a life cycle perspective.* Renew. Energy, 2014. **66**: p. 714-728.
13. Sun, X., D. Huang, and G. Wu, *The current state of offshore wind energy technology development.* Energy, 2012. **41**(1): p. 298-312.
14. Kaldellis, J.K. and M. Kapsali, *Shifting towards offshore wind energy—Recent activity and future development.* Energy Policy, 2012. **53**: p. 136-148.
15. Twidell, J. and G. Gaudiosi, *Offshore wind power*. 2009, Brentwood: Multi-Science Publ.
16. Standard, D., *Offshore standard DNV-OS-J101*. 2010, Høvik: DNV.
17. Lynn, P.A., *Onshore and offshore wind energy : an introduction*. 2012, Wiley: Chichester.
18. Lewandowski, E.M., *The dynamics of marine craft : maneuvering and seakeeping*. 2004, World Scientific Pub.: Singapore.
19. Fox, R.W., A.T. McDonald, and P.J. Pritchard, *Introduction to fluid mechanics*. 6th ed. ed. 2004, Hoboken, N.J: Wiley.
20. Hudspeth, R.T., *Waves and wave forces on coastal and ocean structures*. 2006, World Scientific: Hackensack, N.J.
21. Whitham, G.B., *Linear and nonlinear waves*. Pure and applied mathematics (Wiley). 1974, New York: Wiley.
22. Nielsen, P., *Coastal and estuarine processes*. Advanced series on ocean engineering. Vol. vol. 29. 2009, New Jersey: World Scientific.
23. Jen-Men Lo, R.G.D., *Evaluation of a modified stretched linear wave theory.* Proceedings of 20th Conference on Coastal Engineering, 1986.
24. DNV, *RP-C205 : Enviormental Conditions and Enviormental loads*. 2014.
25. Le Mehaute, B., et al., *Transformation of Monochromatic Waves from Deep to*

Shallow Water. 1980.
26. Dean, R.G. and R.A. Dalrymple, *Coastal processes with engineering applications*. 2002, Cambridge, UK : New York: Cambridge, UK : New York: Cambridge University Press.
27. Marintek, *USFOS Geetting Started* Strcutural Engineering SINTEF GROUP.
28. Patel, M.H., *Dynamics of offshore structures*. 1989, London: Butterworths.
29. T.S.Hedges, *Wave Breaking and Reflection.* Department of Civil Engineering. **University of Liverpool**.
30. Battjes, J.A., *Surf Similarity.* Coastal Engineering, 1974. **14**.
31. Wienke, J. and H. Oumeraci, *Breaking wave impact force on a vertical and inclined slender pile - Theoretical and large-scale model investigations.* Coastal Engineering, 2005. **52**(5): p. 435-462.
32. Gudmestad, O.T., *Lecture notes Wave forces 2010.* 2014.
33. Akira Watanabe, K.H., *Breaking waveforces on a large diameter cell.* Coastal Engineering, 1974. **14**: p. 19.
34. Rao, S.S. and Y.F. Fah, *Mechanical vibrations*. 5th ed.in SI Units. ed. Always learning. 2011, Singapore: Pearson/Prentice Hall.
35. Rausa Heredia, I.E., *Characterization of wave slamming forces for a truss structure within the framework of the WaveSlam project*, in *DEPARTMENT OF CIVIL AND TRANSPORT ENGINEERING*. 2014, NORWEGIAN UNIVERSITY OF SCIENCE AND TECHNOLOGY. p. 180.
36. **Jose, J.P., O.**, *Experimental Analysis of Slamming Load for Truss Structures within the framework of WaveSlam Project.* 2015, University of Stavanger, UiS, Norway / University of Gdańsk, Poland. p. 60.

Attachments:

- Model file
- Control file Hammer test
- Control file quasi static comparison
- Control file Slam from experiment
- Control file Slam according to Monopile theory
- Sketch of Jacket used in WaveSlam experiment

Model File

' NODES axis A

'x= 0 Boundary code

	'id	x	y	z						
NODE		1	0	0	-1.96	0	0	0	1	1	1
NODE		2	0	2.25	-1.96	0	0	0	1	1	1
NODE		3	0	0	-1.79	0	0	0	1	1	1
NODE		4	0	2.25	-1.79	0	0	0	1	1	1
NODE		5	0	1.125	-1.2	0	0	0	1	1	1
NODE		6	0	0	-0.61	0	0	0	1	1	1
NODE		7	0	2.25	-0.61	0	0	0	1	1	1
NODE		8	0	0	-0.51	0	0	0	1	1	1
NODE		801	0	0	-0.06	0	0	0	1	1	1
NODE		9	0	2.25	-0.51	0	0	0	1	1	1
NODE		10	0	1.125	0.08	0	0	0	1	1	1
NODE		11	0	0	0.67	0	0	0	1	1	1
NODE		111	0	0	0.53	0	0	0	1	1	1
NODE		1111	0.344	0	0.489	0	0	0	1	1	1
NODE		112	0	0	0.53	0	0	0	1	1	1
NODE		12	0	2.25	0.67	0	0	0	1	1	1
NODE		13	0	0	0.77	0	0	0	1	1	1
NODE		132	0	0	0.91	0	0	0	1	1	1
NODE		14	0	2.25	0.77	0	0	0	1	1	1
NODE		143	0.344	2.25	0.95	0	0	0	1	1	1
NODE		142	0	2.25	0.91	0	0	0	1	1	1
NODE		15	0	1.125	1.36	0	0	0	1	1	1
%Intrument nodes											
NODE		131	0	0.344	0.95	0	0	0	1	1	1
NODE		141	0	1.906	0.95	0	0	0	1	1	1
NODE	151	0	0.781	1.18	0	0	0	1	1	1	
NODE	152	0	1.469	1.18	0	0	0	1	1	1	
NODE		16	0	0	1.95	0	0	0	1	1	1
NODE		161	0	0	1.81	0	0	0	1	1	1
NODE		17	0	2.25	1.95	0	0	0	1	1	1
NODE		171	0	2.25	1.81	0	0	0	1	1	1
NODE		18	0	0	2.71	0	0	0	1	1	1
NODE		19	0	2.25	2.71	0	0	0	1	1	1

' NODES axis B 'x= 1125

	'id	x	y	z						
NODE		20	1.125	0	-1.2	0	0	0	1	1	1
NODE		21	1.125	2.25	-1.2	0	0	0	1	1	1
NODE		22	1.125	0	0.08	0	0	0	1	1	1
NODE		221	0.781	0	0.26	0	0	0	1	1	1
NODE		23	1.125	2.25	0.08	0	0	0	1	1	1
NODE		231	1.469	2.25	0.26	0	0	0	1	1	1
NODE		24	1.125	0	1.36	0	0	0	1	1	1
NODE		241	1.469	0	1.179	0	0	0	1	1	1
NODE		25	1.125	2.25	1.36	0	0	0	1	1	1

```
NODE 251 0.781 2.25 1.18 0 0 0 1 1 1

'  NODES axis C  'x= 2250

'id x y z
NODE 26 2.25 0 -1.96 0 0 0 1 1 1
NODE 27 2.25 2.25 -1.96 0 0 0 1 1 1
NODE 28 2.25 0 -1.79 0 0 0 1 0 1
NODE 29 2.25 2.25 -1.79 0 0 0 1 0 1
NODE 30 2.25 1.125 -1.2 0 0 0 1 1 1
NODE 31 2.25 0 -0.61 0 0 0 1 1 1
NODE 32 2.25 2.25 -0.61 0 0 0 1 1 1
NODE 33 2.25 0 -0.51 0 0 0 1 1 1
NODE 34 2.25 2.25 -0.51 0 0 0 1 1 1
NODE 35 2.25 1.125 0.08 0 0 0 1 1 1
NODE 36 2.25 0 0.67 0 0 0 1 1 1
NODE 37 2.25 2.25 0.67 0 0 0 1 1 1
NODE 371 1.906 2.25 0.49 0 0 0 1 1 1
NODE 38 2.25 0 0.77 0 0 0 1 1 1
NODE 381 1.906 0 0.95 0 0 0 1 1 1
NODE 39 2.25 2.25 0.77 0 0 0 1 1 1
NODE 40 2.25 1.125 1.36 0 0 0 1 1 1
NODE 41 2.25 0 1.95 0 0 0 1 1 1
NODE 42 2.25 2.25 1.95 0 0 0 1 1 1
NODE 43 2.25 0 2.71 0 0 0 1 1 1
NODE 44 2.25 2.25 2.71 0 0 0 1 1 1
NODE 45 2.25 1.125 2.71 0 0 0 1 1 1
'Fastend in beam above
NODE 46 2 0 2.71 0 1 1 1 1 1
NODE 47 2 2.25 2.71 0 1 1 1 1 1
'Slamload limitation nodes
'A
NODE 48 0 0 0.08 0 0 0 1 1 1
NODE 49 0 2.25 0.08 0 0 0 1 1 1

NODE 50 0 0 1.36 0 0 0 1 1 1
NODE 51 0 2.25 1.36 0 0 0 1 1 1
'Hammer test modification at node 50 & node 51
NODE 501 0 0 1.26 0 0 0 1 1 1
NODE 511 0 2.25 1.26 0 0 0 1 1 1

NODE 601 2.25 2.25 0.08 0 0 0 1 1 1
NODE 602 2.25 0 0.08 0 0 0 1 1 1
'  Geom ID Do Thick
PIPE 1 0.1397 0.005
PIPE 3 0.1397 0.0698
PIPE 4 0.1 0.005 T-bot [Sh_y Sh
'GeoID H T-web W-top T-top W-bot 0.001
IHPROFIL 2 0.1 0.012 0.14 0.0012 0.14
```

		'GeoID	H	T-web		W-top	T-top	W-bot	
IHPROFIL		5	0.14	0.005		0.073	0.007	0.073	0.007
								T-bot	[Sh_y Sh
'	MatID	E-mod	poiss	yield	‹term.exp				
MISOIEP		1	7.00E+10	0.3		3.55E+08	7850	1.20E-05	
MISOIEP		2	7.00E+10	0.3		3.55E+08	8350		
%aluminium									
MISOIEP		3	3.85E+10	0.3		3.55E+08	3350		
%INSTRUMENT									
MISOIEP	4	5.50E+08		0.3		3.55E+08	16000		
%CENTER BEAM									
MISOIEP	5	5.50E+08		0.3		3.55E+08	8350		
%SPRINGTO Ground									
SpriDiag		6	1.45E09	0	0	0	0	0	
SpriDiag		7	1.46E09	0	0	0	0	0	
SPRNG2GR		300	28	6					
SPRNG2GR		301	29	6					
SPRNG2GR		302	46	7					
SPRNG2GR		303	47	7					
'	BEAMS in	axi:	'id	N1		N2	Materialgeometry		
BEAM			1	1		3	1	1	
BEAM			2	2		4	1	1	
BEAM			3	3		5	1	1	
BEAM			4	4		5	1	1	
BEAM			5	5		6	1	1	
BEAM			6	5		7	1	1	
BEAM			7	3		6	1	1	
BEAM			8	4		7	1	1	
BEAM			9	6		8	1	1	
BEAM			10	7		9	1	1	
BEAM			11	8		10	1	1	
BEAM			12	9		10	1	1	
BEAM			13	10		11	1	1	
BEAM			14	10		12	1	1	
%Instrument beam									
BEAM			83	801		48	3	3	
BEAM			15	9		49	1	1	
BEAM			16	11		13	1	1	
BEAM			17	12		14	1	1	
BEAM			18	13		131	4	1	
BEAM			181	131		151	2	1	
BEAM			19	14		141	4	1	
BEAM			191	141		152	2	1	

BEAM	192	151	15	4	1
BEAM	193	15	152	4	1
BEAM	20	15	16	2	1
BEAM	21	15	17	2	1
BEAM	22	50	161	3	3
BEAM	23	51	171	3	3
BEAM	24	16	18	1	1
BEAM	25	17	19	1	1
BEAM	26	18	19	1	2

' BEAMS from axis A to axis B

BEAM	27	3	20	1	1
BEAM	28	20	6	1	1
BEAM	29	4	21	1	1
BEAM	30	21	7	1	1
BEAM	31	8	22	1	1
BEAM	32	22	221	4	1
BEAM	321	221	1111	1	1
BEAM	322	11	1111	4	1
BEAM	33	9	23	1	1
BEAM	34	23	12	1	1
BEAM	35	13	24	1	1
BEAM	36	24	16	1	1
BEAM	37	14	143	4	1
BEAM	371	143	251	1	1
BEAM	372	251	25	4	1
BEAM	38	25	17	1	1

' BEAMS from axis B to axis C

BEAM	39	28	20	1	1
BEAM	40	20	31	1	1
BEAM	41	29	21	1	1
BEAM	42	21	32	1	1
BEAM	43	33	22	1	1
BEAM	44	22	36	1	1
BEAM	45	34	23	1	1
BEAM	46	23	231	4	1
BEAM	461	231	371	1	1
BEAM	462	371	37	4	1
BEAM	47	38	381	4	1
BEAM	471	381	241	1	1
BEAM	472	24	241	4	1
BEAM	48	24	41	1	1
BEAM	49	39	25	1	1

	BEAM	50	25	42	1	1
'	BEAMS in axis C					
	BEAM	51	26	28	1	1
	BEAM	52	27	29	1	1
	BEAM	53	28	30	1	1
	BEAM	54	29	30	1	1
	BEAM	55	30	31	1	1
	BEAM	56	30	32	1	1
	BEAM	57	28	31	1	1
	BEAM	58	29	32	1	1
	BEAM	59	31	33	1	1
	BEAM	60	32	34	1	1
	BEAM	61	33	35	1	1
	BEAM	62	34	35	1	1
	BEAM	63	35	37	1	1
	BEAM	64	35	36	1	1
	BEAM	65	34	601	1	1
	BEAM	651	601	37	1	1
	BEAM	66	33	602	1	1
	BEAM	661	602	36	1	1
	BEAM	67	36	38	1	1
	BEAM	68	37	39	1	1
	BEAM	69	38	40	1	1
	BEAM	70	39	40	1	1
	BEAM	71	38	41	1	1
	BEAM	72	39	42	1	1
	BEAM	73	40	41	1	1
	BEAM	74	40	42	1	1
	BEAM	75	41	43	1	1
	BEAM	77	42	44	1	1
	BEAM	84	44	45	5	2
	BEAM	78	43	45	5	2
'	BEAMS FROM axis A to axis C					
	BEAM	79	18	46	1	2
	BEAM	80	19	47	1	2
	BEAM	81	18	44	1	5
	BEAM	82	45	15	5	4

'Fastend in beam above

BEAM	85	46	43	1	2
BEAM	86	47	44	1	2

'SLAMBEAM modification

BEAM	87	48	111	3	3
BEAM	88	49	12	1	1

%BEAM DUE TO MOD

BEAM	1401	14	142	1	1
BEAM	1701	171	17	1	1
BEAM	1301	13	132	2	1
BEAM	1601	161	16	2	1
BEAM	801	8	801	1	1
BEAM	1111	11	111	1	1

'Hammer test modification at node 50 'hammertest beam

BEAM	89	132	501	3	3
BEAM	91	501	50	3	3

'Hammer test modification at node 51

BEAM	92	511	51	3	3
BEAM	90	142	511	3	3

' LCase aX aY aZ

GRAVITY	1	0	0	-9.81

'Dynamic "fitting"

INTFLUID	1025	Timedep	11	Element	51
INTFLUID	1025	Timedep	11	Element	52
INTFLUID	1025	Timedep	11	Element	53
INTFLUID	1025	Timedep	11	Element	54
INTFLUID	1025	Timedep	11	Element	55
INTFLUID	1025	Timedep	11	Element	56
INTFLUID	1025	Timedep	11	Element	57
INTFLUID	1025	Timedep	11	Element	58
INTFLUID	1025	Timedep	11	Element	59
INTFLUID	1025	Timedep	11	Element	61
INTFLUID	1025	Timedep	11	Element	62
INTFLUID	1025	Timedep	11	Element	41
INTFLUID	1025	Timedep	11	Element	29
INTFLUID	1025	Timedep	11	Element	2
INTFLUID	1025	Timedep	11	Element	8
INTFLUID	1025	Timedep	11	Element	30
INTFLUID	1025	Timedep	11	Element	42
INTFLUID	1025	Timedep	11	Element	10
INTFLUID	1025	Timedep	11	Element	33
INTFLUID	1025	Timedep	11	Element	45
INTFLUID	1025	Timedep	11	Element	4
INTFLUID	1025	Timedep	11	Element	6

INTFLUID	1025	Timedep	11	Element 12
INTFLUID	1025	Timedep	11	Element 5
INTFLUID	1025	Timedep	11	Element 3
INTFLUID	1025	Timedep	11	Element 1
INTFLUID	1025	Timedep	11	Element 7
INTFLUID	1025	Timedep	11	Element 9
INTFLUID	1025	Timedep	11	Element 801
INTFLUID	1025	Timedep	11	Element 11
INTFLUID	1025	Timedep	11	Element 31
INTFLUID	1025	Timedep	11	Element 28
INTFLUID	1025	Timedep	11	Element 27
INTFLUID	1025	Timedep	11	Element 40
INTFLUID	1025	Timedep	11	Element 39

Control file Hammer comparison

```
HEAD          Quadsh Test Case No 2  Axial Loaded plate
            U S F O S  progressive collapse analysis
                 SINTEF  2001   T Holmas
'
'
'      nloads   npostp   mxpstp   mxpdis
 'CUSFOS    5       50      0.10     1.0
'      lcomb    lfact     mxld    nstep     minstp
  '         1      0.1     10.0     200      0.001
'
'      ncnods
CMAXSTEP               12100
'      nodex    idof     dfact
 '         2       1        1.
'
STATIC                                    1              0.1              0.1              0.1
'
DYNAMIC                                2.2084           0.0001           0.0001           0.0001
'      matno    E-mod    poiss yield density thermX  Mod    SigU  EpsU
' MISOIEP    1    210000E6   0.3  400E6  7850     0.0 ! -3    400E6  0.5
LOADHIST                    1                1
LOADHIST                    2                2
LOADHIST                    3                1
'
TIMEHIST                    1 Points                    0                0 0.2 **
%TIMEHIST                   2 Points                    0                0 1.01**
TIMEHIST                    2 Points                    0                0 1.0125 **
'
TimeHist                   11 Points                    0                0              0.2
%Wavedata                   3                1                2                5              0
'BEAMLOAD                   1               81                0                0              0
'
NODELOAD                    2              501             7430                0              0
'
'         lldcs  <type>   wave height    Period   Direction  Phase   Surf_Lev  Depth
WAVEDATA     3      2         0.0       5.55    0     90.0     0.0    4.3

Hyd_CdCm 1.0 2.0

DYNRES_N                      Disp                       501                1
'
'
Eigenval         Time                                  2.5
Eigenval         NumberOf                   20
Eigenval         Algorithm       Lanczos
EigenVal         Modescal                    1

'
DeterOff
CONSIMAS
```

' ---------- E O F ----------

DampRatio ! Rayleigh Damping. 1% at 0.1 and 10 hz

**Continued time histroy

1	0.3	1			
0	1.0101	0.055	1.0102	0.15618	**
0	1.0127	0.3	1.0132	1	1.0137**

1	0.3	1
0	0	5

**

1.0103	0.30741		1.0104	0.489475
0.59	1.0139	0.32	1.0141	0.13

Control file quasi static comparison

```
HEAD          Usfos Wave Load Example


'
'
' ------------------------------------------------------------------------
'     Load Control in Time Domain
' ------------------------------------------------------------------------

 Cmaxstep 30000

%XFOSFULL
'       EndTime   dT    dTres   dTpri
 Static     1.0     0.1     0.1     0.1     !  Apply Deadweight statically
' Static     5.0     0.01    0.01     0.01     !  Static Wave simulation
 Dynamic    4.00     0.001    0.001     0.001
'
'                           - Define Time Histories
'        ID   Type     p1   p2   p3
 TimeHist    1   Point    0 0  0.5 1  100 1   !  Ramp up DeadWeight in 1 sec
                            !  and keep constant thereafter.
'        ID   Type    dTL  StartTime
 TimeHist    2   Switch   0     1.0        !  New Load Calc every analysis step (dTL=0)
'        ID   Typ p3                 p4
'
 TimeHist    11   Point    0 0  0.5 1  100 1  ! INTERNAL FLUID
'         LCase  TimHst             (Connect Load Cases with Time Hist)
 LoadHist     1      1   ! DeadWeight
 LoadHist     2      2   ! "Wet things"

%          Ratio1   Ratio2   Freq1  Freq2
 DampRatio     ! Rayleigh Damping. 1% at 0.1 and 10 hz
%
'        Ildcs  <I Phase   Surf_L Depth
 WAVEDATA      2      2        1.5    0.0                        180                 0              2.75
%
Dynres_G       WaveElev
%
Dynres_G       ReacXDir
%
Hyd_CdCm                   0.7                 2
```

Control file Slam load from experiment

```
HEAD          Usfos Wave Load Example


'
'
' ------------------------------------------------------------------------
'     Load Control in Time Domain
' ------------------------------------------------------------------------

 Cmaxstep 15000

%XFOSFULL
'       EndTime   dT    dTres   dTpri
 Static     1.0     0.1     0.1     0.1     !  Apply Deadweight statically
' Static     5.0     0.01    0.01     0.01     !  Static Wave simulation
 Dynamic    2.7     0.0001    0.0001     0.0001
'
'                           - Define Time Histories
'        ID   Type     p1   p2   p3
 TimeHist    1   Point    0 0  0.5 1  100 1   !  Ramp up DeadWeight in 1 sec
                              !  and keep constant thereafter.
'        ID   Type    dTL  StartTime
 TimeHist    2   Switch   0     1.0        !  New Load Calc every analysis step (dTL=0)
'        ID   Typ p3                 p4
 TIMEHIST                    3  Points                          0                  0              1.45  0 **

'
 TimeHist    11   Point    0 0  0.5 1  100 1  ! INTERNAL FLUID                            - Activate Loads
'         LCase  TimHst             (Connect Load Cases with Time Hist)
 LoadHist     1     1   ! DeadWeight
 LoadHist     2     2   ! "Wet things"
 LOADHist     3     3   ! Imposed load
%          Ratio1   Ratio2   Freq1  Freq2
 DampRatio    ! Rayleigh Damping. 1% at 0.1 and 10 hz
%
'        lldcs  <type>   wave height    Period   Direction  Phase   Surf_Lev  Depth
 WAVEDATA   0     120.0     0.0    2.725
%
Dynres_G       WaveElev
%
Dynres_G       ReacXDir
%
NODELOAD                    3              152             2395
NODELOAD                    3              151             2395
NODELOAD                    3              141             2395
NODELOAD                    3              131             2395

Continueed timehistory
** 1.465                    1            1.495             0.38            1.525                 0  2     0
```

Control file Slam load accoding to Monopile theory

```
HEAD          Usfos Wave Load Example


'
'
' ------------------------------------------------------------------
'     Load Control in Time Domain
' ------------------------------------------------------------------

 Cmaxstep      15000

%XFOSFULL
'       EndTime   dT    dTres   dTpri
 Static     1.0    0.1     0.5     0.5    !  Apply Deadweight statically
' Static     5.0    0.01    0.01    0.01    !  Static Wave simulation
 Dynamic    2.7    0.0001    0.0001    0.0001
'
'                          - Define Time Histories
'        ID   Type     p1   p2   p3
 TimeHist    1   Point    0 0  1 1  100 1   !  Ramp up DeadWeight in 1 sec
                            !  and keep constant thereafter.
'        ID   Type    dTL  StartTime
 TimeHist    2   Switch   0    1.0        !  New Load Calc every analysis step (dTL=0)
'        ID   Typ p3                p4
 %TIMEHIST                   3  Points                        0                0  1.1816 **
'
TIMEHIST                     3  Points                        0                0  1.45 **
%
 TimeHist    11   Point    0 0  1 1  100 1
'                          - Activate Loads
'         LCase  TimHst            (Connect Load Cases with Time Hist)
 LoadHist     1      1   ! DeadWeight
 LoadHist     2      2   ! "Wet things"
 LoadHist     3   ! "SLAM"
 LoadHist     4   ! "SLAM"
 LoadHist     5   ! "SLAM"
 LoadHist     6   ! "SLAM"
 LoadHist     7   ! "SLAM"
 LoadHist     8   ! "SLAM"
 LoadHist     9   ! "SLAM"
 LoadHist     1   ! "SLAM"
 LoadHist     1   ! "SLAM"
 LoadHist     1   ! "SLAM"
 LoadHist     1   ! "SLAM"
 LoadHist     1   ! "SLAM"
 LoadHist     1   ! "SLAM"
%'          Ratio1   Ratio2   Freq1  Freq2
 DampRatio     ! Rayleigh Damping. 1% at 0.1 and 10 hz

'------------------------------------------------------------------
```

```
'      Define Wave & Current
'-------------------------------------------------------------------
'
'         Ildcs  <I wave height   Period          Direction       Phase          Surf_Lev        Depth
 WAVEDATA                  0               5               0                              100 0  2.75
'
'Estimated impact from slamming
'BEAMLOAD L ElemID          qx1             qy1             qz1             qx2             qy2
 BEAMLOAD                 15          1401        13886.3             0               0               0
 BEAMLOAD                  3          1301        13886.3             0               0               0
 BEAMLOAD                  4            18        13886.3             0               0               0
 BEAMLOAD                  5            19        13886.3             0               0               0
 BEAMLOAD                  6           192        13886.3             0               0               0
 BEAMLOAD                  7           193        13886.3             0               0               0
 BEAMLOAD                  8           191 13886.3  0              0               0
 BEAMLOAD                  9           181        13886.3             0               0               0
 BEAMLOAD                 10            90 13886.3  0              0               0
 BEAMLOAD                 11            89 13886.3  0              0               0
 BEAMLOAD                 12            92 13886.3  0              0               0
 BEAMLOAD                 13            91 13886.3  0              0               0
 BEAMLOAD                 14            88 13886.3  0              0               0

'Wave Type 1 : Airy, Extrapolated
'         1.1 : Airy, Stretched
'         2 : Stoke's 5'th (Skjelbreia, Hendrickson, 1961)
'         3 : User Defined
'         4 : Stream Function Theory (Dean, Dalrymple) Unit



'
'                                 - Account for buoyancy
' BUOYANCY

' Rel_Velo              ! Account for Relative Velocity

'
' ---------------------------------------------------------------------
'    Define Drag and Mass Coeffs-
' ---------------------------------------------------------------------
'
  Hyd_CdCm 0.7 2.0
'
' ---------------------------------------------------------------
'  Save Dynamic Results for Visualization in Xact
' ---------------------------------------------------------------
'                                 - Global Results
 Dynres_G      WaveLoad    ! Wave Forces
 Dynres_Glob   WaveOvtm    ! Wave OverTurning Moment
 Dynres_Glob   ReacBSH     ! Reaction, Base Shear
```

```
 Dynres_Glob   ReacOvtm    ! Reaction, Overturning Moment
 Dynres_Glob   WaveElev    ! Plot of Surface elevation
'
'
'            ResTyp   Elem Id    End  Dof
 Dynres_Elem     Force      11        2    2
'
'
'       ncnods
' CNODES     1
'       nodex    idof     dfact
'         8      1       1
'
'
'
% DeterOff
'
' ------------------------------ E O F ---------------------------
```

```
**continued time history
              0          1.2191               1          1.2566               0               2               0

              0          1.4551               1          1.4602               0               2               0
```

Attachment: SKETCH of Jacket used in WaveSlam experiment

Front View

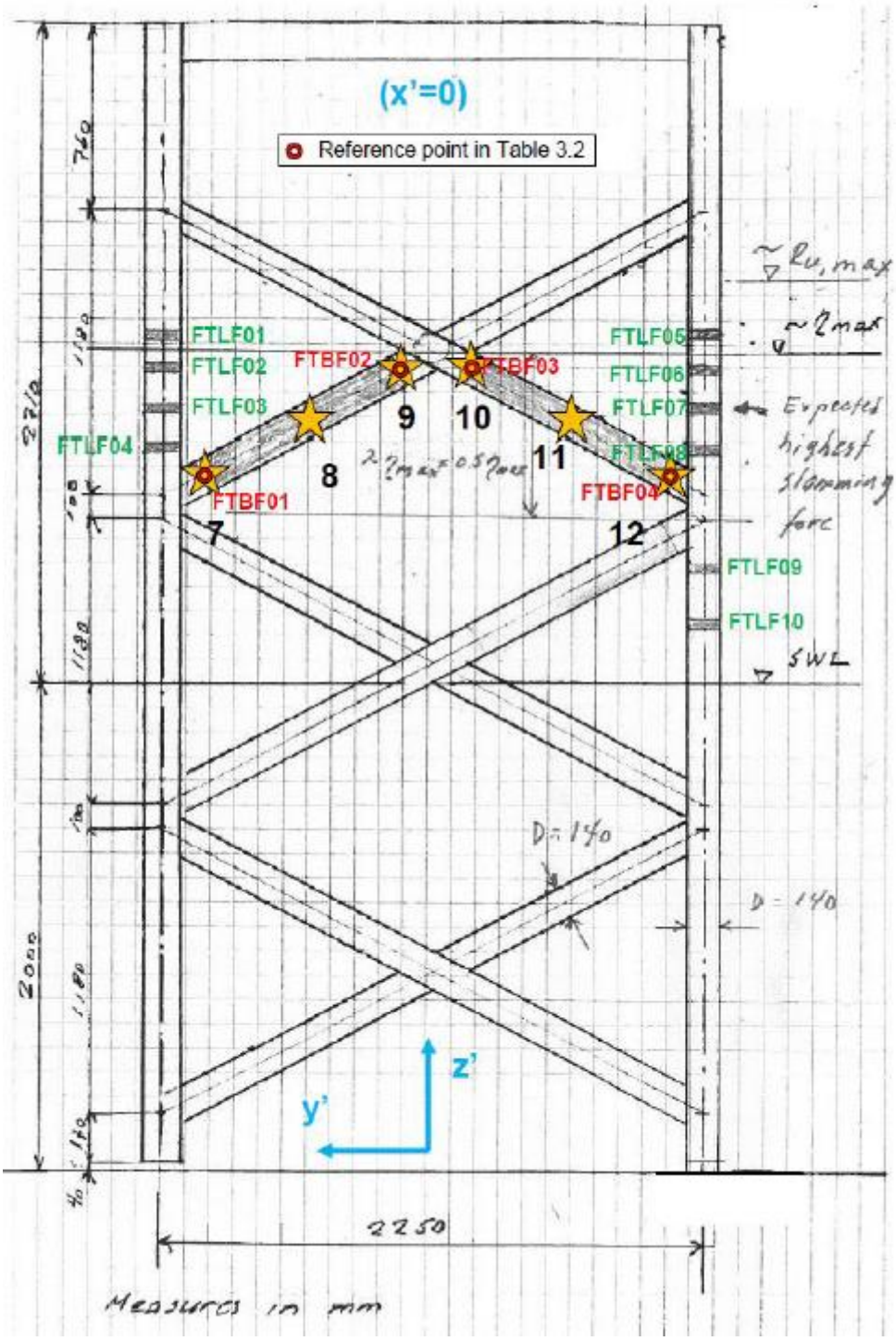

Side view 1

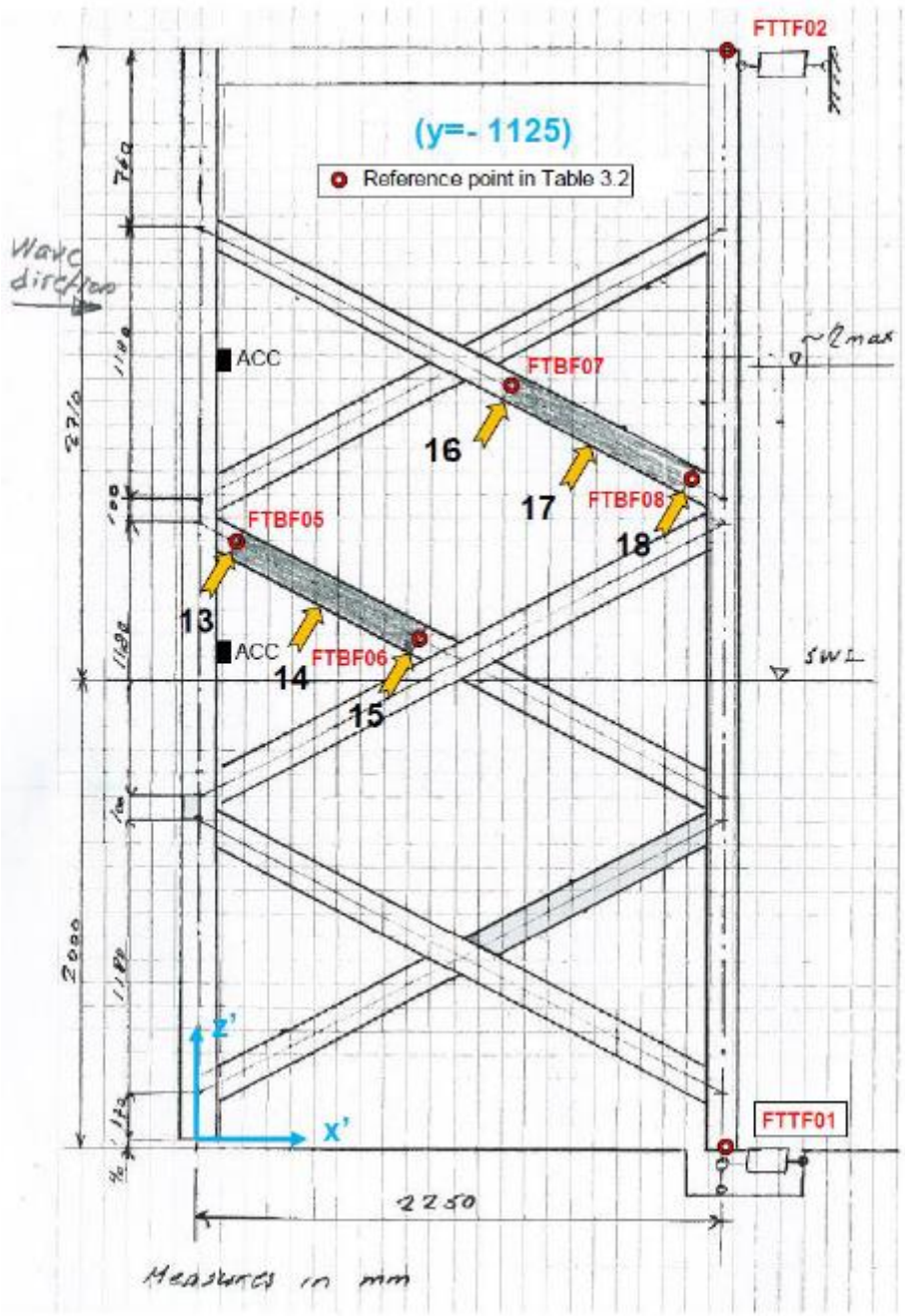
FTTF02
(y=- 1125)
Reference point in Table 3.2
Wave direction
ACC
FTBF07
16
17
FTBF08
18
FTBF05
13
ACC
14
FTBF06
15
SWL
z'
x'
FTTF01
2250
Measures in mm

Side View 2

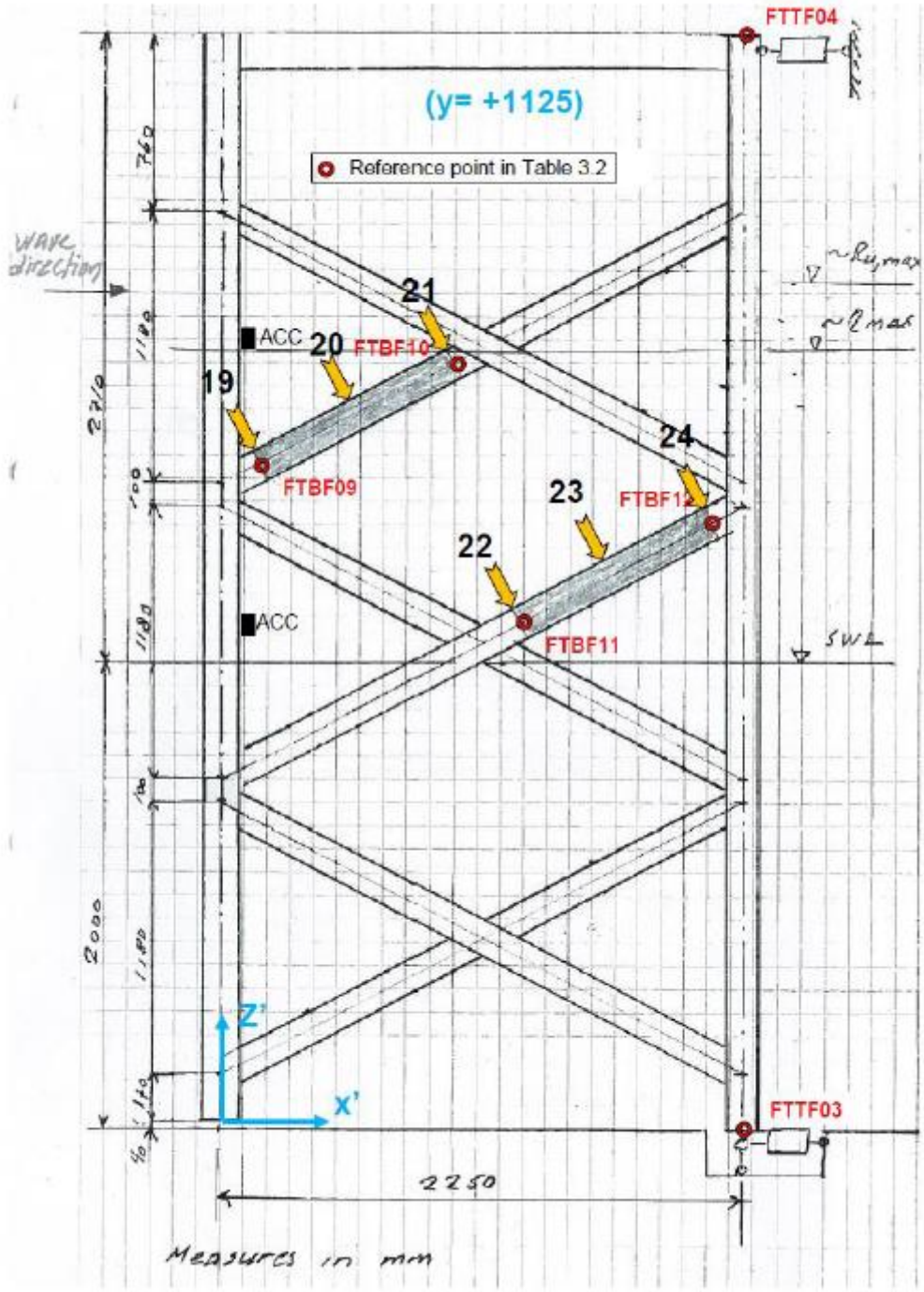
FTTF04
(y= +1125)
Reference point in Table 3.2
wave direction
21
20
FTBF10
19
ACC
FTBF09
24
23
FTBF12
22
ACC
FTBF11
SWL
FTTF03
Z'
X'
2250
Measures in mm